STATE OF OHIO
Bob Taft, Governor
DEPARTMENT OF NATURAL RESOURCES
Samuel W. Speck, Director
DIVISION OF GEOLOGICAL SURVEY
Thomas M. Berg, Chief

Report of Investigations No. 146

SUBSURFACE GEOLOGY OF THE SERPENT MOUND DISTURBANCE, ADAMS, HIGHLAND, AND PIKE COUNTIES, OHIO

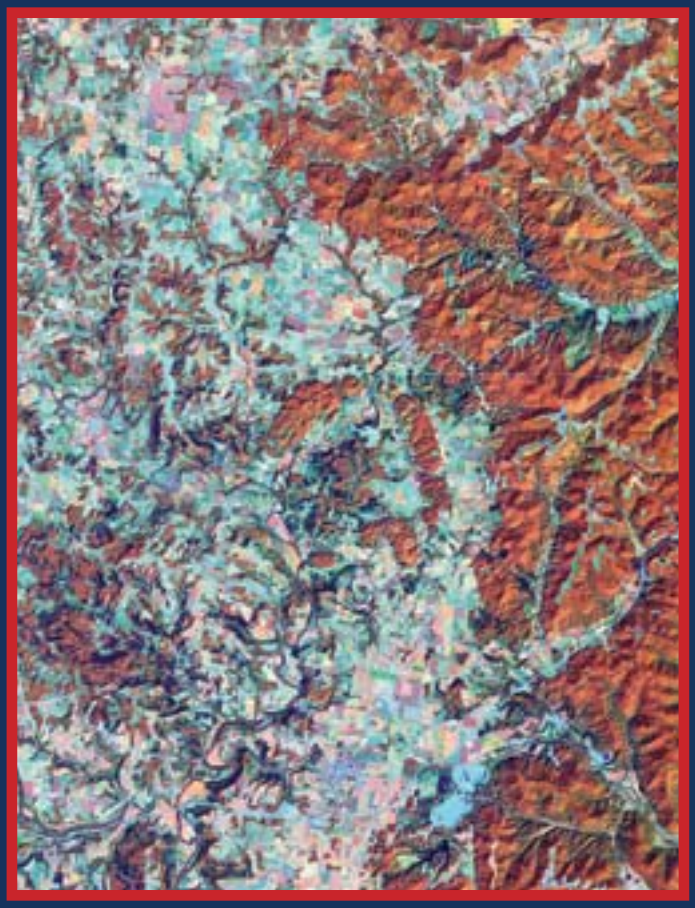

by
Mark T. Baranoski, Gregory A. Schumacher,
Doyle R. Watts, Richard W. Carlton,
and
Belgasem M. El-Saiti

Columbus
2003

DIVISION OF GEOLOGICAL SURVEY
4383 FOUNTAIN SQUARE DRIVE
COLUMBUS, OHIO 43224-1362
(614) 265-6576
(614) 447-1918 (FAX)
e-mail: geo.survey@dnr.state.oh.us
World Wide Web: http://www.ohiodnr.com/geosurvey/

STATE OF OHIO
Bob Taft, Governor
DEPARTMENT OF NATURAL RESOURCES
Samuel W. Speck, Director
DIVISION OF GEOLOGICAL SURVEY
Thomas M. Berg, Chief

Report of Investigations No. 146

SUBSURFACE GEOLOGY OF THE SERPENT MOUND DISTURBANCE, ADAMS, HIGHLAND, AND PIKE COUNTIES, OHIO

by

Mark T. Baranoski
Ohio Division of Geological Survey

Gregory A. Schumacher
Ohio Division of Geological Survey

Doyle R. Watts
Wright State University (formerly at University of Glasgow)

Richard W. Carlton
Ohio Division of Geological Survey (now retired)
and
Belgasem M. El-Saiti
Gar Younis University, Bengazi, Libya (formerly at University of Glasgow)

Columbus
2003

Front cover: Landsat Thematic Mapper (TM) satellite false-color image taken in September 1994 showing the circular Serpent Mound disturbance and the Plum Run Quarry Fault adjacent to the western limit of the Appalachian Plateaus in southern Ohio (see interpretation opposite). Image area covers approximately 888 square km (343 square miles). Image spectral bands are bands 2, 3, and 4, which determine relative intensities of blue, green, and red, respectively. The bands range in wavelength between 0.52 and 0.60 micrometers, 0.63 and 0.69 micrometers, and 0.76 and 0.90 micrometers, respectively. Reddish-orange hues generally indicate deciduous tree cover on rugged topographic relief. Light-blue to purple hues indicate highly reflective surfaces such as roads, manmade features, and water bodies. Image processing provided by Ohio Department of Natural Resources, Division of Real Estate and Land Management.

Back cover: Aerial view of the Serpent Mound effigy, Adams County, Ohio. Photo by Tom Root. Reproduced with the permission of the Ohio Historical Society.

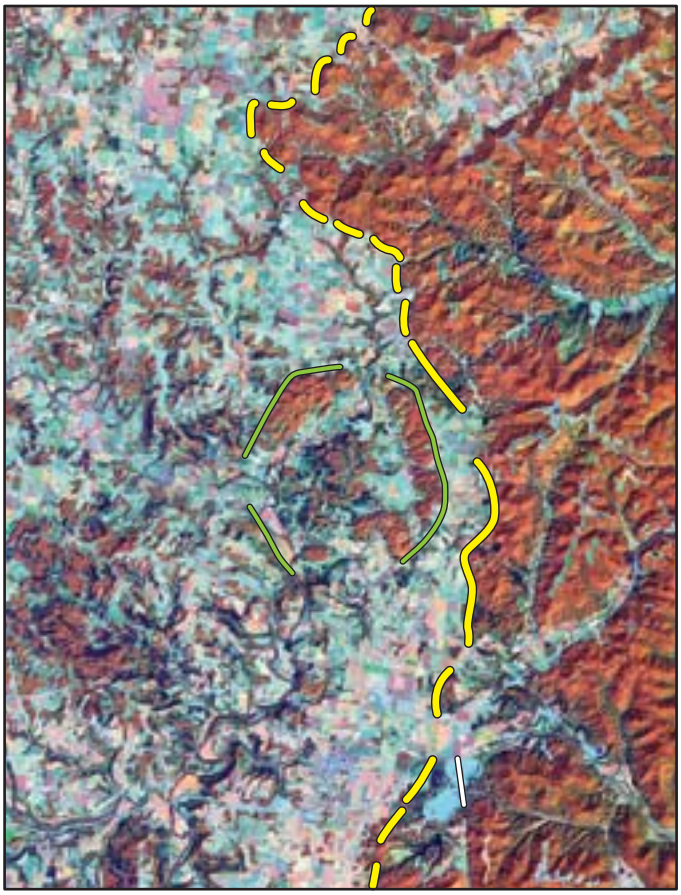

Western edge of the Appalachian Plateaus escarpment

Boundary fault zone of the Serpent Mound disturbance

Plum Run Quarry Fault

INTERPRETATION OF FRONT-COVER IMAGE

CONTENTS

FIGURES

TABLES

PLATES

SUBSURFACE GEOLOGY OF THE SERPENT MOUND DISTURBANCE, ADAMS, HIGHLAND, AND PIKE COUNTIES, OHIO

by
Mark T. Baranoski
Gregory A. Schumacher
Doyle R. Watts
Richard W. Carlton
and
Belgasem M. B. El-Saiti

ABSTRACT

The Serpent Mound disturbance is an area of geologically complex rocks in southern Ohio near the junction of Adams, Highland, and Pike Counties. The disturbance takes its name from but should not to be confused with the Serpent Mound effigy mound, an archaeological site located in the southwest portion of the geologic structure. The Serpent Mound geologic disturbance is a circular structure about 8 km (5 miles) in diameter and consists of three structural elements: a central uplift, a transition zone, and a ring graben. The disturbed area contains highly faulted and folded sedimentary rocks of Ordovician through Mississippian age. The origin of the structure generally has been attributed to either an exogenic event, such as a meteorite impact, or an endogenic event, such as explosive release of highly pressurized gas trapped beneath the Earth's surface. Paleomagnetic data suggest that the disturbance formed prior to the Late Permian (256 million years ago).

Core DGS 3274, drilled in the central uplift, contains 903 meters of severely deformed (fractured, faulted, and brecciated) to mildly deformed sedimentary rocks ranging in age from Late Cambrian (?) to Late Devonian. Shatter cones and shock metamorphism in the form of planar deformation features in quartz, as well as a small iridium anomaly found in a breccia from this core, provide convincing evidence for a meteorite-impact origin of the Serpent Mound disturbance. Core DGS 3275, drilled in the transition zone, penetrates 629 meters of severely deformed to undeformed sedimentary rocks ranging in age from Late Cambrian (?) to Middle Silurian. Core DGS 3275 has fewer breccias and less deformation than core DGS 3274, but does contain shatter cones and most of the types of small-scale structures reported in DGS 3274. No systematic search for iridium or shock metamorphic features was performed on core DGS 3275.

Core and seismic data indicate that, in the central uplift, strata above the Ordovician-age Carntown unit of the Black River Group (equivalent to drillers' "Gull River" limestone) are highly disturbed and discontinuous. Cores DGS 3274 and 3275 also show complex cross-cutting structural relationships and mineralization. These features indicate relative timing of structural events and support the seismic interpretation of multiple episodes of deformation. These younger rocks in the central uplift, in some cases, have been displaced a maximum of 275 meters above their expected level, when compared to similar strata outside the disturbance. Conversely, the Carntown unit and the underlying Wells Creek Formation can be traced across the Serpent Mound disturbance on seismic profiles and appear to be displaced downward at least 276 meters below their expected elevations. Seismic data indicate that Paleozoic rocks below the Carntown are thinner than expected for the region, which may partially account for the Carntown unit and older rocks being lower than expected. Much of the depression below the Serpent Mound disturbance, not accounted for by thinning, may be the result of movement along pre-existing Precambrian faults, which were reactivated after the formation of the Carntown unit.

Although the Carntown unit and the Wells Creek Formation can be traced across the Serpent Mound disturbance on seismic profiles, both units are broken by faults extending upward from the Precambrian. Evidence suggests that post-Carntown faulting may have occurred before the formation of the Serpent Mound disturbance as well as after its formation.

A localized, oblong, positive magnetic anomaly is slightly offset in relation to the surface outline of the Serpent Mound disturbance. This magnetic anomaly is on trend with the northwest-trending contours of regional total magnetic intensity maps. A localized gravity anomaly beneath the central uplift appears to be related to the impact. The core and geophysical evidence suggests that a meteorite impact occurred on or near a pre-exisiting geologic structure.

INTRODUCTION

The Serpent Mound disturbance is a nearly circular area, about 8 km (5 miles)[1] in diameter, of intensely faulted and folded Ordovician- to Mississippian-age rocks exposed at the surface near the junction of Adams, Highland, and Pike Counties in south-central Ohio (fig. 1). The disturbed nature of the rock strata in this area is in sharp contrast to relatively flat lying strata outside the area. The surface geology of the Serpent Mound disturbance has been well documented by numerous studies over the past 160+ years (see section on Previous work). All of these studies were driven by either scientific curiosity related to the origin of the disturbance or by its economic potential.

John Locke (1838) was the first to describe the area and gave it the name "Sunken Mountain." Walter Bucher (1925) renamed the feature the Serpent Mound **cryptovolcanic**[2] structure after the aboriginal serpent-shaped effigy mound (see back cover), located on a bluff overlooking Ohio Brush Creek on the southwestern side of the disturbance. This shared name has sometimes led to confusion between the geologic area and the archaeological site. However, there is no known relationship between the Serpent Mound disturbance and the archaeological site other than location. For more information on the archaeological significance of the area, the reader is referred to Fletcher and others (1996).

Bucher (1936) and Reidel and others (1982) divided

[1]Metric units of measure are used throughout this report; English equivalents are given in parentheses for map/road distances. English units, with metric equivalents, have been used in the core, sample, and geophysical-log descriptions in the tables and appendixes because the original records on file at the Ohio Division of Geological Survey use English units.

[2]Some terms, particularly those related to structural geology and geophysics, that may be unfamiliar to some readers are defined in the glossary (Appendix A). These terms are in **boldface** type where they are first used in the text. For definitions of other terms, please refer to the American Geological Institute *Glossary of geology* (Jackson, 1997).

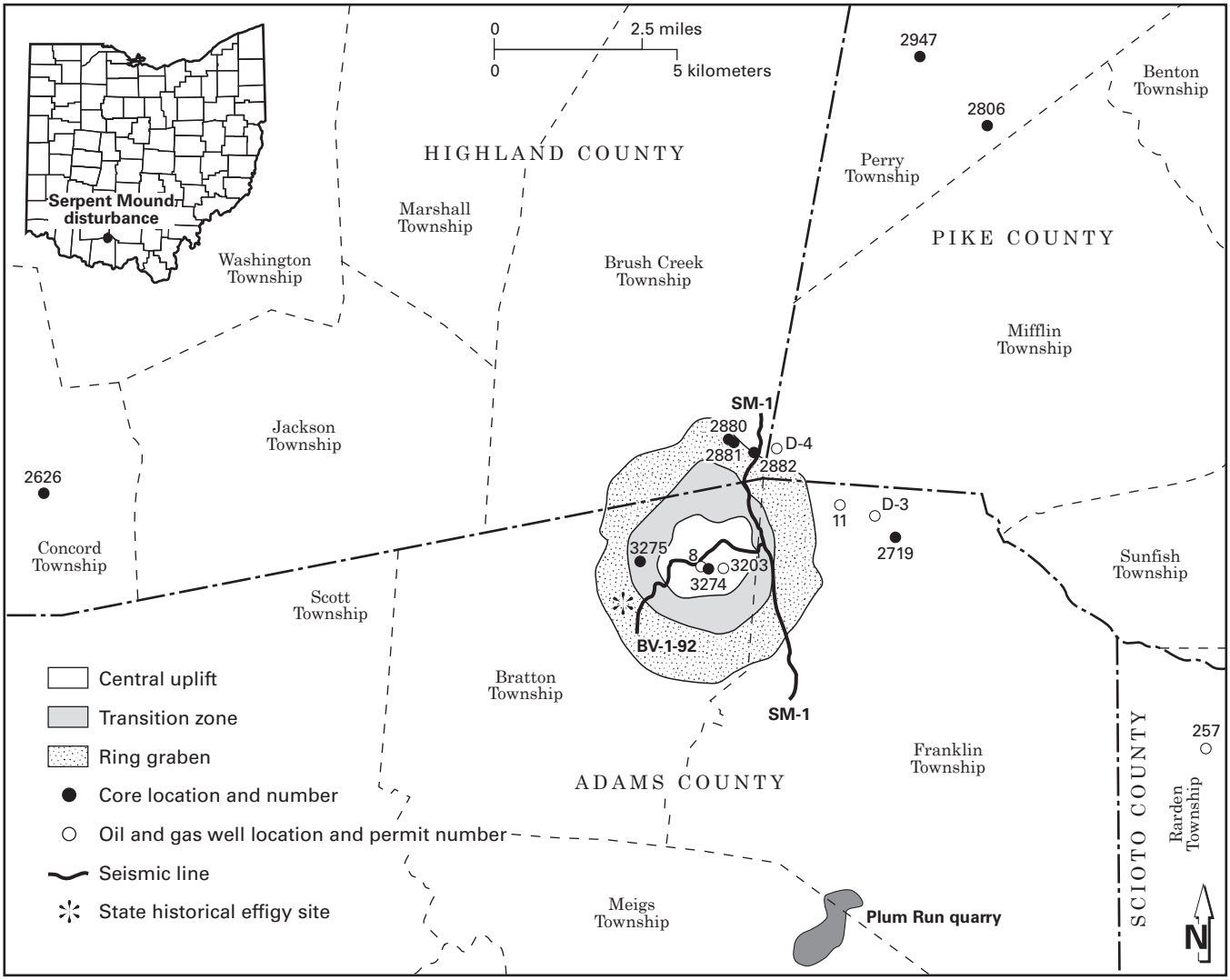

FIGURE 1.—Location of structural zones of the Serpent Mound disturbance based on descriptions from Bucher (1936), Reidel (1975), and Reidel and others (1982). Also shown are location of wells, cores, seismic lines, and selected cultural features.

the Serpent Mound disturbance into three structural zones largely on the basis of surface mapping: a central uplift, a transition zone, and a **ring graben** (fig. 1). Strata in the central uplift are characterized by highly disturbed, faulted, and folded rocks of Ordovician and Silurian age, which have been uplifted a minimum of 122 meters and possibly as much as 275 meters. Surrounding the central uplift is a transition zone of mostly Silurian rocks characterized by both radially and concentrically folded and faulted strata that have minor vertical displacement. The ring graben on the outer perimeter of the Serpent Mound disturbance is characterized by fault-bounded strata that have been displaced below their undisturbed structural positions a minimum of 60 meters and possibly as much as 245 meters (Reidel and others, 1982). Mississippian and Devonian rocks are preserved in the graben.

A single hypothesis regarding the origin of the Serpent Mound disturbance has been elusive because of the lack of subsurface data (Reidel and others, 1982). Two basic modes of origin have been proposed: an **exogenic**, meteorite-impact hypothesis and an **endogenic** hypothesis that assumes some force within the Earth created the disturbance. Although both models are discussed in this report, the presence of planar deformation features (PDF's) and a small iridium anomaly provide convincing evidence for a meteorite impact in the Serpent Mound area (Carlton and others, 1998b).

The primary objectives of this report are to present new, significant subsurface information on the Serpent Mound disturbance and to describe the geologic history of this structure. In addition, this report provides a brief review of the important published, unpublished, and open-file literature on the Serpent Mound disturbance.

This report focuses on two primary sources of new information. The most important new data come from two continuous cores, Division of Geological Survey (DGS) cores 3274 and 3275, drilled into the Serpent Mound disturbance by John L. Carroll Mineral Exploration in 1979. These cores were donated to the Survey in 1993. Core DGS 3274 was drilled in the central uplift (fig. 1) and reached a depth of 903 meters. DGS 3275 was drilled in the transition zone and reached a depth of 629 meters. Examination of the cores has revealed a structurally complex, faulted, and brecciated assemblage of Silurian, Ordovician, and possibly Cambrian strata.

The second source of new information is geophysical data, including reprocessed **seismic reflection** profiles (SM-1 and BV-1-92) and **magnetic** and **gravity surveys** taken in 1996 across the Serpent Mound disturbance (see fig. 22). The seismic data reveal a complex and only partially understood relationship between the Serpent Mound disturbance and the local subsurface geology. The magnetic and gravity data acquired for this investigation complement older data sets and help to characterize the three-dimensional geophysical nature of the disturbance. **Paleomagnetic analysis** of hematitic limestones was used to determine the approximate age of the Serpent Mound disturbance.

Data from three cores (DGS 2880, 2881, and 2882) and two sets of cuttings from wells drilled within the perimeter of the disturbance provided additional subsurface information on the Serpent Mound disturbance. Data from two cores (DGS 2626 and DGS 2719) and four sets of cuttings from wells drilled beyond the perimeter of the disturbance were used primarily for comparative purposes. Table 1 summarizes the drill-hole data used in this investigation.

Numerous published abstracts have reported preliminary findings of this project: Baranoski, Schumacher, Carlton, Watts, El-Saiti, and Koeberl (1998); Baranoski and Watts (1997); Baranoski, Watts, El-Saiti, Schumacher, and Carlton (1998a, b); Carlton, Koeberl, Baranoski, and Schumacher (1998a); Koeberl, Buchanan, and Carlton (1998); Schumacher, Baranoski, Carlton, Watts, and El-Saiti (1998); Watts, El-Saiti, Baranoski, and Schumacher (1998); and Watts, El-Saiti, Memmi, Weaver, and Baranoski (1998). Baranoski, Schumacher, Watts, Carlton, and El-Saiti (1997) and Baranoski and Watts (2001) reported on the hydrocarbon potential of the area. El-Saiti (1998) completed a Ph.D. dissertation on the geophysical characteristics of the disturbance. Carlton and others (1998b) published the first report that documented the presence of PDF's and an iridium anomaly in the Serpent Mound disturbance. Most of this published information is included in this report.

ACKNOWLEDGMENTS

The authors express their sincere appreciation to the many scientists, landowners, archivists, Ohio Department of Natural Resources (ODNR) employees, and others who assisted or contributed in some way to this investigation. We are indebted to the following people and their organizations: John L. Carroll, owner of John L. Carroll Mineral Exploration (New York, New York), who donated the deep continuous cores to the Ohio Division of Geological Survey; the Serpent Mound Working Group, particularly Arie Janssens (consultant) and Michael C. Hansen (Ohio Division of Geological Survey); the late Perry Dean, President of Paragon Geophysical, for field acquisition of the seismic line BV-1-92; Tom McGovern and Lauren Geophysical for seismic processing of seismic line BV-1-92; Columbia Natural Resources for processed and raw seismic data for line SM-1; the Royal Society of London for financial assistance (to Watts) for the geophysical field work and additional seismic data processing; Landmark Graphics Corp. and Geophysical Microcomputer Applications, Inc., for technical support and assistance with seismic processing and modeling software; and The Robertson Trust for providing funds to purchase geophysical software for the University of Glasgow (Scotland) while Doyle Watts was employed there. Wright State University provided equipment and facilities to support the geophysical field work. Rob Van der Voo of the University of Michigan and Anne M. Grunow of the Byrd Polar Research Center at The Ohio State University made their laboratory facilities available. Stephen P. Reidel (Battelle Pacific Northwest National Laboratory) and Raymond R. Anderson (Iowa Geological Survey Bureau) provided insightful technical reviews of an early draft of the manuscript. Thomas M. Berg, Merrianne Hackathorn, Michael C. Hansen, Dennis N. Hull, E. Mac Swinford, and Lawrence H. Wickstrom (all of Ohio Division of Geological Survey) and Emily L. Eby reviewed the manuscript and suggested many editorial and technical improvements. We

TABLE 1.—*Basic information for*

County[1]	Township	Lease name	Operator	Permit no.	Data type
Adams	Bratton	Brown	John L. Carroll Mineral Exploration	12	core DGS 3274
Adams	Bratton	McCleese	John L. Carroll Mineral Exploration	13	core DGS 3275
Adams	Bratton	Kaeser	Simpson Oil & Gas Co.	8	sample cuttings
Adams	Bratton	Parker	Sinking Springs Oil Co.	3203	open-file sample description
Adams	Franklin	Tira	Tira Syndicate	D-3	open-file sample description
Adams	Franklin	Justice	North American Exploration, Inc./ Phillips Petroleum Co.	NA	core DGS 2719
Adams	Franklin	Russell/Tener	Oxford Oil Co.	11	sample cuttings, geophysical log
Highland	Brush Creek	Humphrey	Cominco American, Inc.	8	core DGS 2880
Highland	Brush Creek	Humphrey	Cominco American, Inc.	9	core DGS 2881
Highland	Brush Creek	Adams/Shoemaker	Cominco American, Inc.	10	core DGS 2882
Highland	Concord	Goins	Ohio Division of Geological Survey	NA	core DGS 2626, geophysical log
Pike	Mifflin	Kessler	Sinking Springs Oil Co.	D-4	open-file sample description
Pike	Perry	Attinger	Karl Wehmeyer	21	core DGS 2947
Pike	Perry	Hatfield	Phillips Petroleum Corp.	NA	core DGS 2806
Scioto	Rarden	Smith	Adobe Oil & Gas Corp.	257	geophysical log

[1]See figure 1 for locations.
[2]BX, diameter = $1^1/_2$" (3.8 cm); NCQ, diameter = $1^7/_8$" (4.8 cm); NX, diameter = 2" (5.1 cm); ST, diameter = 4" (10.2 cm); NA, not applicable.

also thank the following individuals for their help: Ernest H. Carlson (Kent State University); Stuart L. Dean (University of Toledo); Kees A. DeJong and David L. Meyer (University of Cincinnati); Ernest C. Hauser, Byron Kulander, Benjamin H. Richard, Ronald G. Schmidt, and Paul J. Wolfe (Wright State University); Frank L. Koucky (College of Wooster); Roxanne Kukuk and Richard Terry (Boonschoft Museum of Discovery, Dayton); Robert L. Malcuit (Denison University); Michael R. Sandy (University of Dayton); and John F. Simpson (consultant). Michael D. Williams of the ODNR, Office of Marketing Services took most of the core photographs. Gary M. Schaal (now retired) of the ODNR, Division of Real Estate and Land Management provided the Landsat TM image for the cover. Lisa Van Doren drafted the figures and plates for this report.

PREVIOUS WORK

Previous studies concerning the Serpent Mound disturbance that are cited in this report are not of equal importance; many are abstracts, unpublished reports, theses, field guides, or open-file maps. The studies that have either mapping or historical significance are reviewed below. Papers that are less relevant to our investigation are listed in table 2. References to previous work related to other aspects of this report can be found in the appropriate sections.

The faulted, folded, and displaced rocks of the Serpent Mound disturbance were first described by John Locke during the First Geological Survey of the State of Ohio (Locke, 1838). In late August 1837, John Locke traveled to Locust Grove in northeastern Adams County to examine the many sulfur springs of the region. Massie's Spring, located about 3.2 km (2 miles) northwest of Locust Grove and within the ring graben of the Serpent Mound disturbance, was the first spring studied. Locke noted that he traveled on rocks of the "cliff limestone" (Bisher and Lilley Formations and the Peebles Dolomite; see fig. 5) on the relatively flat uplands and expected to encounter the "greate marle stratum" (Estill Shale) as they descended into the valley of Crooked Creek, south of the spring within the ring graben. The following passage from Locke (1838, p. 266) describes the discovery of the Serpent Mound disturbance:

As we descended into the channel of Crooked Creek, I did not find as I had expected, the greate marle stratum. Its place seems to be occupied by thin layers of limestone. Although we travelled on that level which should have presented us with the cliff limestone, yet we were surprised with its total disappearance as we approached the spring, and in its place was found the sandstone in large upturned and broken masses. In short, it became evident that a region of no small extent had sunk down several hundred feet, producing faults, dislocations and upturnings of the layers of the rocks.

Locke named this region of Adams County the "Sunken Mountain" because of the downward displacement of the strata in this area. Edward Orton, in his 1871 report describing the geology of Highland County for the Second Geological Survey of Ohio, provided additional information about the size, variability of bedding dip, and magnitude of fault displacement. Orton (1871, p. 289) stated:

Faults occur in the immediate neighborhood of Sinking Spring of considerable extent, the Waverly sandstone [Bedford Shale and Berea Sandstone] *walling against the Pentamerous division of the Niagara group* [Peebles Dolomite]. *The disturbed area extends for six or eight miles* [8-10 km] *in each direction. There is nothing like uniformity of dip throughout the region. Waverly sandstone, slates, the various limestones of the county, are involved in inextricable confusion.*

August F. Foerste and Raymond A. Lamborn were the

drill holes used in this investigation

Total depth of hole	Completion date	Geologic unit at total depth	Interval of core, well cuttings, or sample descriptions examined	Percent of core missing	Core diameter[2]	Location in relation to Serpent Mound disturbance
2,962 ft (903 m)	6/29/79	Knox Dolomite	11-2,962 ft (3-903 m)	9	NX, BX	central uplift
2,065 ft (629 m)	8/31/79	Knox Dolomite	17-2,065 ft (5-629 m)	4	NX, BX	transition zone
1,760 ft (536 m)	1/73	Ordovician undivided	20-1,750 ft (6-533 m)	NA	NA	central uplift
1,525 ft (465 m)	1921	Ordovician undivided	85-1,015 ft (26-465 m)	NA	NA	central uplift
2,162 ft (659 m)	6/29/39	Rose Run sandstone	1,447-2,162 ft (441-659 m)	NA	NA	outside disturbance
422 ft (129 m)	11/24/80	Tymochtee and Greenfield Dolomites undivided?	0-422 ft (0-129 m)	0	ST	outside disturbance
3,886 ft (1,184 m)	7/7/79	Precambrian	2,700-3,886 ft (823-1,184 m)	NA	NA	outside disturbance
275 ft (84 m)	6/30/71	Brassfield Formation	20-275 ft (6-84 m)	5	BX	ring graben
313 ft (95 m)	7/10/71	Brassfield Formation	20-313 ft (6-95 m)	0	BX	ring graben
290 ft (88 m)	7/13/71	Brassfield Formation	20-290 ft (6-88 m)	5	BX	ring graben
1,762 ft (537 m)	10/8/87	Wells Creek Formation	51-1,762 ft (16-537 m)	0	NCQ	outside disturbance
1,792 ft (546 m)	1922	Black River Group	1,018-1,792 ft (310-546 m)	NA	NA	outside disturbance
534 ft (163 m)	11/1/61	Drakes Formation	20-534 ft (6-163 m)	0	ST	outside disturbance
449 ft (137 m)	12/9/80	Tymochtee and Greenfield Dolomites undivided?	12-449 ft (4-137 m)	0	ST	outside disturbance
4,432 ft (1,351 m)	11/1/79	Precambrian	samples not available	NA	NA	outside disturbance

TABLE 2.—*Additional published and unpublished studies in the area of the Serpent Mound disturbance*

The references listed in this table are not cited in the body of the report but are included in the References cited. The references are organized by subject and are briefly annotated.

General geology

Stout, 1941: speculated that the Serpent Mound structure was related to the Bowling Green fault and not to Appalachian Valley and Ridge structures.

Hansen, 1998: summary article on past and recent work.

Geologic mapping

Bucher, 1935: discusses earlier work (see Bucher 1921, 1925, 1933).

Galbraith and Koucky, 1969: discusses local structure in the area.

Reidel, 1970: mapping and structure of western portion of structure.

Jacobs, 1971: discusses local structure in the area.

Stryker, 1971: mapping and structure of northern portion of structure.

Wachter, 1971: mapping and structure of southwestern portion of structure.

Swinford, 1983: mapping and structure of southeastern portion of structure.

Geophysical studies

Sappenfield, 1950: unpublished M.S. thesis, magnetic survey of the area.

Istok, 1978: unpublished M.S. thesis, paleomagnetic study of the area.

Mineralization

Botoman and Stieglitz, 1978: discusses Mississippi Valley-type sufide mineralization.

McFarland and others, 1993 (abs.): mentions trace elements in the area.

McFarland and Carlson, 1994 (abs.): mentions sulfur isotope study.

McFarland and Talnagi, 1994 (abs.): mentions trace elements in the area.

McFarland and Carlson, 1996 (abs.): mentions brine migration supported by mineralization studies.

McFarland, 1999: investigation of mineralization using sulfur isotopes, fluid inclusions, and trace elements.

Origin

Dietz, 1959, 1968: discusses shatter cones found in structures.

Worthing, 1965: discusses structures in eastern North America.

Reidel, 1981 (abs.): mentions hydrotectonic model for the structure.

Hansen, 1982: speculates kimberlite origin for the structure.

Field guides

Summerson and others, 1963

Forsyth and Bowman, 1963

Koucky, 1975

Reidel and Koucky, 1981

Koucky and Reidel, 1987

Baranoski and Brockman, 1998

Miscellaneous

Heirendt, 1988: unpublished M.S. thesis, soil-gas survey of the area.

first geologists to map the details of the Serpent Mound disturbance. The files of the Ohio Division of Geological Survey contain two geologic maps, dated 1918 and 1919, of the Bainbridge 15-minute quadrangle by Foerste and Lamborn. These manuscript maps indicate a circular feature defined by an outer faulted ring of Devonian and Mississippian rocks and a central area of Ordovician rocks (fig. 2A). The 1920 *Geologic map of Ohio*, compiled by John A. Bownocker, was the first published map to show a circular feature in northeastern Adams County and adjacent areas (fig. 2B). Because the 1920 *Geologic map of Ohio* was of much smaller scale (1:500,000), many of the Serpent Mound structural features and geology were more generalized than those found on Foerste and Lamborn's maps. The Ordovician rocks in the area of the central uplift are not shown on the 1920 map.

Walter Bucher (1933, 1936) published the first detailed geologic map of the Serpent Mound disturbance. His map shows the disturbance as a circular feature of faulted and folded rocks bounded by normal faults or sharp flexures. He subdivided the disturbance into three regions: the uplifted center of intensely faulted and folded Ordovician shales and limestones, the outer ring depression of locally folded and faulted Silurian, Devonian, and Mississippian rocks, and a transition zone of small fault blocks of Silurian rocks that separate the uplifted center and outer depressed ring graben. Bucher proposed that the Serpent Mound disturbance was produced by the explosive release of confined volcanic gases (cryptovolcanism). Ironically, in his discussion on the age of the Serpent Mound disturbance, Bucher (1936, p. 1063) indicated that ". . . this circle of hills suggests a lunar crater."

Stephen P. Reidel (1972, 1975) mapped the structural complexities of the Serpent Mound disturbance in detail and confirmed the main structural components of Bucher (1933, 1936). Reidel (1975) defined three prominent structural components: a circular uplifted central area (central uplift of this report), an intermediate ring area (transition zone of this report), and a depressed outer ring of synclines (ring graben of this report).

REGIONAL GEOLOGIC SETTING

PRECAMBRIAN GEOLOGY

The Serpent Mound disturbance is located near the boundary of two Precambrian provinces of the eastern Midcontinent. The older of the two provinces, the Granite-Rhyolite Province (Denison and others, 1984), underlies western Ohio. Depths to rocks of the Granite-Rhyolite Province in western Ohio range from 800 to 6,100 meters below sea level (Drahovzal and others, 1992, p. 12, fig. 6). The Grenville Province (Bass, 1960) lies east of the Granite-Rhyolite Province and is buried beneath hundreds to thousands of meters of Paleozoic sedimentary rocks.

The Granite-Rhyolite Province is the Precambrian craton in Ohio and has been down-faulted and structurally deformed by continental **rifting** during the development of the East Continent Rift Basin (Drahovzal and others, 1992). This basin extends from northwestern Ohio to central Kentucky and westward into Indiana (fig. 3) and is thought to be part of the Midcontinent Rift System (Drahovzal and others, 1992). During and subsequent to the rifting, the East Continent Rift Basin was filled with as much as 6,900 meters of clastic sedimentary and volcanic rocks, including the Middle Run Formation described by Shrake (1991) and Shrake and others (1991).

The Grenville Province is an extension of the Grenville Metamorphic Terrane exposed in southern Canada and consists of regionally metamorphosed igneous and sedimentary rocks. The Grenville thrust sheets are thought to have, in part, overridden the older Granite-Rhyolite Province and the East Continent Rift Basin. The Grenville Province consists of many structural features and localized zones of weakness that affected faulting and sedimentation during the Paleozoic (Beardsley and Cable, 1983; Riley and others, 1993).

The structural contact between the Granite-Rhyolite and Grenville Provinces is referred to as the Grenville Front Tectonic Zone and consists of complexly metamorphosed and folded thrust-belt rocks (Bass, 1960; Rudman and others, 1965; Muehlberger and others, 1967; Bayley and Muehlberger, 1968; Lidiak and Zietz, 1976). This zone is about 50 km (31 miles) wide (Culotta and others, 1990), and its eastern edge lies very near the Serpent Mound disturbance.

A second major structural feature in the area, the Kentucky River Fault System (Ammerman and Keller, 1979), lies 97 km (60 miles) south of the Serpent Mound disturbance (fig. 3). This fault system is the northern boundary fault of the Rome Trough (McGuire and Howell, 1963). Movement along the Kentucky River Fault System and Rome Trough was limited primarily to Early and Middle Cambrian time, during a late phase of crustal extension related to a Precambrian **aulacogen** (Riley and others, 1993). Hansen (1984, p. 4) suggested that present-day earthquakes in northern Kentucky along this zone of weakness may indicate movement on Precambrian faults is still occurring.

The Serpent Mound disturbance is situated on a northwest-trending geophysical anomaly that is depicted on maps by Hildenbrand and Kucks (1984a, b) and contour maps made using the data from Hildenbrand and Kucks (1984a). The coincidence of the disturbance with this geophysical trend, and its implications on interpreting the complex geologic history of the area from the Precambrian to present, is discussed in the section on Geophysical data (p. 24).

PALEOZOIC FOLDING AND FAULTING

Ohio is located on portions of three regional Paleozoic sedimentary and structural basins that unconformably overlie the Precambrian basement complex: the Appalachian, Illinois, and Michigan Basins (fig. 4). The basins are separated by the Cincinnati-Kankakee Arch system, Findlay Arch, and Indiana-Ohio Platform, which are considered regional structurally positive features (Green, 1957). The basins developed during the Paleozoic Era as a result of periodic subsidence, faulting, and structural adjustment in the Precambrian basement complex along plate tectonic boundaries and associated zones of weakness.

Many folds and faults have been observed in and around the Serpent Mound disturbance (Bucher, 1921, 1933, 1936; Schmidt and others, 1961; Galbraith, 1968; Reidel, 1975;

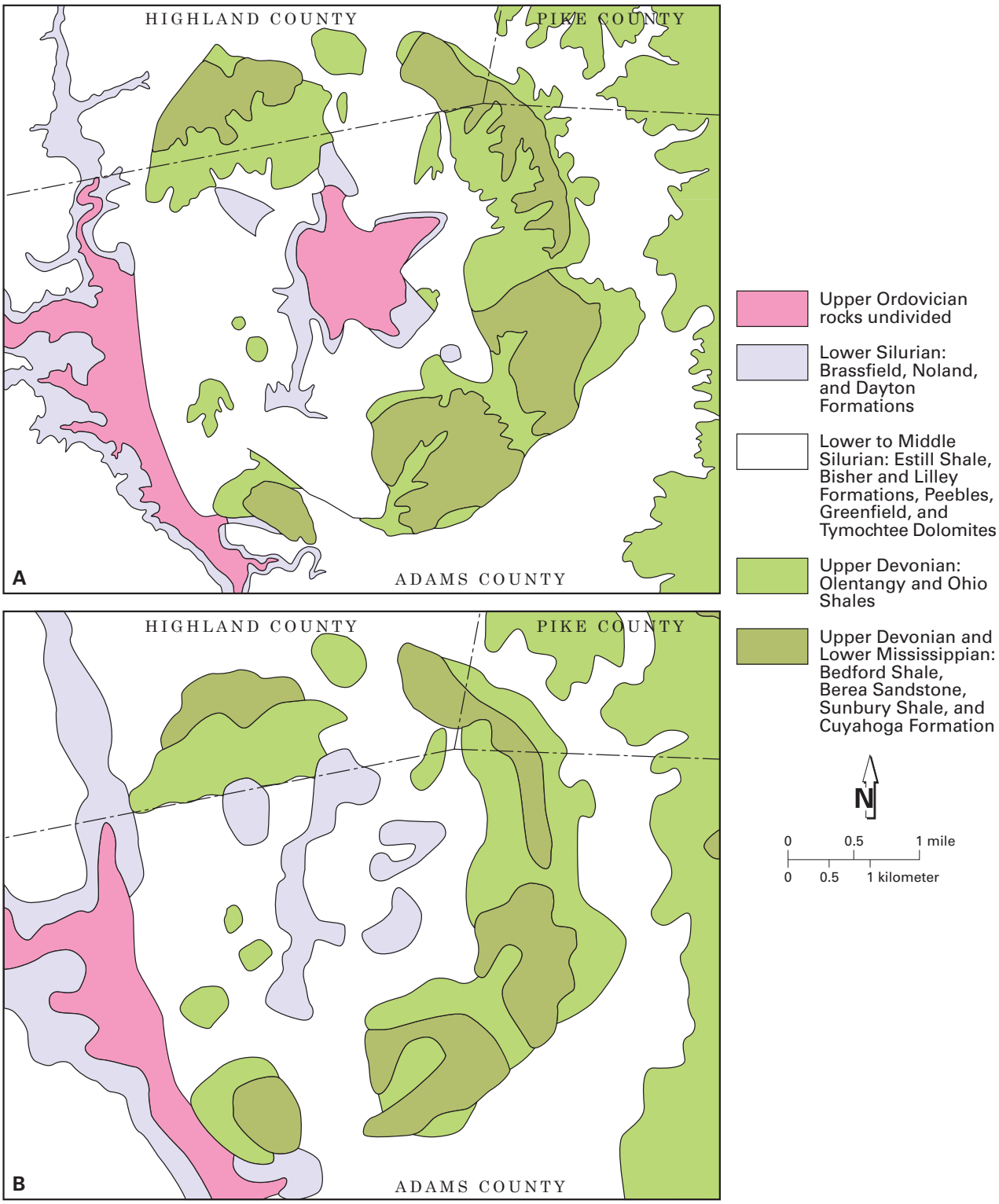

FIGURE 2.—Comparison between the geologic maps of Foerste and Lamborn and Bownocker. **A**, portion of the unpublished Bainbridge 15-minute quadrangle (scale 1:62,500) mapped by Foerste and Lamborn in 1918 and 1919, from file maps at the Division of Geological Survey. **B**, portion of the published 1:500,000-scale geologic map of Ohio by Bownocker (1920), enlarged to 1:62,500 scale. Both maps have been modified from the originals. Note that the unit contacts illustrated from the Bainbridge quadrangle (**A**) have been generalized to accommodate the smaller map scale of the 1920 map (**B**); also note the slight southwest shift of the geologic contacts in relation to the county lines on the 1920 map. The Ordovician rocks that Foerste and Lamborn mapped in the central uplift are shown as Lower to Middle Silurian rocks on Bownocker's map. The authors assume this omission was an oversight in map production.

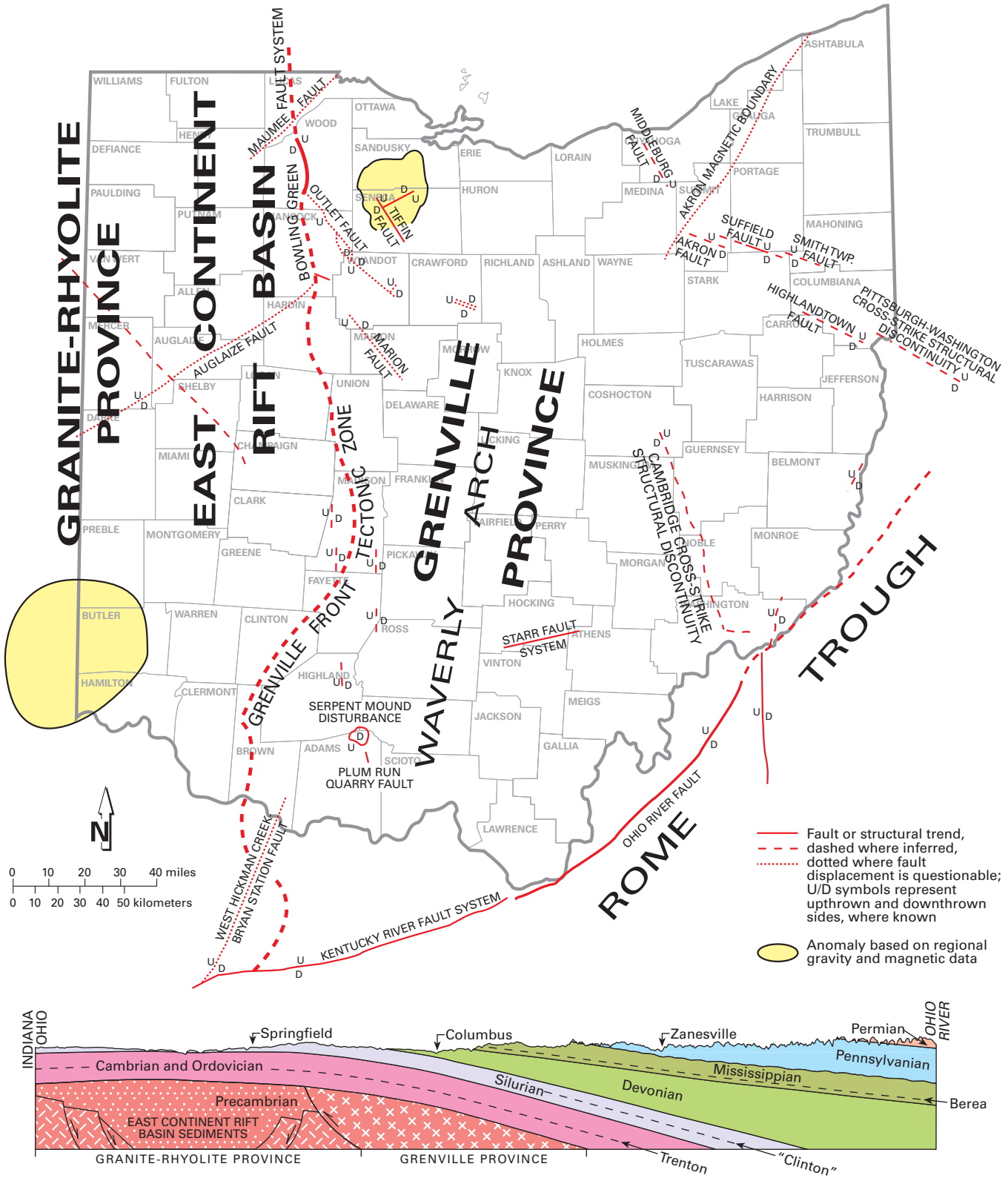

FIGURE 3.—Location of selected basement features in Ohio, modified from Baranoski and Wickstrom (1994), and diagrammatic east-west cross section of Ohio showing Paleozoic sedimentary units and Precambrian provinces.

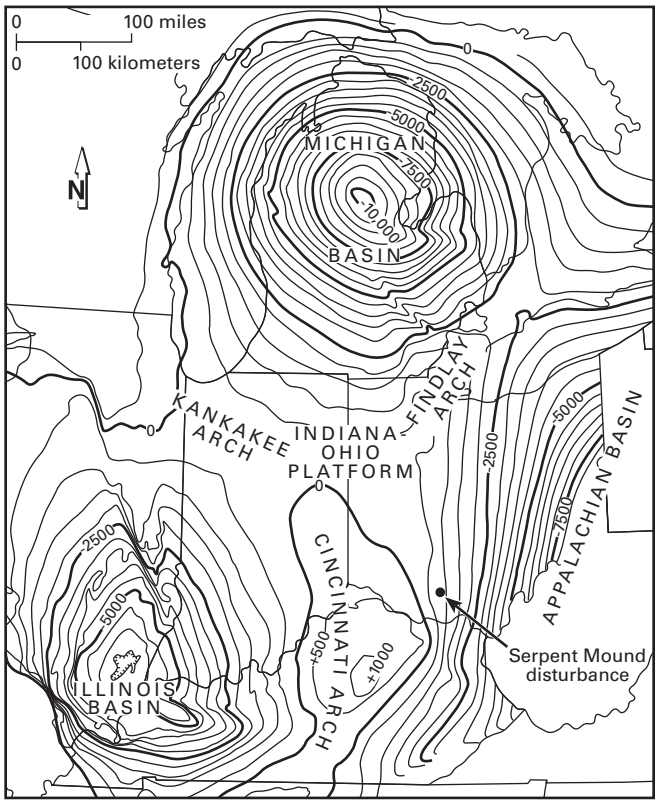

FIGURE 4.—Regional structural features and generalized structure on the top of the Trenton Limestone and equivalents in part of the east-central stable craton of North America (from Wickstrom, 1990). Contour interval is 500 feet (152 meters).

Reidel and others, 1982; Swinford, 1985, 1991). The Waverly Arch, located 16 km (10 miles) east of the Serpent Mound disturbance (fig. 3), is a controversial geologic feature that originally was proposed by Woodward (1961, p. 1645) as a "broad low concealed arch extending from north-central Ohio southward into eastern Kentucky . . . ." Although Woodward did not directly implicate the Precambrian basement structure in the formation of the Waverly Arch, Cable and Beardsley (1984) and Riley and others (1993) speculated that the Waverly Arch was related to episodic movement of the Precambrian basement during crustal convergence from latest Cambrian through Middle Ordovician time (Riley and others, 1993).

Bucher (1933, 1936) observed a dominant northwest-oriented fault trend both within and adjacent to the disturbance. He described these faults as vertical to subvertical and noted that some faults were filled with breccia. A series of north-northwest-oriented grabens, bounded by normal faults and folds, has been observed at the Plum Run quarry (fig. 1), 10 km (6 miles) southeast of the central uplift (Schmidt and others, 1961). Horizontal **slickensides** observed along faults in the Plum Run quarry during this study indicate strike-slip movement accompanied vertical movement as the grabens developed. The grabens formed as part of a regional episode of north-to-northwest faulting in this area (Reidel and others, 1982).

Fractures and faults in the Serpent Mound disturbance reported by Reidel and others (1982) and the core studies and geophysical data described below are strong evidence for a pre-existing Precambrian zone of weakness prior to the formation of the Serpent Mound disturbance. Swinford (1985) suggested that basement faulting controlled development of a north-south- to north-northeast-trending monocline in Adams County west of the Plum Run quarry.

The Plum Run quarry lies in a graben containing the Silurian Peebles and Greenfield Dolomites (see fig. 5). The presence of asphaltic material in the Peebles Dolomite allows relative timing constraints to be placed on faulting in the Plum Run quarry and the Serpent Mound disturbance. Typically, the Peebles in Highland County contains some asphalt-filled vugs (Bowman, 1956). Meyer and Sweeney (1968, p. 99) listed eight locations in Highland and Adams Counties where asphaltic deposits have been reported in Silurian rocks. Asphaltic deposits in the Peebles in the graben at Plum Run are sparse, in contrast to apparently higher concentrations of asphaltic material in the Greenfield Dolomite within the graben (R. S. Bowman, personal commun., 1996). The apparent difference in asphaltic content of the Peebles and the Greenfield suggests that fluid migration occurred laterally after faulting took place at Plum Run. By inference, the presence of asphaltic-rich Peebles in core DGS 3275 suggests that the Serpent Mound disturbance formed after the asphalt was deposited and the Plum Run graben formed. Small amounts of black shale, presumed to be Late Devonian in age, were recovered from a strike-slip fault-zone breccia in the quarry during this study.

Migration of fluids out of the Appalachian Basin and into western Ohio occurred during the Late Paleozoic Alleghany Orogeny (McCabe and Elmore, 1989). The regional asphaltic deposits in the Peebles Dolomite seem to be relict indicators of this migration. Further work is needed to verify this interpretation.

PALEOZOIC STATIGRAPHY

Paleozoic sedimentary rocks on the western flank of the Appalachian Basin range in thickness from 800 meters in north-central Ohio to 4,200 meters in eastern Ohio. The undeformed bedrock sequence adjacent to the Serpent Mound disturbance consists of approximately 1,128 meters of Paleozoic sedimentary rocks unconformably overlying Precambrian basement rocks (fig. 5). The Paleozoic rocks range in age from Middle (?) Cambrian to Early Mississippian and consist of dolomite, limestone, shale, and sandstone, with minor amounts of siltstone, K-bentonite, and chert. The Precambrian through Early Mississippian stratigraphic units in southwestern Ohio are described in Appendix B. The Paleozoic history of the area is summarized below.

Deposition of the lowermost Paleozoic rocks in Ohio began in Middle Cambrian time and continued into Early Ordovician time. These rocks, the Mount Simon Sandstone through the Knox Dolomite (fig. 5), represent an overall transgressive sequence deposited on an eroded Precambrian surface. The Precambrian surface may have up to 100 meters of relief (Janssens, 1973). Regional facies changes are evident in the Cambrian Mount Simon Sand-

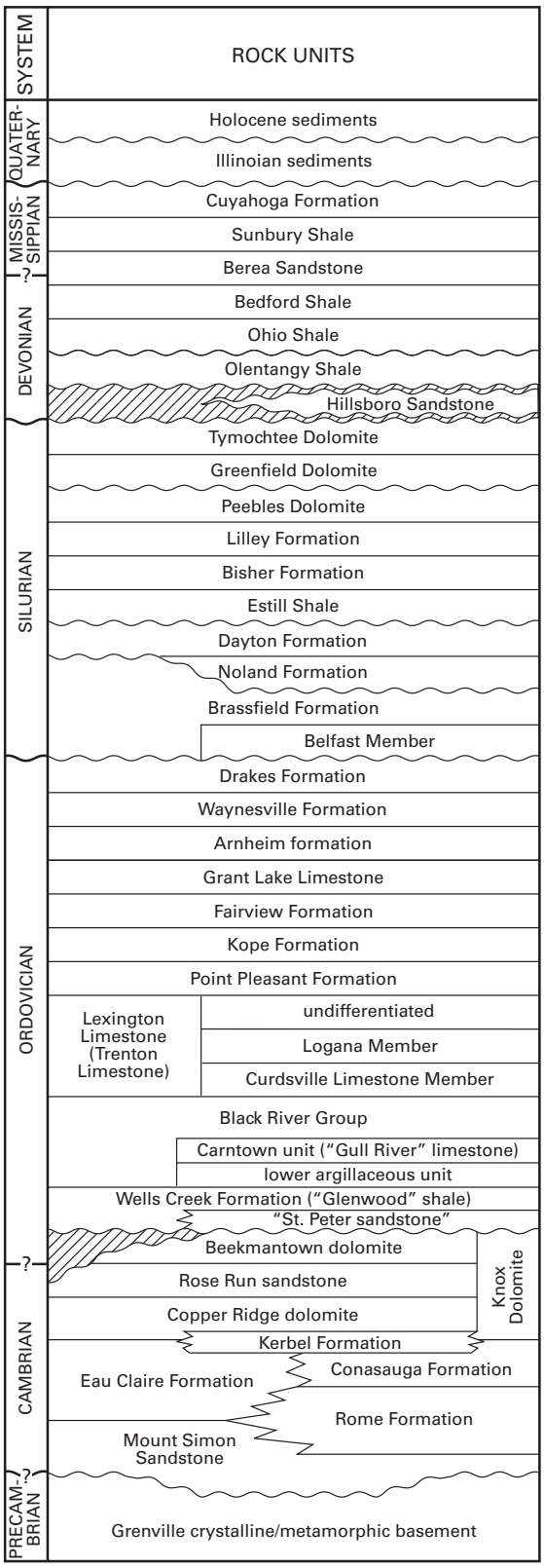

FIGURE 5.—Generalized stratigraphic nomenclature for surface and subsurface geologic units in southern Ohio in the vicinity of the Serpent Mound disturbance. Informal terms are shown in lower case. See Appendix B for generalized unit descriptions.

stone and Eau Claire, Rome, Conasauga, and Kerbel Formations and the Cambrian-Ordovician Knox Dolomite. These facies may be related to crustal movement along the Grenville Front. Locally, a paleotopographic high was present during Late Cambrian time in Adams and Highland Counties along a northwest-trending geophysical anomaly. Sporadic uplift (tectonic inversion) resulting in nondeposition and/or erosion began near the end of Rome Formation deposition, continued into Conasauga Formation deposition, and ended during deposition of the Knox Dolomite (see fig. 25). During Early? to Middle? Ordovician time, the regional Knox unconformity was formed by extensive erosion of an emergent carbonate platform (Riley and others, 1993). The local paleotopographic high in Adams and Highland Counties was removed by erosion prior to deposition of the Middle Ordovician Carntown unit of the Black River Group. Paleotopography on the Knox Dolomite in the area of Ohio reached a maximum of 45 meters (Janssens, 1973).

Tropical seas returned to the Ohio region in the latter part of Middle Ordovician time and inundated the subsiding Knox platform. The "St. Peter sandstone" and the Wells Creek Formation were deposited on the regional Knox unconformity. Shallow marine sedimentation continued through Middle and Late Ordovician time, depositing approximately 500 meters of subtidal to supratidal limestone and shale of the Black River Group through the Drakes Formation.

After deposition of Drakes Formation sediments, sea level dropped and land again emerged. An unconformity developed in Late Ordovician-Early Silurian time owing to regional uplift of the eastern North American craton, coupled with the vast continental glaciation in the southern hemisphere (Dennison, 1976; Hambrey, 1985; Ettensohn, 1991).

By Silurian time, the seas had returned, repeatedly flooding and retreating from the coastal lowlands on the western flank of the Appalachian Basin (McDowell, 1983; Gordon and Ettensohn, 1984). In Ohio, lagoonal, intertidal, and shallow marine carbonates and shales of the Brassfield Formation through the Tymochtee Dolomite accumulated on a series of carbonate ramps as seas migrated back and forth across Ohio. Local and regional unconformities developed on the tops of the Brassfield Formation, the Dayton Formation, the Peebles Dolomite, and the Tymochtee Dolomite as erosion or nondeposition occurred with each marine regression (Rexroad and others, 1965; Kleffner, 1987; Kleffner and Ausich, 1988).

At the close of the Silurian, regional uplift associated with the beginning of the Acadian Orogeny drained the seas from southern Ohio (Ettensohn 1985, 1987; Scotese and McKerrow, 1990). Caves and sinkholes developed on the emergent Silurian carbonate rocks in Early to Middle Devonian time (Kahle, 1988; Court and Kahle, 1993). Fine-grained eolian sands of the Middle Devonian (?) Hillsboro Sandstone accumulated as cavity fillings or as locally restricted bedded sandstone overlying the Silurian carbonate rocks (Carman and Schillhahn, 1930; Summerson and Swann, 1970).

During Late Devonian time, tropical seas again inun-

dated the region. Southern Ohio subsided into a foreland basin that developed west of the Catskill Mountains of eastern New York (Ettensohn 1992; Pashin and Ettensohn, 1995). In Late Devonian time, the basin became partially restricted and the Upper Devonian Olentangy and Ohio Shales were deposited. The Upper Devonian-Lower Mississippian Bedford Shale and Berea Sandstone represent the progradation of eroded sediments of the Catskill Delta into southern Ohio (Pashin and Ettensohn, 1995). An Early Mississippian marine transgression resulted in the deposition of the Sunbury Shale, followed by delta progradation and deposition of the Cuyahoga Formation as a result of renewed mountain building in eastern North America (Pashin and Ettensohn, 1995). Rocks younger than the Mississippian-age Cuyahoga Formation have not been identified within the Serpent Mound disturbance, and the thickness of post-Cuyahoga sedimentary rocks at the time of formation of the disturbance is unknown.

Undisturbed Pleistocene-age sediments have been mapped in the northwestern portion of the disturbance (Reidel, 1975; Goldthwait and Van Horn, 1993), indicating that the Serpent Mound disturbance is older than the Illinoian glacial stage of the Pleistocene Epoch. Holocene-age alluvium and colluvium of variable thickness and soils generally less than 1.5 meters thick (Williams and others, 1977; Lucht and Brown, 1994) blanket much of the bedrock in area of the Serpent Mound disturbance.

CORE AND OIL AND GAS WELL DATA

Cores, cuttings from oil and gas wells, geophysical logs, and well-sample descriptions were examined in order to compare and correlate undeformed units outside the Serpent Mound disturbance with deformed strata inside the disturbance. Each available core in the area was examined to look for significant variations in lithostratigraphy, the presence of breccia, and structural deformation outside the known limits of the disturbance. The location of the cores and oil and gas wells is shown in figure 1; more detailed information on the drill holes is given in table 1. The cores, well cuttings, geophysical logs, and sample descriptions used in this study are stored at the Ohio Division of Geological Survey.

The condition of the cores ranged from excellent to poor; some intervals had been damaged by water, rodents, insects, plants, etc. Prior to examination and logging, an attempt was made to match the tops and bottoms of cores in each box with core tops and bottoms in adjacent boxes. However, none of the cores were marked with orientation lines indicating the up direction and in a few instances tops and bottoms within a core box could not be determined. Drillers' blocks generally placed at intervals of about 3 or 4.6 meters were missing in portions of some boxes.

CORE EXAMINATION PROCEDURES AND TERMINOLOGY

Detailed core descriptions were prepared using a checklist (Appendix C) generated, in part, using the methodology of Kulander and others (1990). A protractor was used to measure the relative orientations of bedding planes, faults, and fractures. All angles were measured from the horizontal (perpendicular to the core length). For example, a fault and a bedding plane might be recorded as a 60° fault oblique to beds dipping 30°. The true strike-dip orientations of planar features with respect to north is not known because the cores were not oriented. Dips reported for planar features and bed thicknesses are "apparent." Most measured fault-plane surfaces were small scale and had minor offsets, at least partly because of the small size of most of the cores.

Breccia terminology used for meteorite-impact rocks (see Pilkington and Grieve, 1992; Anderson and others, 1996) has not been used in this report primarily because insufficient information on Serpent Mound breccias is available to use impact-breccia classification with certainty. For example, small black clasts discovered during the petrographic examination of core samples may be impact-melt clasts, but these clasts are highly altered and their origin is far from established. It is essential when using impact-breccia terminology to know whether melt-rock clasts are present in the rock before assigning a name to the specimen. Furthermore, impact-breccia terminology is still controversial (Witzke and Anderson, 1996, p. 141) and does not adequately describe all impact breccias.

The Peebles and Knox Dolomites are known to contain breccias formed by karst, sedimentary, and soil-forming processes (Dolly and Bush, 1972; Mussman and Read, 1986; Kahle, 1988; Court and Kahle, 1993; Potter, 1996). Breccias resulting from tectonic stresses also may be present. Impact, sedimentary, and tectonic breccia types cannot be systematically differentiated at this time.

Numerous large fault blocks of coherent rock were penetrated by the drill bit in cores DGS 3274 and 3275. These blocks range in size from slightly larger than the core diameter to tens of meters in estimated thickness when measured along the core length. The lateral extent of these blocks is unknown, but the haphazard arrangement, association with breccias, presence of folding, and anomalous stratigraphic position indicate these blocks moved from their original stratigraphic position during the formation of the Serpent Mound disturbance. Thus, the term "block" as used in this report denotes rock units or clasts larger than the core diameter that the authors believe have been moved from their original structural position.

In the megascopic study of the cores, two major types of breccias were observed on the basis of the dominant clast lithology. The first type of breccia has one dominant clast lithology (70 percent or more of sample) and is referred to in this report by the dominant clast lithology, for example, limestone-clast breccia or shale-clast breccia (fig. 6). The clasts and matrix are derived from adjacent lithostratigraphic units and have not moved far (millimeters to meters) from the present-day position of the parent rock. However, the parent rock may be a large **allochthonous** block that has moved an unknown distance. These breccias also may be **cataclastic**.

The second type of breccia contains multiple clast lithologies and in some instances multiple lithostratigraphic units and has the appearance of minor to significant structural movement from the original to final clast position. This type is termed a mixed-lithic breccia (fig. 7).

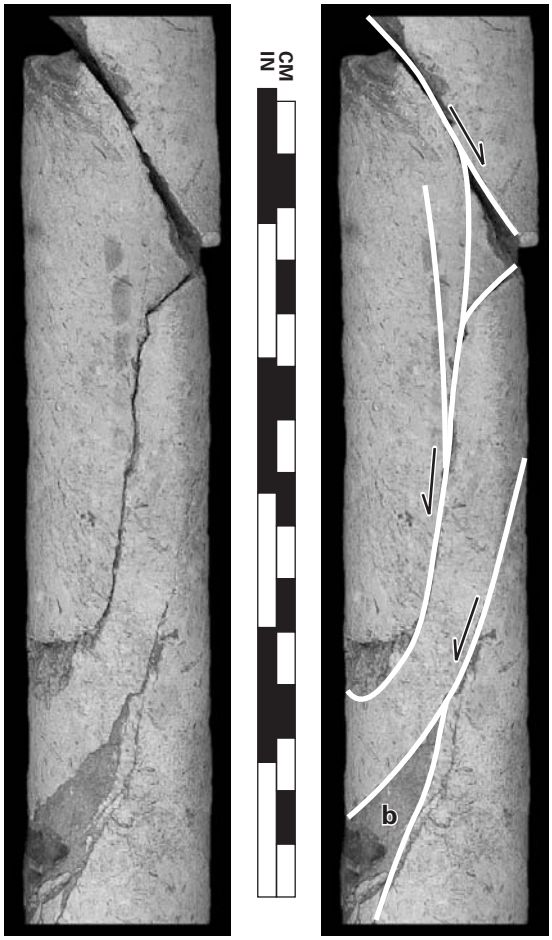

FIGURE 6.—Limestone-clast and shale-clast breccia along normal faults from core DGS 3274. ***Please note***—for all core photos in this report, two images are provided: an uninterpreted image on the left and an interpreted image on the right. Lines on interpreted image indicate faults and arrows indicate relative direction of fault movement. Small triangular-shaped area (**b**) in lower part of core section is shale-clast breccia. DGS 3274, box 135, 1,255 feet (382 meters), Ordovician Lexington Limestone.

DATA BEYOND THE BOUNDARY OF THE SERPENT MOUND DISTURBANCE

The Kessler well (fig. 1; table 1) was drilled in Perry Township, Pike County, in the winter of 1921-22 less than 1.6 km (1 mile) from the northeast boundary fault mapped by Reidel (1975). This well reached a depth of 547 meters. Oil and gas shows from the Kessler well were not reported, but a description of cuttings from this well indicates an anomalous black shale and quartz sandstone in the Ordovician Black River Group.

The Tira well was a dry hole drilled in 1939 in Franklin Township, Adams County, about 3 km (2 miles) beyond the eastern edge of the disturbance. This well reached a depth of 659 meters. The sample descriptions for this well did not indicate any structural or lithologic anomalies.

The Russell/Tener well was drilled in 1979 in Franklin Township, Adams County, about 0.8 km (0.5 mile) beyond Reidel's (1975) eastern boundary of the Serpent Mound disturbance. This well was drilled into the Precambrian to a depth of 1,184 meters and was part of a regional exploration play (K. Smith, Oxford Oil Company, personal commun., 1997). A gas show was reported in the Lexington Limestone (Trenton), and well cuttings suggest 61 meters of pre-Mount Simon arkose (?) is present. Stratigraphic thicknesses in the Russell/Tener well were used for comparison with thicknesses inside the Serpent Mound disturbance. A **density log** from this well was used to compute **acoustic impedance** and to produce a **synthetic seismogram** for the interpretation of data from seismic lines SM-1 and BV-1-92 (see pls. 2, 3).

As part of a statewide geologic mapping program, the Division of Geological Survey drilled core DGS 2626 in 1987 in Concord Township, Highland County, about 19 km (11.8 miles) west and updip from the center of the Serpent Mound disturbance. The core and geophysical logs from this site were used to determine thicknesses of shallow (Silurian and Ordovician) strata in the region outside the Serpent Mound disturbance. Samples of hematitic limestone from undeformed strata of the Silurian Brassfield Formation from this core were used for paleomagnetic analysis (Watts, in press).

The Smith well was an exploratory oil and gas well drilled in 1979 in Rarden Township, Scioto County, about 14 km (8.7 miles) southeast of the center of the structure. This well was drilled to a depth of 1,351 meters and penetrated Precambrian crystalline rocks; it is the deepest well drilled in the vicinity of the Serpent Mound disturbance. The Smith well served as a control standard for shallow and deep strata outside the disturbance.

Three shallow cores, DGS 2719, 2806, and 2947, were drilled 15 km (9.3 miles) or less northeast of the central uplift. Core DGS 2719 was drilled in Adams County in 1980 for mineral exploration purposes, core DGS 2806 was drilled in Pike County in 1980 for oil shale potential, and core DGS 2947 was drilled in Pike County in 1961 for a stratigraphic test related to oil and gas exploration. Examination of these cores did not reveal evidence of any significant stratigraphic or structural anomalies.

The drill-hole information from outside the Serpent Mound disturbance was used to estimate the regional dip and thickness of rock strata prior to formation of the disturbance. Although the cores were not oriented and drillers' records or surveys indicating borehole inclination do not exist, both the cores and subsequent measurements were assumed to be vertical. The true thickness of dipping beds was calculated using standard trigonometric methods (Appendix C) to increase our confidence in borehole verticality, to verify thickness of lithostratigraphic units, and to aid in structural interpretation. The calculated thicknesses of units within the Serpent Mound disturbance were compared to thicknesses of corresponding units in nearby undisturbed areas (table 3).

The regional subsurface dip on the top of the Carntown unit of the Black River Group between core DGS 2626 and the Russell/Tener well is about 6.2 meters/km (33 feet/mile) to the east. Dip on the Carntown unit increases east of the Russell/Tener well toward the Smith well to about 10.7 meters/km (57 feet/mile). The structure map on the

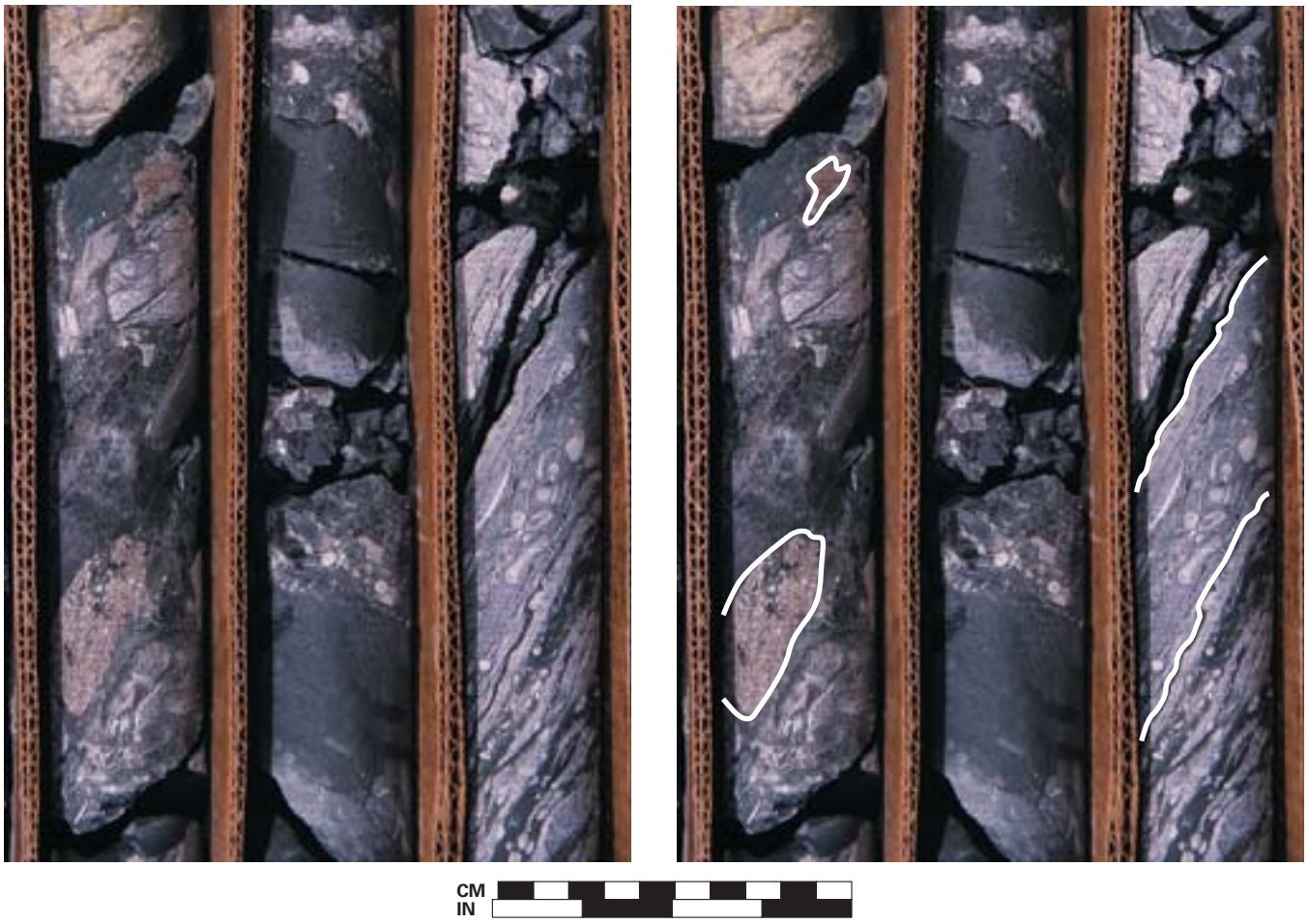

FIGURE 7.—Mixed-lithic breccias from middle highly brecciated interval of core DGS 3274 showing clasts of Ordovician shale and limestone, clasts of red-orange hematitic limestone (outlined in white on right-center core section) of the Brassfield Formation (Silurian), faulting, and variable apparent bedding dip. White lines on core section on far right indicate dipping bedding laminae in a large clast. DGS 3274, box 165, 1,523.5 feet (464 meters) to 1,529 feet (466 meters).

Knox unconformity of Baranoski and Riley (1993) indicates a similar increase in dip east of the Russell/Tener well. Swinford (1985, p. 227) noted an increase in dip from 6-8 to 10-11 meters/km (32 to 58 feet/mile) on rocks exposed at the surface south of the Serpent Mound disturbance and attributed the increase to a northeast-trending monocline. Swinford (1985, p. 228) suggested that the structures observed at the surface in the area were controlled by the Precambrian basement.

DATA WITHIN THE BOUNDARY OF THE SERPENT MOUND DISTURBANCE

Two oil and gas wells have been drilled in the central uplift of the Serpent Mound disturbance, in Bratton Township, Adams County. The Parker well (fig. 1; table 1) was drilled in late 1921 and reached a total depth of 465 meters. An oil show was reported at 338 meters in the Upper Ordovician shales. The sample description for the Parker well indicates brecciated carbonate lithologies. The stratigraphic tops of the Brassfield Formation and the Lexington Limestone in this well are higher than expected. The Kaeser well was drilled in 1973 and reached a total depth of 536 meters without reported oil or gas shows. John Simpson (personal commun., 1997) of the Simpson Oil Company chose the highest topographic location on the central uplift for the location of the Kaeser well on the basis of his work with productive piercement shale domes in other parts of the country. Simpson's prospect involved a model that speculated on the presence of structurally high Rose Run sandstone, an informal unit in the Knox Dolomite, within the central uplift. The well did not penetrate the Knox and was abandoned because of mechanical problems. Sample cuttings from this well show possible breccia lithologies.

Five continuous cores have been drilled in the Serpent Mound disturbance searching for economic mineral deposits. In 1971, Cominco American, Inc., drilled three core holes, each less than 152 meters in length, into the outer ring graben in Brush Creek Township, Highland County. These cores later were donated to the Survey and were designated

TABLE 3.—*Thickness of stratigraphic units from cores, geophysical logs, well cuttings, and sample descriptions examined in this investigation*[1]

Core no./well name and permit no.		DGS 2626/Goins	DGS 2880/ Humphrey 8	DGS 2280	DGS 2881/ Humphrey 9	DGS 2881	DGS 2882/ Adams/Shoemaker 10	DGS 2882	DGS 3274/ Brown 12	DGS 3274
Structural location		outside disturbance	ring graben	rotated[2]	ring graben	rotated[2]	ring graben	rotated[2]	central uplift	rotated[2]
Approximate length of missing core		0	13 ft (4 m)		0		14 ft (4 m)		270 ft (82 m)	
Stratigraphic unit	Berea Sandstone									
	Bedford Shale									
	Olentangy and Ohio Shales undivided									
	Tymochtee and Greenfield Dolomites undivided									
	Peebles Dolomite		22 ft (7 m)		29 ft (9 m)		45 ft (14 m)			
	Lilley and Bisher Formations undivided	23+ ft (7+ m)[3]	84 ft (26 m)	84 ft (26 m)	89 ft (27 m)	84 ft (26 m)	89 ft (27 m)	86 ft (26 m)		
	Estill Shale	89 ft (27 m)	112 ft (34 m)	110 ft (34 m)	115 ft (35 m)	111 ft (34 m)	118 ft (36 m)	116 ft (35 m)		
	Dayton, Noland, and Brassfield Formations undivided	37 ft (11 m)	37+ ft (11+ m)	37+ ft (11+ m)	60+ ft (18+ m)	49+ ft (15+ m)	18+ ft (5+ m)	17+ ft (5+ m)		
	Drakes Formation	26 ft (8 m)								
	Waynesville Formation and Arnheim formation undivided	236 ft (72 m)								
	Grant Lake Limestone	98 ft (30 m)							[4]	[4]
	Fairview Formation	100 ft (30 m)							[4]	[4]
	Kope Formation	260 ft (79 m)							[4]	[4]
	Point Pleasant Formation	117 ft (36 m)							[4]	[4]
	Lexington Limestone	202 ft (62 m)							290 ft (89 m)	222 ft (68 m)
	Black River Group	505 ft (154 m)							[4]	[4]
	Wells Creek Formation	18+ ft (6+ m)							[4]	[4]
	Knox Dolomite								[4]	[4]
	Kerbel Formation									
	Conasauga Formation									
	Rome Formation									
	Mount Simon Sandstone									
	Precambrian									

TABLE 3.—*Thickness of stratigraphic units from cores, geophysical logs, well cuttings, and sample descriptions examined in this investigation*[1] (cont.)

	Core no./well name and permit no. Structural location Approximate length of missing core	DGS 3275/ McCleese 13 transition zone 89 ft (27 m)	DGS 3275 rotated[2]	DGS 2719/ Justice outside disturbance 0	DGS 2947/ Attinger 21 outside disturbance 0	DGS 2806/ Hatfield outside disturbance 0	NA/Russell/ Tener 11 outside disturbance NA	NA/ Smith 257 outside disturbance NA
Stratigraphic unit	Berea Sandstone							107 ft (33 m)
	Bedford Shale			17+ ft (5+ m)		114- ft (35- m)		59 ft (18 m)
	Olentangy and Ohio Shales undivided			301 ft (92 m)	69+ ft (21+ m)	317 ft (97 m)		407 ft (124 m)
	Tymochtee and Greenfield Dolomites undivided			3+ ft (1+ m)	20 ft (6 m)	4+ ft (1+ m)		[4]
	Peebles Dolomite	101+ ft (31+ m)	81 ft (25 m)		[4]			[4]
	Lilley and Bisher Formations undivided	102 ft (31 m)	77 ft (23 m)		156- ft (48- m)		214- ft (65- m)	197- ft (60- m)
	Estill Shale	104 ft (32 m)	100 ft (30 m)		51 ft (16 m)		124 ft (38 m)	137 ft (42 m)
	Dayton, Noland, and Brassfield Formations undivided	63 ft (19 m)	52 ft (16 m)		104 ft (32 m)		83 ft (25 m)	95 ft (29 m)
	Drakes Formation	18 ft (6 m)	16 ft (5 m)		69+ ft (21+ m)		[4]	[4]
	Waynesville Formation and Arnheim formation undivided	[4]	[4]				230 ft (70 m)	222 ft (68 m)
	Grant Lake Limestone	[4]	[4]				104 ft (32 m)	108 ft (33 m)
	Fairview Formation	[4]	[4]				[4]	[4]
	Kope Formation	[4]	[4]				267 ft (81 m)	270 ft (82 m)
	Point Pleasant Formation	[4]	[4]				120 ft (37 m)	117 ft (36 m)
	Lexington Limestone	207 ft (63 m)	206 ft (63 m)				215 ft (66 m)	223 ft (68 m)
	Black River Group	501 ft (153 m)	499 ft (152 m)				502 ft (153 m)	522 ft (159 m)
	Wells Creek Formation	45 ft (14 m)	45 ft (14 m)				36 ft (11 m)	18 ft (6 m)
	Knox Dolomite	245+ ft (75+ m)	244+ ft (75+ m)				835 ft (255 m)	844 ft (257 m)
	Kerbel Formation						157 ft (48 m)	155 ft (47 m)
	Conasauga Formation						295 ft (90 m)	285 ft (87 m)
	Rome Formation						277 ft (84 m)	285 ft (87 m)
	Mount Simon Sandstone						119 ft (36 m)	132 ft (40 m)
	Precambrian						200+ ft (61+ m)	[4]

[1]See figure 1 for locations of cores and wells. DGS 2626, Russell/Tener 11, and Smith 257 are reference boreholes in which unit thicknesses are considered to be undeformed.

[2]"Rotated" indicates that bedding thickness has been rotated to the assumed predisturbance horizontal position. See Appendix C for trigonometric methods.

[3]Footages have been rounded to the nearest foot; + or - indicates that the values straddle adjacent stratigraphic units because units were not differentiated or that entire thickness of the unit was not drilled. See core descriptions on plate 1 for actual measured stratigraphic contacts.

[4]Unit contact could not be determined because of faulting or brecciation.

as DGS 2880, 2881, and 2882. Reidel (1972) determined that the iron and zinc content of these cores was less than 1 percent of the total constituents present. The rocks throughout the cores are mildly to moderately deformed, and deformation generally decreases with depth (see pl. 1).

In 1979, John L. Carroll Mineral Exploration drilled two core holes in Bratton Township, Adams County, to explore for possible mineral deposits deep in the structure. The first hole (core DGS 3274) was drilled within the central uplift to a depth of 903 meters. The second hole (core DGS 3275) was drilled about 1.8 km (1.1 miles) west of core DGS 3274 in the transition zone and reached a depth of 629 meters. Neither core penetrated units below the Knox Dolomite. Economic mineral deposits were not discovered in either core. John L. Carroll Mineral Exploration did not make company core descriptions available.

Division of Geological Survey geologists examined the two Carroll cores in detail in 1996. Some core intervals were found to be missing (91 meters in DGS 3274 and 25 meters in DGS 3275). Much of the missing core is thought to be either mineralized zones that John L. Carroll Mineral Exploration kept for detailed analysis or possibly bentonite beds that may have washed out in drilling. Specific details regarding faults, breccias, **shatter cones**, **slickenlines**, **stylolites**, mineralization, and other features can be found in the lithologic descriptions and graphic logs for cores DGS 3274, 3275, 2880, 2881, and 2882 on plate 1. A general discussion of cores DGS 3274 (including petrography and geochemical results) and 3275 is presented below.

Megascopic description of core DGS 3274

Reidel (1975) mapped undifferentiated Upper Ordovician rocks at the surface at the drill-site location for core DGS 3274. Approximately 30 meters north of the location for core DGS 3274, an east-west-trending curvilinear fault separates undifferentiated Ordovician rocks on the south from vertical and subvertical beds of the Silurian Estill Shale (Rochester Shale of Reidel, 1975) and Brassfield Formation on the north. Strike of the Silurian rocks is approximately north-south.

Core DGS 3274 (pl. 1) contains 903 meters of fractured, faulted, brecciated, and undeformed to severely deformed Upper Cambrian (?) to Upper Devonian limestone, shale, dolomite, and sandstone; 91 meters of core is missing. Breccias are common throughout the core. Lower and Middle Silurian, and Upper Devonian units are represented as clasts within mixed-lithic breccias and are not found as large discrete blocks. Stratigraphic units are repeated throughout the core (fig. 8), and there is no simple decrease in structural complexity with depth, as there is in cores DGS 2880, 2881, 2882, and 3275.

The fractures and faults in the core are generally small scale, less than several millimeters in width and several centimeters or more in length. Direction of movement and/or offset along faults is generally indeterminate because of poorly developed slickenlines or lack of offset strata. In some cases, breccia-filled fractures show laminations, flow structures (?), crude particle sorting, and/or possible oriented, elongated rock fragments, which are parallel or subparallel to the enclosing fracture or fault surfaces. In general, the matrix and the cement in the breccias are calcareous. Mineralized **anastomosing** fractures are present throughout both brecciated and unbrecciated core. Where stylolites are present, they are parallel or subparallel to bedding planes and are rarely observed at oblique to high angles to bedding. Slickenlines generally are developed parallel to subparallel with the dip of the fault surface and rarely perpendicular to the fault plane.

The megascopic examination of core DGS 3274 revealed a general lack of mineralization; it is possible that the 91 meters of missing core could have been mineralized. The little mineralization that is present includes disseminated and fracture-filling calcite and sulfides (pyrite and sphalerite). Lesser amounts of dolomite and glauconite were observed. Small accumulations of dark insoluble residue, possibly organic rich, were observed along stylolite surfaces and small slickenlined faults in the Lexington Limestone and Black River Group.

Shatter cones are abundant in core DGS 3274 (pl. 1; fig. 9). They appear as striated, fractured rock surfaces that have a conical shape in ideal form. In most instances, they have subplanar surfaces oriented at an oblique angle to bedding dips. They generally occur in well-indurated carbonates but also are found in shales. The shatter-cone surface may have a "smeared" light and dark texture/color as shown in figure 9A. The authors have observed similar shatter cones in Ordovician limestone slabs collected from the surface of the central uplift (fig. 9B). Shatter-cone surfaces can be confused with slickenlined faults, but the merging striae of shatter cones, in contrast to the parallel striae of slickenlines, can be used to distinguish them.

Cross-cutting relationships between mineral- and breccia-filled fractures and faults, shatter cones, and stylolites are present in core DGS 3274, particularly below 869 meters. Shatter cones were observed cutting through fractures as well as terminating against them, suggesting episodes of deformation before and after the formation of the shatter cones (fig. 10A). Faulting was observed to cut breccias (fig. 10B), and breccias were observed as fracture fillings (figs. 10C, 10D).

The authors have subdivided core DGS 3274 into four intervals (pl. 1; fig. 8): (1) an upper highly disturbed block interval from 3.4 to 432 meters, (2) a middle highly brecciated interval from 432 to 517 meters, (3) a middle moderately brecciated interval from 517 to 869 meters, and (4) a lower highly brecciated interval from 869 to 903 meters. The highly disturbed block interval is characterized by fault blocks of Ordovician carbonate containing internal faults and cataclastic brecciation. The large blocks commonly are separated by carbonate-clast breccias that have a minor shale-clast component. Moderately to highly deformed, folded, faulted, and brecciated beds of Lexington Limestone, Kope and Fairview Formations, and Grant Lake Limestone generally dip from 10° to 90°; some beds are overturned (figs. 11A, 11B).

The middle highly brecciated interval is characterized by faulted and moderately to severely brecciated rocks ranging in age from Middle Ordovician to Late Devonian. Discrete and complete lithostratigraphic units are absent

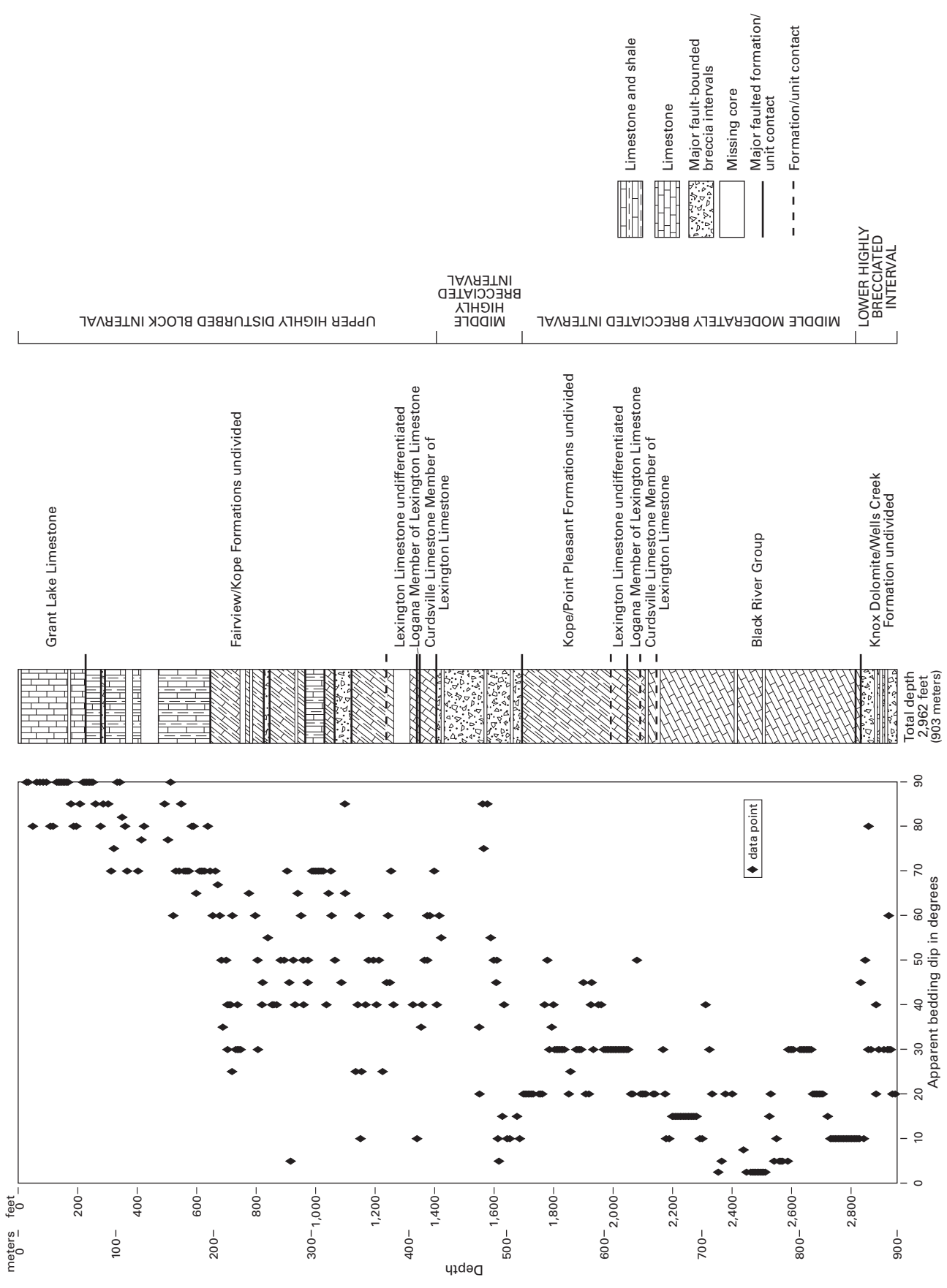

FIGURE 8.—Plot of apparent bedding dips and generalized lithostratigraphy for core DGS 3274. See plate 1 for more detail.

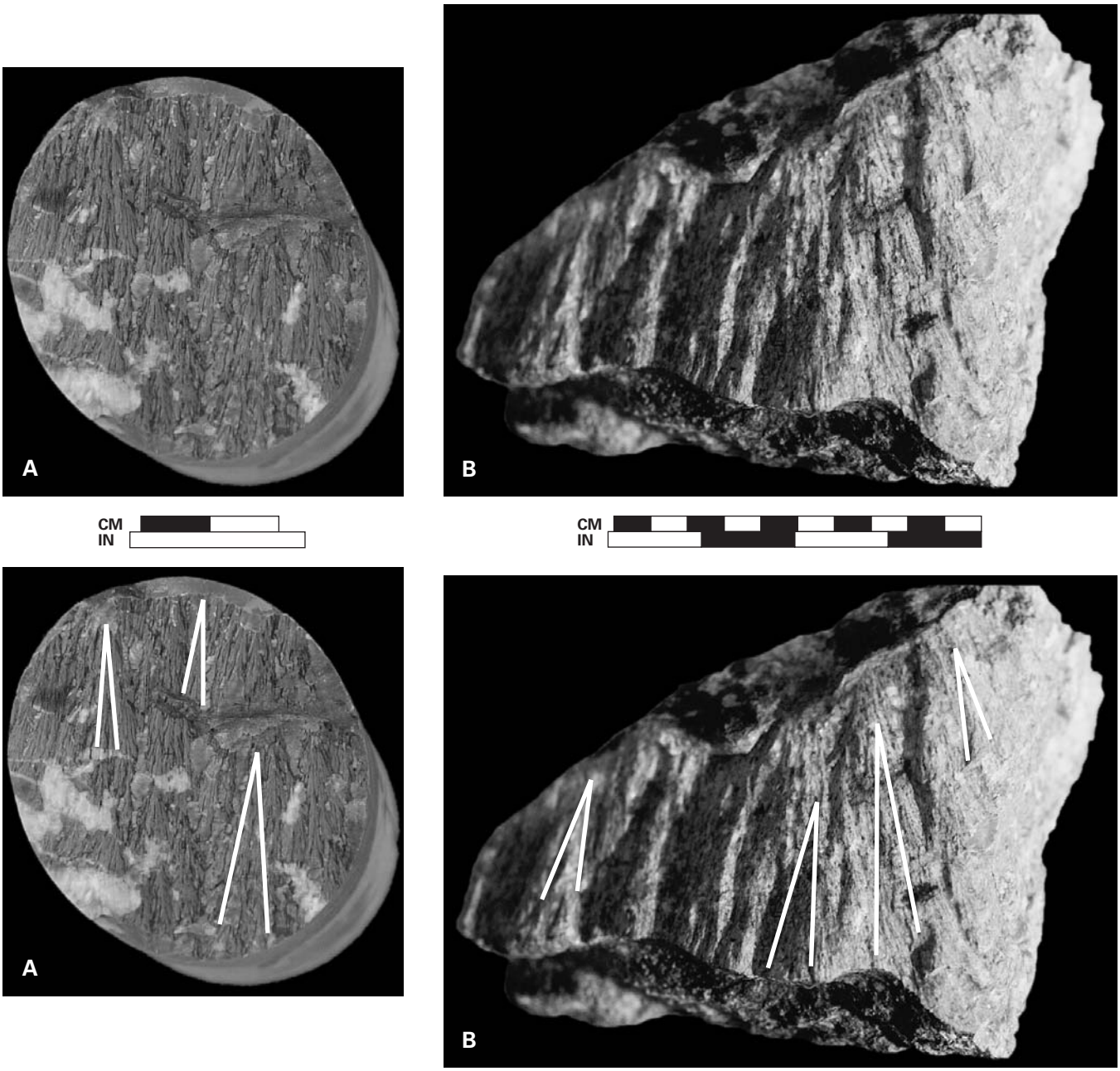

FIGURE 9.—Shatter cones in core and hand samples. A few of the apices on both figures are outlined in white. **A**, end view of core showing shatter cones along a planar surface that is dipping 30º from the horizontal relative to vertical core axis; note light and dark texture and relief. DGS 3274, box 296, 2,735 feet (833 meters), Ordovician Black River Group. **B**, shatter cones in a fresh, broken cobble of Ordovician limestone from a surface exposure in the central uplift of the Serpent Mound disturbance; note light and dark texture. Shatter cones in this sample are subparallel to bedding.

from this interval (pl. 1). Mixed-lithic breccias (fig. 12) dominate the entire interval, separated by large blocks and clasts of undeformed to highly deformed Lexington Limestone (Curdsville Limestone Member), Kope and Fairview Formations, Grant Lake Limestone, and Waynesville (?) and Drakes Formations. Folded beds, overturned strata, and beds dipping 10° to 85° are common.

The middle moderately brecciated interval is characterized by undeformed to moderately deformed Upper Ordovician carbonates and shales. The lower argillaceous unit and the Carntown unit of the Black River Group, the Curdsville Limestone Member and the Logana Member of the Lexington Limestone, and the Point Pleasant and Kope Formations are present in this interval and dip from 0° to 50° (pl. 1). Dips generally diminish with depth below 655 meters.

The lower highly brecciated interval consists of moderately to severely deformed, folded, faulted, and brecciated Wells Creek Formation and Knox Dolomite. Clasts of Rose Run sandstone and Copper Ridge dolomite (informal units within the Knox Dolomite) were tentatively identified. The

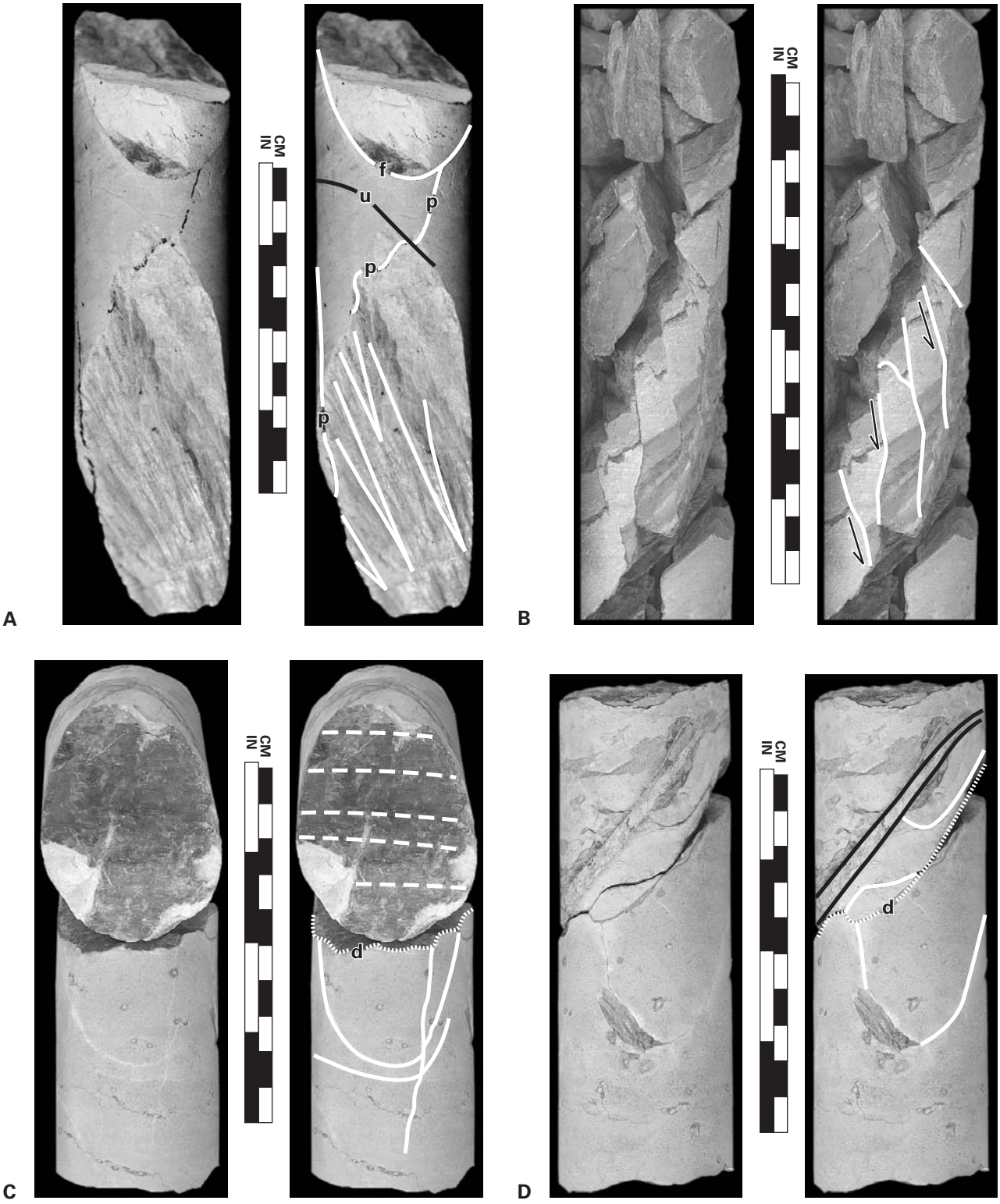

FIGURE 10.—Examples of multiple episodes of deformation from core DGS 3274. **A**, shatter cones (narrow **V**'s in lower portion of core section) cut across pyrite-filled pre-existing fracture (**p**). An unmineralized fracture (**u**) cuts across the core, and a breccia-filled fracture or fault (**f**) is at the top of the core section. DGS 3274, box 312, 2,897 feet (883 meters), Cambrian-Ordovician Knox Dolomite. **B**, en echelon normal faults in mixed-lithic breccia; vertical to subvertical lines indicate faults, arrows indicate relative direction of fault movement. DGS 3274, box 135, 930 feet (283 meters), Ordovician Fairview and Kope Formations undivided. **C**, longitudinal portion of core (bottom) shows faulting and calcite-filled fractures (indicated by solid lines). Cross-sectional portion of core (top) shows dark, irregular, faulted surface and slickenlines; (trend indicated by dashed lines). Area labeled **d** is a fault that also is seen in figure 10D. DGS 3274, box 300, 2,779 feet (847 meters), Ordovician Black River Group. **D**, same section as **C**, reassembled. White lines indicate faults; area labeled **d** is the same fault shown in figure 10C. Black lines indicate a breccia-filled fracture.

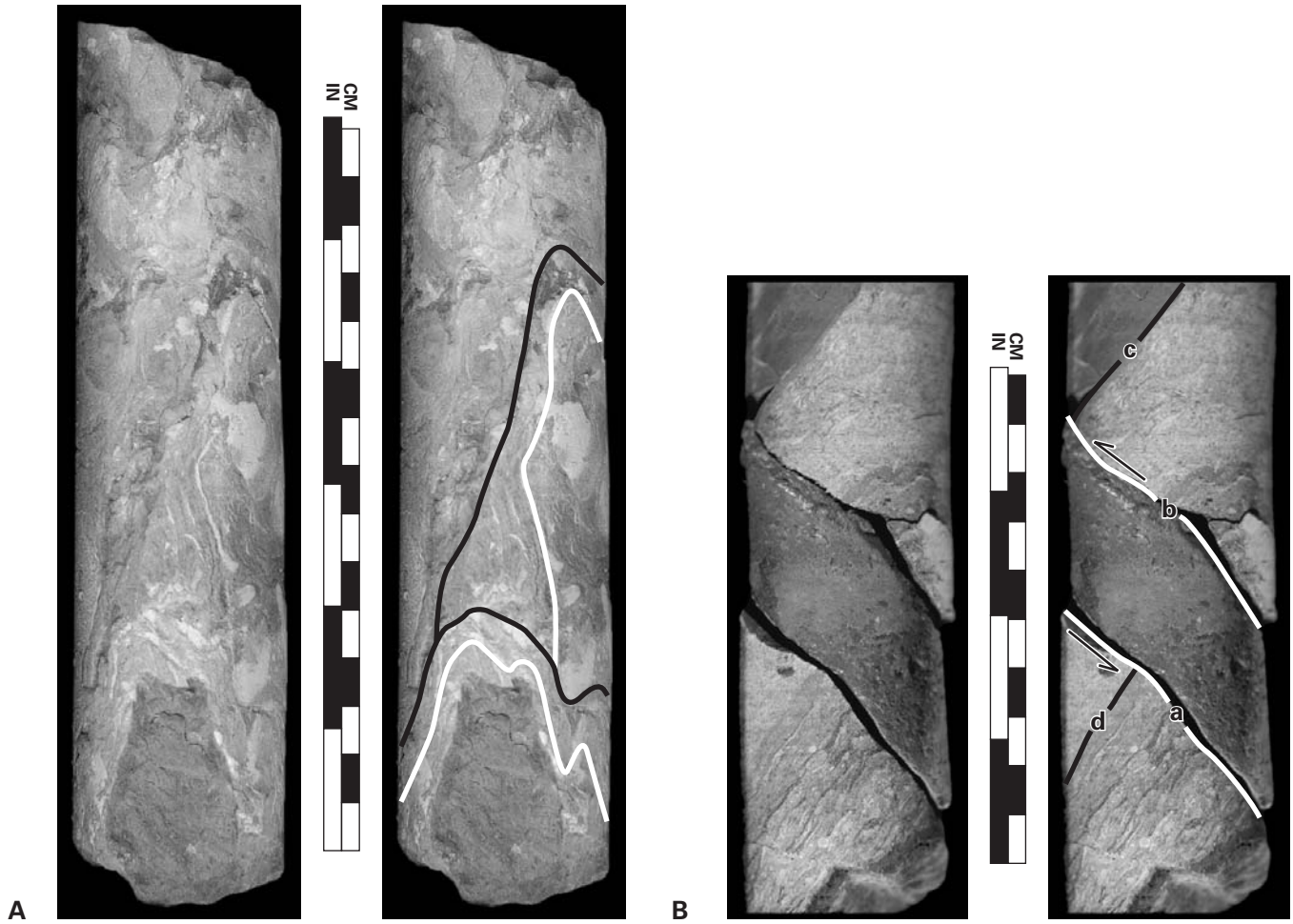

FIGURE 11.—Examples of the upper highly disturbed block interval of core DGS 3274. **A**, faulted and folded clasts of Ordovician Grant Lake Limestone from mixed-lithic breccia. White lines indicate folded bedding laminae; black lines outline clasts. DGS 3274, box 23, 223 feet (68 meters). **B**, reverse fault filled with breccia containing very small (less than 3 mm in diameter) shale and carbonate clasts and a few black impact-melt (?) clasts embedded in a very finely pulverized matrix. White lines (**a** and **b**) indicate faults, and arrows indicate relative direction of fault movement; black lines (**c** and **d**) indicate bedding laminae. DGS 3274, box 100, 922.5 feet (281 meters), Ordovician Fairview and Kope Formations undivided.

upper part of the Knox Dolomite is not present, and the lower contact with the underlying Kerbel/Conasauga Formation, if present, was not cored.

Mixed-lithic breccias are present throughout the lower highly brecciated interval and separate major blocks. Complete, unfaulted lithostratigraphic units are absent. Recognizable units occur as discrete, moderately to highly brecciated and fractured fault blocks. The contact between the Wells Creek Formation and the Black River Group is missing, as are the uppermost and lowermost portions of the Wells Creek Formation. Beds dip from 20° to 80°, folded beds are common, and small faults are rare.

Petrography of core DGS 3274

Twenty samples from core DGS 3274 were selected for petrographic examination (table 4; Appendix D). Because the Serpent Mound disturbance is considered by many geologists (Cohen and others, 1961; Dietz, 1960; Koeberl and Anderson, 1996) to be the result of an impact, a systematic petrographic search of core DGS 3274 was made for shock metamorphic features such as **planar deformation features** (PDF's) in quartz and altered impact-melt clasts. PDF's in quartz grains were discovered almost immediately in thin-sectioned samples of breccia (Carlton and others, 1998b). PDF's are discussed in more detail in the section on Origin of the Serpent Mound disturbance (p. 34). Consequently, a 15-cm section of mixed-lithic breccia (sample SM1-36) from the middle highly brecciated interval (438 meters) was prepared for grain-mount studies. Quartz grains containing PDF's from sample SM1-36 were sent to Christian Koeberl, University of Vienna (Austria), for confirmation and determination of crystallographic orientation of PDF's using a universal stage with four axes.

The entire length of core DGS 3274 penetrates sedimentary-clast breccias; clasts range in size from microscopic to

FIGURE 12.—Poorly sorted mixed-lithic breccia from core DGS 3274. The matrix is slightly calcareous. The breccia contains many green and gray shale and claystone clasts and gray limestone clasts. Box 155, 1,436 feet (438 meters).

large megascopic to fault blocks up to tens of meters thick. All but two of the thin-sectioned samples contain identifiable clasts and matrix material at the scale of a standard (27 by 46 mm) thin section. The two exceptions (samples SM1-15 and SM1-27) are samples of large clasts (chert and sandstone, respectively) that cover the entire area of the thin section. Most (15) of the samples are limestone-clast breccias having subordinate amounts of shale, claystone, sandstone, siltstone, chert, and possibly altered impact-melt(?) clasts. Three breccia samples (SM1-4, SM1-7, and SM1-13) contain more shale or claystone clasts than carbonate clasts, and one breccia (SM1-28B; fig. 13) contains mostly medium- to coarse-grained sandstone clasts. PDF's were identified in seven of the thin-sectioned samples (fig. 14) and in grain mounts from sample SM1-36. Most of the PDF's observed were in subangular quartz grains less than 90 micrometers in diameter from the upper 495 meters of the core. The PDF-bearing quartz grains resemble in size and shape sedimentary quartz grains from Devonian- and Mississippian-age sandstone, siltstone, and shale in outcrops near the Serpent Mound disturbance. Many of the quartz grains in sample SM1-36 in the very fine sand to silt size range contain PDF's. A maximum of six sets of PDF's per grain was observed. An analysis of 170 sets of PDF's that could be assigned with confidence to a rational crystallographic plane, out of 232 sets determined, show a maximum at the $\{10\bar{1}3\}$ orientation (fig. 15). PDF's were not observed in the quartz clasts of the Rose Run sandstone in core DGS 3274 or core DGS 3275.

In core DGS 3274, small black clasts ranging in size from less than 1 mm to more than 1 cm are present in small amounts in seven of the samples examined petrographically (SM1-16, SM1-23, SM1-25, SM1-28A, SM1-29A, SM1-33A, SM1-33B; table 4). The black clasts may be blocky and angular to moderately rounded (fig. 16). Under high magnification in transmitted light, the matrix is gray, cloudy, microcrystalline to cryptocrystalline carbonate filled with black opaque grains (pyrite?) 1 to 4 micrometers diameter. Larger inclusions of quartz and carbonate grains 30 to 150 micrometers in diameter occur within the black clasts. Similar dark material was observed filling fractures and faults (fig. 17). Meteorite impacts into sedimentary rocks, especially carbonate rocks, are thought to result in the creation of large amounts of gas (Kieffer, 1980). According to Grieve and Pilkington (1996), the abundance of volatiles causes increased alteration of impact-melt glasses to carbonate and hydrated phases. The black carbonate clasts in the breccias from the Serpent Mound disturbance may represent fragments of altered impact-melt rock (?), but additional work needs to be performed on these clasts before their identity can be certain.

Geochemistry of core DGS 3274

As part of this investigation, three samples (SM1-4, SM1-16A, SM1-16B) were sent to Christian Koeberl (University of Vienna, Austria) for major and trace element analyses by standard X-ray fluorescence (XRF) and instrumental neutron activation analysis (INAA) procedures (see Koeberl and Reimold, 1995, for procedural details). Sample SM1-4 is a mixed-lithic breccia. Sample SM1-16 is a breccia containing limestone clasts (host rock) that have dikelike fractures filled with a black, fine-grained matrix. The host rock (SM1-16B) and the black matrix material (SM1-16A) were analyzed separately.

One target of the analyses was iridium (Ir), which is several orders of magnitude more abundant in **chondritic** and iron meteorites than in Earth's crustal rocks. Chondritic meteorites contain about 400 to 800 parts per billion (ppb) Ir; the average Ir content of crustal rocks is about 0.02 ppb (Taylor and McLennan, 1985). Thus, if the Serpent Mound breccias were enriched in Ir compared to the carbonate-rich host rock, that enrichment would be considered good evidence for an impact origin. According to Koeberl and others (1998), the results of the analyses show the two breccias have a minor but significant enrichment in Ir; in particular, sample SM1-16A (black matrix) is enriched to 0.2 ppb compared to sample SM1-16B (host rock). This enrichment indicates a possible meteoritic component of about 0.05 percent.

Megascopic description of core DGS 3275

Reidel (1975) mapped undivided Silurian Tymochtee

TABLE 4.—*Major breccia intervals from core DGS 3274 and characterization of thin-sectioned samples*[1]

Major breccia interval in feet	Thickness in feet (meters)	Thin-section sample no.	Depth in feet (meters)	Breccia classification where determined	Clast description	PDF's present	Possible clasts of altered impact-melt rock(?) present
42.0-45.0	3.0 (0.9)						
82.0-84.0	2.0 (0.6)						
145.0-150.0	5.0 (1.5)						
220.0-225.3	5.3 (1.6)						
278.0-296.0	18.0 (5.5)						
476.8-477.4	0.6 (0.2)						
703.5-706.0	2.5 (0.8)						
831.0-849.0	18.0 (5.5)						
		SM1-07	960.9-961.1 (292.9)	claystone-clast breccia	98% claystone, 2% limestone		X
970.8-971.5	0.7 (0.2)			mixed-lithic breccia			
973.5-975.2	1.7 (0.5)			mixed-lithic breccia			
1050.0-1053.0	3.0 (0.9)						
1064.7-1065.5	0.8 (0.2)						
1069.5-1126.5	57.0 (17.4)			mixed-lithic breccia			
		SM1-09	1122.4-1122.6 (342.1-342.3)	limestone-clast breccia	90% limestone, 10% shale/claystone	X	
1134.5-1135.5	1.0 (0.3)						
1239.0-1240.0	1.0 (0.3)			mixed-lithic breccia			
1242.5-1243.5	1.0 (0.3)			mixed-lithic breccia			
1328.0-1337.0	9.0 (2.7)			mixed-lithic breccia			
		SM1-13	1348.8-1349.1 (411.1-411.2)	mixed-lithic breccia	60% shale, 40% limestone		X
1356.0-1360.0	4.0 (1.2)						
		SM1-15	1395.1-1395.5 (425.2-425.4)	cataclastic chert	clast in breccia		
1408.0-1412.5	4.5 (1.4)						
		SM1-16	1412.1-1412.6 (430.4-430.6)	limestone-clast breccia	97% limestone, 3% shale/claystone	X	X
1417.0-1696.5	279.5 (85.2)			mixed-lithic breccia			
		SM1-01A	1435.2-1435.5 (437.5)	mixed-lithic breccia	45% limestone, 35% shale/claystone, 20% dolomite	X	
		SM1-04	1435.8-1436.3 (437.6-437.8)	mixed-lithic breccia	65% claystone, 35% limestone	X	
		SM1-02	1623.6-1624.0 (494.8-495.0)	limestone-clast breccia	75% limestone, 25% shale/claystone	X	
1772.0-1774.0	2.0 (0.6)						
1806.6-1807.0	0.4 (0.1)						
1837.7-1838.8	1.1 (0.3)						
1873.0-1874.0	1.0 (0.3)						
1877.0-1878.3	1.3 (0.4)						
1899.5-1903.8	4.3 (1.3)						
1917.0-1919.3	2.3 (0.7)						
1927.0-1927.9	0.9 (0.3)						
2053.0-2054.5	1.5 (0.5)						
2071.6-2071.7	0.1 (0.03)						
2076.5-2077.1	0.6 (0.2)	SM1-03A	2076.5-2076.8 (632.9-633.0)	limestone-clast breccia	80% limestone, 20% shale/claystone		X
		SM1-03B	2076.5-2076.8 (632.9-633.0)	limestone-clast breccia	95% limestone, 5% shale/claystone		X
2078.0-2080.2	2.2 (0.7)						
		SM1-19	2290.3-2290.4 (698.1)	limestone-clast breccia	82% limestone, 15% breccia, 3% shale/claystone		X
2312.5-2314.7	2.5 (0.8)						

2385.0-2387.0	2.0 (0.6)	SM1-33A	2385.1-2385.5 (727.0-727.1)	limestone-clast breccia	97% limestone, 2% sandstone, 1% altered impact-melt rock(?)		X
		SM1-33B	2385.1-2385.5 (727.0-727.1)	limestone-clast breccia	98% limestone, 1% altered impact-melt rock(?), 1% breccia		X
2435.0-2437.0	2.0 (0.6)						
2468.0-2491.0	23.0 (7.0)	SM1-23	2480.4-2480.5 (756.0-756.1)	limestone-clast breccia	99% limestone, 1% altered impact-melt rock(?)		X
		SM1-21	2482.7-2482.9 (756.7-756.8)	limestone-clast breccia	100% limestone		
2545.7-2546.0	0.3 (0.1)						
2644.4-2644.8	0.4 (0.1)	SM1-25	2644.4-2644.7 (806.0-806.1)	limestone-clast breccia	99% limestone, 1% shale/claystone		X
2645.5-2645.7	0.2 (0.1)						
2806.0-2806.1	0.1 (0.03)			mixed-lithic breccia			
2819.0-2822.3	3.3 (1.0)					X	
2825.7-2826.8	1.1 (0.4)			mixed-lithic breccia	79% dolomite, 20% sandstone, 1% shale/claystone		
2851.7-2962.0	110.3 (33.6)	SM1-28A	2852.6-2852.9 (869.5-869.6)	dolomite-clast breccia			X
		SM1-28B	2852.6-2852.9 (869.5-869.6)	sandstone-clast breccia	81% sandstone, 18% dolomite, 1% claystone		
		SM1-27	2856.7-2856.9 (870.7-870.8)	cataclastic sandstone			
		SM1-29A	2870.6-2871.0 (875.0-875.1)	mixed-lithic breccia	55% dolomite, 25% shale/claystone, 20% sandstone		X

[1]See Appendix D for detailed descriptions of samples.

Dolomite, Greenfield Dolomite, and Peebles Dolomite at the surface at the drill-site location for core DGS 3275. Reidel also mapped three faults within 100 meters of the core site; these faults trend north 15° west, north 80° west, and north 50° east. An extensively brecciated outcrop at an abandoned quarry in Silurian-age dolomite is located about 90 meters east of the drill site.

Core DGS 3275 (pl. 1) penetrates 629 meters of fractured, faulted, brecciated, and undeformed to severely deformed strata (table 5). These strata range in age from Late Cambrian (?) to Middle Silurian and consist primarily of limestones, shales, dolomites, and sandstones. The authors have subdivided core DGS 3275 into three intervals: (1) an upper moderately deformed interval from 5 meters to 126 meters; (2) a middle highly brecciated interval from 126 meters to 221 meters, and (3) a lower, relatively undeformed interval from 221 meters to 629 meters. There is marked decrease in degree of deformation downward; this decrease is reflected in the decreasing bed dips (fig. 18).

The upper interval consists of moderately deformed and brecciated rocks of the Drakes, Brassfield, Noland (?), and Dayton Formations, Estill Shale, Bisher and Lilley Formations, and Peebles Dolomite. Beds dip from 15° to 50° (pl. 1). Minor small-scale faults, fractures, and breccias are present throughout the interval. Fractures are filled with breccia or mineralized with calcite. Shatter cones, **en echelon tension gashes**, anastomosing fractures, and multiple directions of movement on slickenlined surfaces are rare. The Peebles Dolomite in particular has abundant asphaltic material disseminated in the breccia matrix and filling vugs, pore spaces, and anastomosing fractures.

The middle highly brecciated interval contains moderately to severely deformed, faulted, and brecciated strata of the Kope and Fairview Formations, Grant Lake Limestone, and Arnheim and Waynesville Formations. This interval consists of a chaotic assemblage of rock strata broken into fragments from sand size to blocks tens of meters or more in diameter (as measured along the core length). Some of the blocks have been complexly faulted and folded (fig. 19). Beds dip 20° to 90° (figs. 19, 20). Normal and reverse faults are common, but shatter cones, stylolites, and slickenlines are rare.

The lower interval is moderately deformed to undeformed and only mildly faulted and brecciated. This interval consists of the Knox Dolomite (including the Rose Run sandstone and Copper Ridge dolomite), Wells Creek Formation, Black River Group, Lexington Limestone (Lexington undifferentiated and Curdsville Limestone and Logana Members), and undifferentiated Point Pleasant and Kope Formations. Bedding dips diminish below 221 meters and range from 0° to 20° (fig. 18). Minor, small-scale faults and breccia (figs. 20, 21) are present throughout the interval. Folded strata are rare, as are shatter cones, en echelon tension gashes, anastomosing fractures, and slickenlines having multiple directions of movement.

Only six thin sections were made from core DGS 3275. Three of the thin sections were from large carbonate clasts that covered the entire surface of the thin sections. No PDF's were expected in these thin sections. The fourth thin section was from a chert clast that covered the entire thin- section

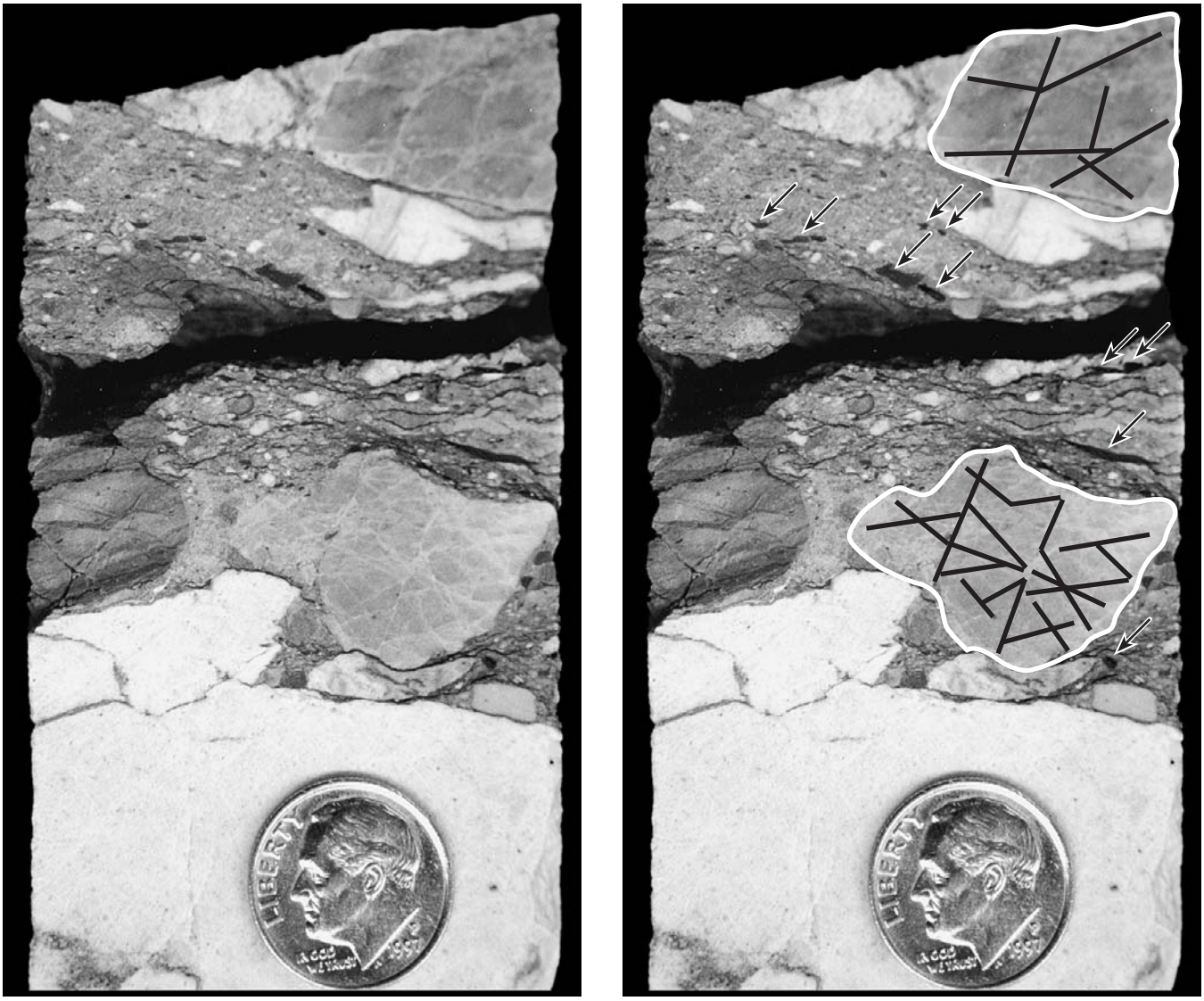

FIGURE 13.—Sandstone-clast breccia from core DGS 3274. Conjugate fractures are faintly visible in the large, noncalcareous, fine- to medium-grained, subrounded sandstone clast on which the coin lies at bottom of photo. Conjugate fractures (black lines) are very pronounced in the calcareous gray dolomite clasts (outlined in white). Many smaller clasts of shale, sandstone, and carbonate as well as a few black impact-melt (?) clasts (arrows) are visible. Sample SM1-28B, box 308, 2,853 feet (870 meters). U.S. dime gives scale.

surface. The other two thin sections were from sandstone clasts that covered the entire thin-section surface. The chert and sandstone thin sections were examined for PDF's but none were found. The chert and sandstone thin sections were made from samples taken near the bottom of the core, where PDF's were less likely to occur.

GEOPHYSICAL DATA

SEISMIC REFLECTION PROFILES AND REPROCESSING

Two seismic reflection profiles across the Serpent Mound disturbance were interpreted for this report. Seismic profile SM-1, acquired by Columbia Natural Resources in 1989, followed Ohio Route 41 and crossed through the transition zone and ring graben along the eastern part of the disturbance (see fig. 22). Seismic profile BV-1-92, acquired by Paragon Geophysical Corporation in 1992, began at Ohio Route 73, crossed the central uplift of the disturbance in a sinuous northeasterly direction, and ended at Ohio Route 41. Data-processing techniques were used to account for the location of the sources and receivers along a winding road. Some of the structures imaged on the seismic profiles may represent reflections from features out of the plane of the profile (sideswipes). A sideswipe also may be caused by

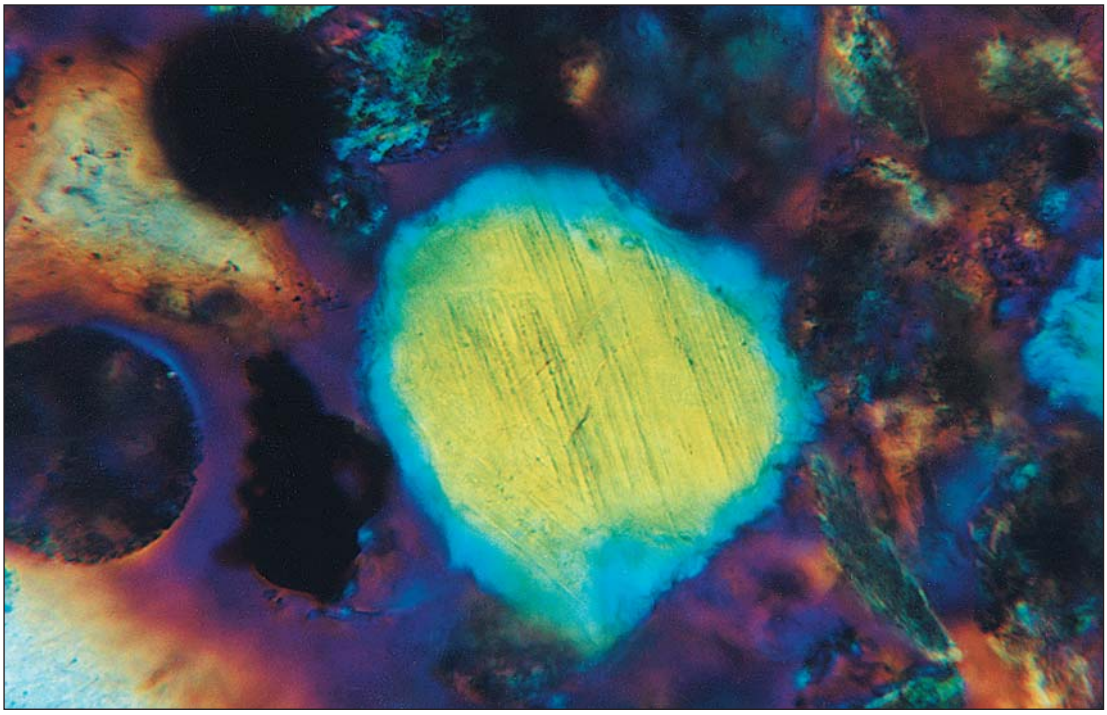

FIGURE 14.—Photomicrograph of sedimentary quartz grain (center of photo) in sample SM1-36C from core DGS 3274 (1,439 feet/439 meters) showing PDF's, which appear as dark lines within the grain. The quartz grain is 104 micrometers in diameter. The grain-mounted thin section was photographed in transmitted light with gypsum plate and crossed nicols.

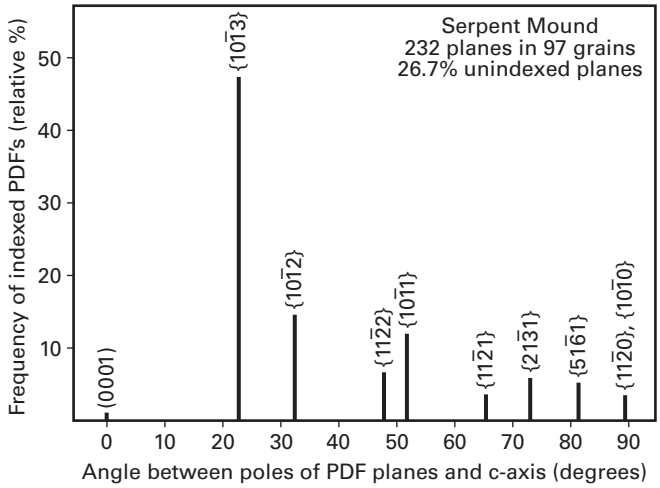

FIGURE 15.—Histogram of angles between poles of the PDF planes in quartz and the C-axis. Modified from Carlton and others (1998b).

diffractions—seismic waves produced by the interaction of the seismic source signal and abrupt lateral discontinuities such as faults or breccia zones.

Baranoski (1993) reported on the original processed seismic data from BV-1-92 and SM-1 and outlined the general stratigraphic and structural features of the Serpent Mound disturbance. In 1996, the seismic data for both SM-1 and BV-1-92 were reprocessed at the University of Glasgow (Scotland). The sections resulting from the reprocessing and details of the processing steps are shown on plates 2 and 3. For both seismic sections, the vertical axis is displayed as two-way travel times in milliseconds (ms; 10^{-3} second), rather than as calculated depths, because of the considerable uncertainty in the velocity of the seismic waves. The chaotic nature of the rocks in the Serpent Mound disturbance and severe faulting are major factors in this uncertainty.

Reflectors on the SM-1 and BV-1-92 profiles were matched with stratigraphic units using a synthetic seismogram computed from the geophysical log for the Russell/Tener well; the synthetic seismogram is included on plates 2 and 3. Only a density log was available for the Russell/Tener well, and assumptions had to be made on the relationship between the density of the rocks and the velocity of sound energy in order to calculate the reflectivity of the rock layers. The Russell/Tener well projects onto the SM-1 profile at about station 174.

The SM-1 seismic profile (pl. 2) shows a broad faulted depression and a faulted **ring anticline**(?) at the north and south ends of the line. The anticline on the south end of the profile is associated with steeply dipping reverse faults that appear to extend into the basement. A curvilinear anticline crossing Ohio Route 41 about 1 km (0.6 mile) south of Sinking Spring (see Reidel, 1975) may be a surface expression of a smaller anticline noted on the north end of the SM-1 profile.

Using the synthetic seismogram generated from the

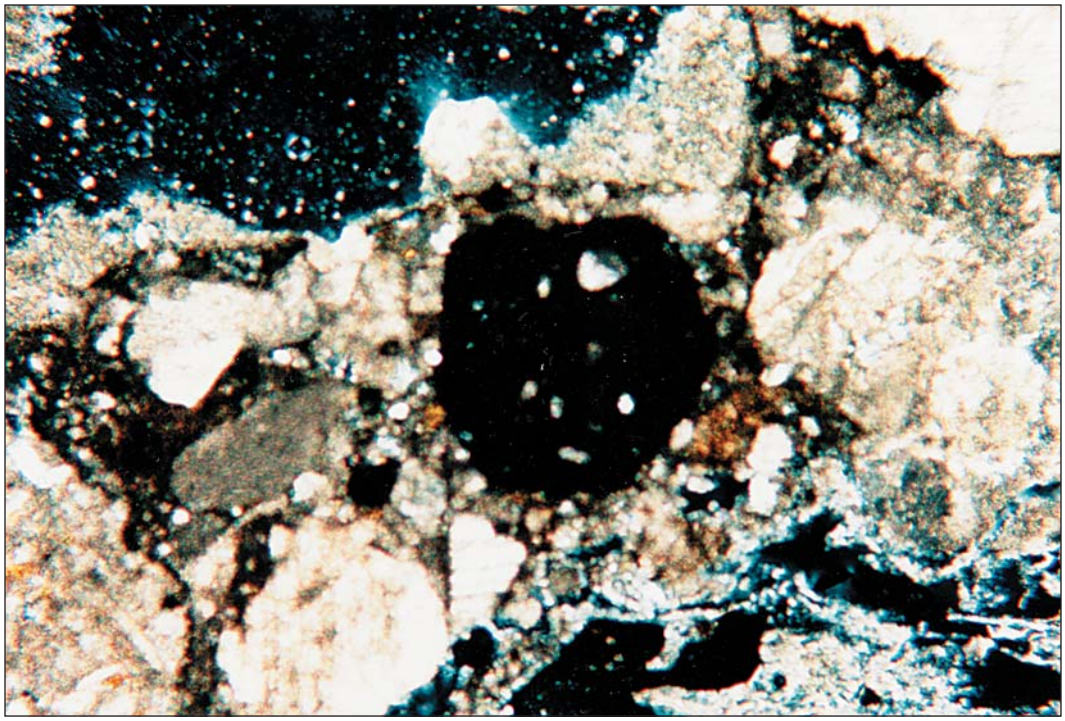

FIGURE 16.—Photomicrograph of black, altered impact-melt (?) clast (center of photo) in sample SM1-16 from core DGS 3274 (1,413 feet/431 meters). The clast is about 710 micrometers in diameter and contains smaller clasts. The photograph was taken in transmitted, plane-polarized light.

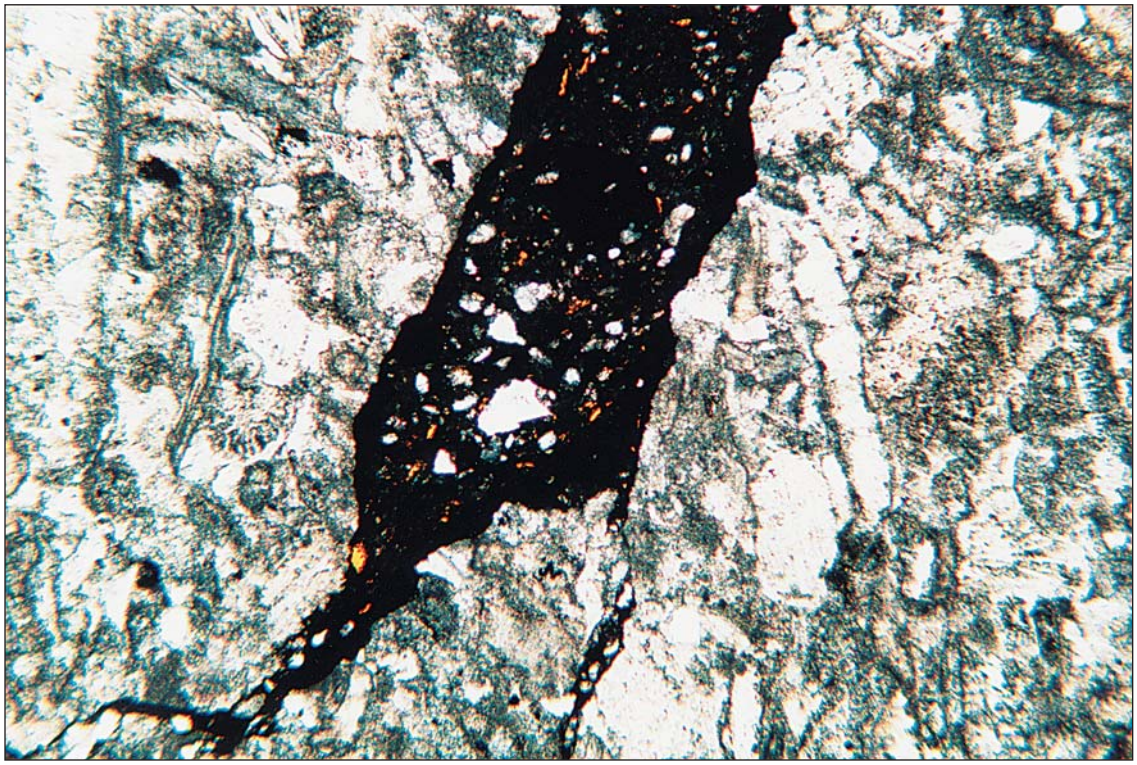

FIGURE 17.—Photomicrograph of a small dike (dark area) in a fossiliferous limestone in sample SM1-16 from core DGS 3274 (1,413 feet/431 meters). The dike matrix is black, aphanitic material thought to be similar in composition to the altered impact-melt (?) clast shown in figure 16. Larger clasts in the black matrix include yellow kerogenlike material, quartz, shale, and carbonate grains. Maximum width of dike in this photo is about 610 micrometers.

TABLE 5.—*Breccia intervals from core DGS 3275*

Breccia interval in feet	Thickness in feet (meters)	Breccia classification
156.0-158.0	2.0 (0.6)	
271.5-275.0	3.5 (1.1)	
322.0-328.0	6.0 (1.8)	
352.0-353.0	1.0 (0.3)	
361.0-365.6	4.6 (1.4)	
415.0-478.5	63.5 (19.4)	mixed-lithic breccia
658.0-725.0	67.0 (20.4)	mixed-lithic breccia
1381.0-1383.0	2.0 (0.6)	
1456.0-1458.0	2.0 (0.6)	
1478.0-1479.0	1.0 (0.3)	
1655.6-1660.0	4.4 (1.3)	
1660.5-1661.5	1.0 (0.3)	
1755.3-1761.0	5.7 (1.7)	
1767.3-1769.0	1.7 (0.5)	
1841.3-1842.9	1.6 (0.5)	
1875.0-1878.0	3.0 (0.9)	
1894.5-1895.3	0.8 (0.2)	mixed-lithic breccia
1932.5-1933.0	0.5 (0.2)	
2006.1-2006.9	0.8 (0.2)	

Russell/Tener well data for reference, the top of the Carntown unit of the Black River Group at a depth of 562 meters below the surface was correlated to reflectors at 160 ms on the SM-1 seismic profile (pl. 2). In like manner, the Conasauga Formation at a depth of 906 meters in the Russell/Tener well was correlated to reflectors at 280 ms, and the Precambrian basement at 1,178 meters to reflectors at 390 ms.

Reflectors corresponding to the Carntown unit and the Wells Creek Formation can be traced across the SM-1 profile, but are broken by faults extending into the Precambrian basement at stations 265, 280, 300, and 335. A minor fault is depicted along the northern part of the SM-1 profile between stations 130 and 140. The Conasauga and Rome reflectors are well developed along the entire line; the lowest point on the Conasauga reflector is below station 265 and has a travel time of 305 ms. The two-way travel time for the interval (mostly Knox Dolomite) that separates the Carntown reflector from the deeper Conasauga reflector ranges from 100 to 110 ms.

The Mount Simon reflector and the underlying Precambrian reflectors are discontinuous, but are observable on the SM-1 seismic profile. The discontinuous nature of the Mount Simon reflector is typical even in undisturbed areas because of topographic relief on the underlying Precambrian unconformity surface. Precambrian reflectors that have the greatest depth on the SM-1 profile are below station 270, at 405 ms.

The BV-1-92 seismic profile (pl. 3) shows a faulted depression beneath the central uplift and transition zone. The depression is slightly asymmetrical on the northeast end of the profile and does not intersect or cross the ring graben. The southwestern part of the line crosses part of the ring graben, but does not indicate significant structural variation. Key reflection characteristics, discussed below, are a lens- shaped area beneath the central uplift, absence of Knox and Rome reflectors, and presence of Precambrian reflectors.

On the BV-1-92 seismic profile (pl. 3), reflectors above the Carntown unit show no continuity and apparently reflect the chaotic nature of the Serpent Mound rocks. The structural low area observable in the Carntown to Precambrian reflectors on BV-1-92 may be somewhat shorter horizontally than it appears because of the sinuous path of the seismic line.

The drill-site location for core DGS 3274 is about 150 meters southeast of station 244 on the BV-1-92 profile; this core displays the disrupted nature of the rocks in the central uplift of the Serpent Mound disturbance. A lens-shaped area (lightest blue area on pl. 3) that has discontinuous reflectors above the Carntown reflector is delineated between stations 150 and 295 on BV-1-92. In core DGS 3274, in the section above the Carntown unit, large blocks of Ordovician rock have been displaced, overturned, and brecciated. Vertically oriented Grant Lake Limestone at the top of core DGS 3274 is at an elevation of 293 meters, which is a minimum of 244 meters above its expected elevation.

The northeastern end of the BV-1-92 seismic profile ties into station 249 on the SM-1 seismic profile. Seismic reflectors associated with the Carntown unit and underlying stratigraphic units (Wells Creek Formation, Knox Dolomite, Conasauga and Rome Formations, Mount Simon Sandstone, and Precambrian basement) on BV-1-92 at the intersection point (station 249) can be traced onto and identified on SM-1. As on SM-1, the reflectors associated with the Carntown unit, the Wells Creek Formation, and the Copper Ridge dolomite on BV-1-92 are more continuous than the overlying reflectors. They can be traced through a series of high-angle normal and reverse faults beneath the central uplift. Beekmantown reflectors on SM-1 may be present on BV-1-92 at the northeast end of the profile. The problematic occurrence of the Beekmantown reflectors on BV-1-92 may be the result of data having a lower **frequency** content or may be due to actual pinching out of the strata across the structure. Riley and others (1993) indicated that the subcrop contacts of the Beekmantown dolomite and Rose Run sandstone pass through northeastern Adams County very close to the Serpent Mound disturbance.

On the BV-1-92 seismic profile, the Carntown and deeper reflectors depict a narrow, highly faulted, and structurally complex depression. The Carntown reflector increases in depth toward the middle of the central uplift; it is lowest beneath station 240 at 315 ms (pl. 3). Between stations 195 and 315 this reflector is broken by at least three faults that extend into the underlying Conasauga and the Precambrian basement. If the top of the Carntown unit, identified in core DGS 3274 at an elevation of 550 meters below mean sea level, correlates with the Carntown reflector identified in BV-1-92, then this elevation may be assumed to represent the approximate depth of the Carntown on the seismic profile. The Carntown unit in the Russell/Tener well is at an elevation of 302 meters below mean sea level. Extrapolating this elevation updip to core DGS 3274 provides an estimated predisturbance elevation of the top of the Carntown in core DGS 3274 at 274 meters below mean sea level, a difference

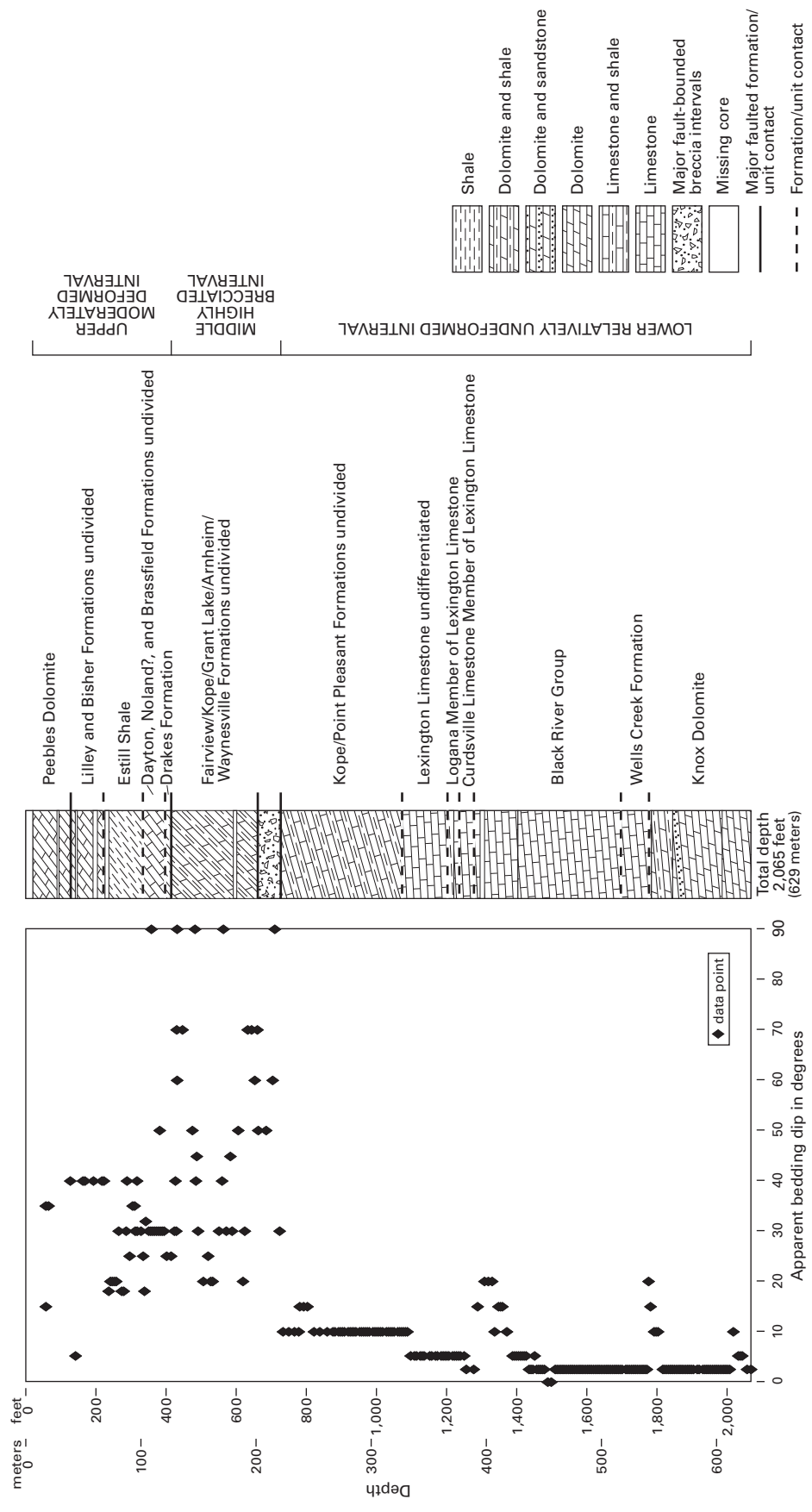

FIGURE 18.—Plot of apparent bedding dips and generalized lithostratigraphy for core DGS 3275. See plate 1 for more detail.

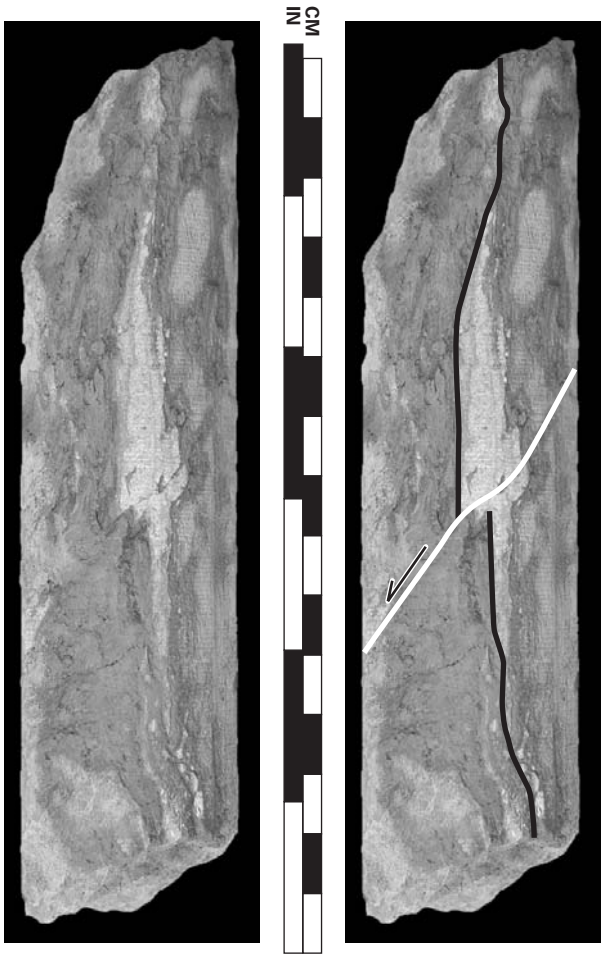

FIGURE 19.—Clast in mixed-lithic breccia from core DGS 3275 that indicates multiple episodes of deformation, folded vertical to overturned bedding, and a normal fault. Black lines indicate folded bedding laminae that are cut by a fault (white line); arrow indicates relative direction of fault movement. DGS 3275, box 40, 424 feet (129 meters), breccia zone.

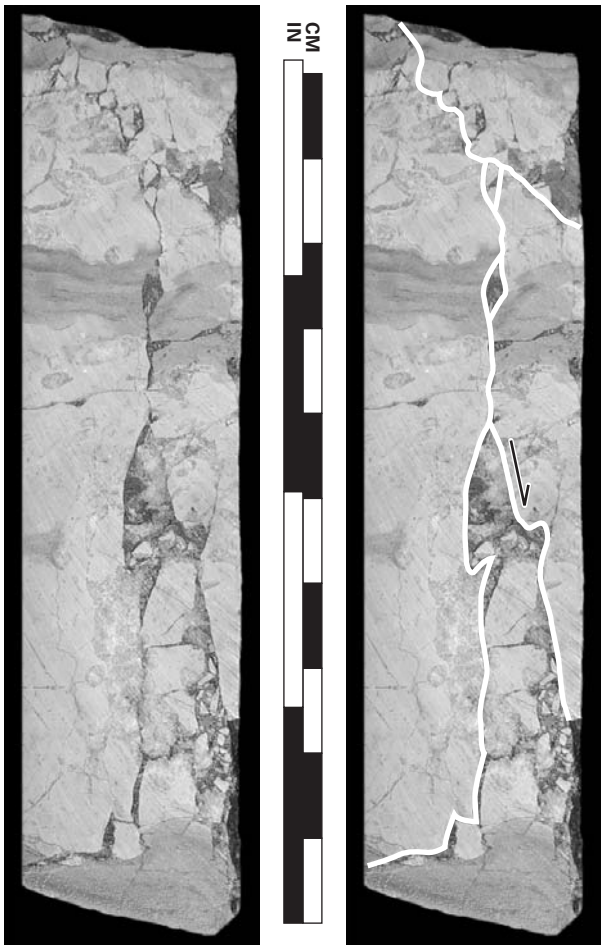

FIGURE 20.—Small normal fault in core DGS 3275 filled with mixed-lithic breccia. Note dark matrix material and angular clasts derived from the walls of the fault. White lines indicate faults and arrow indicates relative direction of fault movement. DGS 3275, box 144, 1,456 feet (444 meters), Ordovician Black River Group.

of 276 meters. This difference implies a depression of at least 276 meters below the central uplift. However, there is at least 34 meters of breccia below the Carntown unit at the base of core DGS 3274. If the Carntown in core DGS 3274 is part of an allochthonous block, then the Carntown unit that corresponds to the reflector may lie below the depth penetrated by core DGS 3274. If so, the depression shown on plate 3 could be significantly deeper.

The Conasauga reflector is well developed along the entire BV-1-92 seismic profile. The lowest point on the Conasauga reflector is beneath station 250 at 400 ms. The interval between the Conasauga reflector and the Carntown reflector represents the Knox Dolomite, which ranges from 110 ms at either end of BV-1-92 to 60 ms beneath the central uplift. The 50-ms difference suggests an estimated 150 meters of Knox Dolomite may be missing beneath the central uplift (medium-blue area, pl. 3). Likewise, the interval between the Conasauga reflector and the underlying Rome reflector decreases from 80 ms at each end of the profile to about 60 ms directly beneath the central uplift (brightest blue area, pl. 3) suggesting a thinning of about 60 meters.

Thinning below the Carntown unit may account for a portion of the structural depression observed in BV-1-92. The thinning may be the result of several factors: (1) poor **resolution** on BV-1-92 of the breccia at the bottom of core DGS 3274, assuming the breccia represents Knox Dolomite, (2) a fault-bounded Cambrian paleotopographic high that was deeply eroded or an area of nondeposition on a emergent landmass prior to Carntown deposition, (3) facies changes and/or pinch-outs in the Knox Dolomite, Conasauga Formation, and upper part of the Rome Formation, (4) solution collapse of Cambrian-age carbonates or evaporites followed by localized subsidence, or (5) fault reactivation and downdropping of Paleozoic and Precambrian strata as a direct result of meteorite impact. The observed Cambrian and Precambrian (?) facies changes and thickness variations

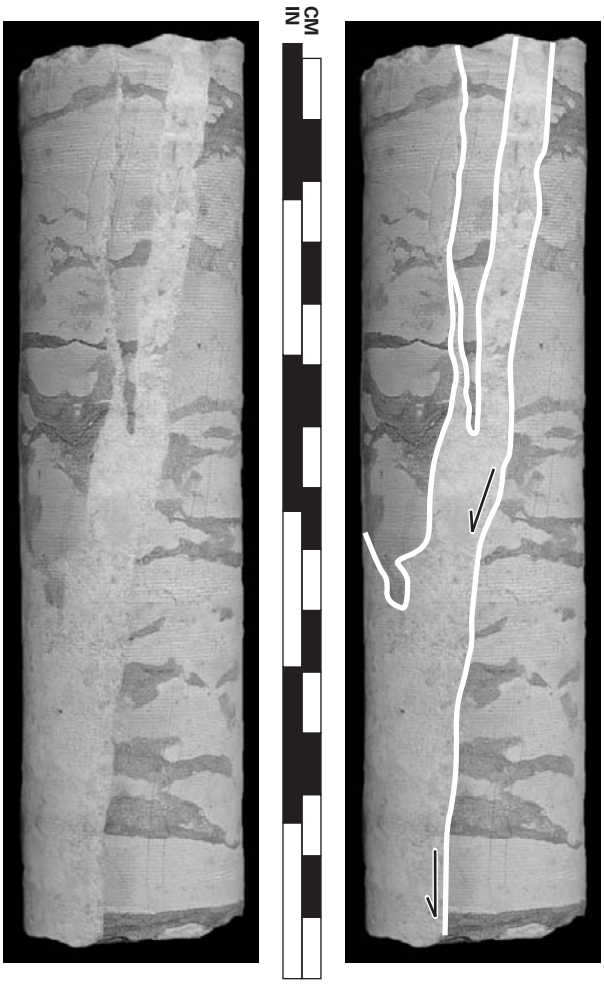

FIGURE 21.—Small-scale, high-angle, subvertical, calcite-filled normal fault (white lines) in core DGS 3275; arrows indicate relative direction of fault movement. DGS 3275, box 167, 1,693 feet (516 meters), Ordovician Carntown unit of Black River Group.

observed on the seismic profiles beneath the central uplift resulted from movement along pre-existing Precambrian faults directly beneath the structure. This interpretation is supported by the numerous faults observed on the seismic profiles and structures observed in cores DGS 3274 and 3275. Factors 1, 4, and 5 above cannot be evaluated because of a lack of wells penetrating Cambrian rocks and the Precambrian crystalline basement below the central uplift. The depression of the reflectors and the thinning of the intervals between them as they pass beneath the central uplift are distinctive features of the BV-1-92 seismic profile. The thin interval of the upper part of the Rome Formation to the Knox unconformity as interpreted on BV-1-92 is coincident with the northwest-trending geophysical anomaly shown on figure 24. The depression cannot be due solely to a velocity pull down (lowering of seismic velocities) beneath the central uplift because the evidence from core DGS 3274 also indicates a physical depression of the Carntown unit beneath the central uplift (assuming a vertical core).

Reflectors beneath the Mount Simon reflector can be identified on both the BV-1-92 and SM-1 profiles. The interval between the pre-Mount Simon and the Mount Simon Sandstone reflectors ranges from 30 to 80 ms on both profiles. Directly beneath the central uplift on BV-1-92 (pl. 3), the interval between the Mount Simon Sandstone and the pre-Mount Simon is estimated to be 320 meters. This is about 250 meters thicker than the Mount Simon Sandstone to pre-Mount Simon interval in the Russell/Tener well. Possible arkose present beneath the Mount Simon Sandstone in the Russell/Tener well may represent the extra 250 meters of sediment indicated on the seismic profile. If so, the arkose (?) may be similar in depositional history to the Middle Run Formation present in Precambrian (?) basins below the Mount Simon Sandstone 50 km (31 miles) to the west.

GRAVITY DATA

The first published regional **gravity anomaly** map of Ohio (Heiskanen and Uotila, 1956) shows a linear gravity high trending northwest-southeast through Scioto, northeastern Adams, western Pike, and Highland Counties. From Highland County, a northerly trend extends into Fayette and Madison Counties and becomes one of the highest positive gravity anomalies in the state. Unfortunately, Heiskanen and Uotila's (1956) map is not sufficiently detailed to show features that might be directly related to the Serpent Mound disturbance.

Bull and others (1967) published the first detailed gravity survey of the Serpent Mound area. Their paper was based on Zahn's (1965) M.S. thesis. On the Bouguer gravity anomaly map of Bull and others (1967, fig. 2), the contour lines trend northwest-southeast and decrease regularly from -12 **milligals** to -22 milligals at the southwestern edge. Their study was confined to the Serpent Mound disturbance and the immediately surrounding area. They noted that the regional Bouguer anomaly trend (Heiskanen and Uotila, 1956) is to the southwest, including a -40-milligal reading about 11 km (7 miles) southwest of the Serpent Mound disturbance. Bull and others (1967, p. 368) attributed the anomaly variation to unknown horizontal density differences in the basement rocks and concluded that their gravity data could not be used to determine the origin of the Serpent Mound disturbance.

Unpublished M.S. theses by Flaugher (1973) and Langford (1984) reported on gravity anomalies within and around the Serpent Mound disturbance. The Bouguer anomaly map constructed by Flaugher (1973) shows a northwest-southeast-trending gravity high characterized by steep gradients on each flank. This gravity high is the same one depicted on Heiskanen and Uotila's (1956) map. The Serpent Mound disturbance lies on the southwest flank.

The regional gravity anomaly north of the Serpent Mound disturbance mapped by Heiskanen and Uotila (1956) and redefined and studied in more detail by Flaugher (1973) and Langford (1984) can be readily identified on the complete Bouguer gravity anomaly map of Ohio compiled by Hildenbrand and Kucks (1984b). This map has a 2-milligal contour interval and shows many closed gravity contours, especially in a north-south zone in west-central Ohio. The

closed-contour anomalies are probably related to the Grenville Front Tectonic Zone or to structural weaknesses in the Precambrian basement (Lucius and Von Frese, 1988; Culotta and others, 1990). None of the gravity highs or lows shown on the Hildenbrand and Kucks (1984b) map appears to be spatially related to the Serpent Mound disturbance.

As part of our investigation, a high-resolution gravity survey was conducted during the summer of 1996 along the course of seismic line BV-1-92. The survey followed Horner Chapel Road north from its intersection with Ohio Route 73 to the intersection with Parker Ridge Road, and then easterly to the intersection with Ohio Route 41 (see fig. 22). A U.S. Geological Survey bench mark 637 meters north from the intersection of Ohio Route 124 and Ohio Route 41 in Sinking Spring was used as gravity base station G-0. Base station G-1 was established at the intersection of Parker Ridge Road and Ohio Route 41, and base station G-2 was at the intersection of Horner Chapel Road and Ohio Route 73. Elevations and latitude and longitude coordinates for these stations are given in the caption of figure 22. The gravity station interval was approximately 50 meters from base station G-1 westward across the central uplift to base station G-2.

A La Coste-Romberg model G gravity meter and a Worden Prospector gravity meter were operated simultaneously during the survey to provide a cross check on both instruments so that possible tares (abrupt changes of the null point of the meter) could be detected. Instrument drift was measured by returning to station G-1 every three hours and to station G-0 at the beginning and end of each survey day. Results from the La Coste-Romberg meter were more accurate than those from the Worden meter and were used in this investigation. Elevations and locations of seven gravity stations along the traverse, including stations G-1 and G-2, were determined using a differential global positioning system (GPS) and station G-0 for reference. The elevations and locations of intermediate stations along the traverse were determined using an optical theodolite because only up to six GPS stations could be surveyed at the appropriate precision in a single day. The theodolite stations were then tied to the GPS-determined stations. The gravity data were corrected for instrument drift, latitude change, and elevation. The Bouguer corrections included a terrain correction calculated using a Hammer chart and topographic maps at a scale of 1:24,000. The Bouguer anomaly profile derived from the gravity survey and calculated with respect to station G-1 is shown on plate 3.

The Bouguer gravity profile (pl. 3) generally becomes less negative from the southwest to the northeast, but levels out and dips or becomes more negative (about -2 milligals) over the central uplift, then begins to become less negative again on the northeastern part of the transition zone. The drop over the central uplift coincides with the location of the depression of reflectors on seismic line BV-1-92. The highly deformed central uplift has a greater concentration of faults, fractures, and breccias than the adjacent transition zone or ring graben. The greater degree of faulting and brecciation results in a decrease in the average density of rocks in the central uplift, leading to the local negative anomaly. The missing part of the Knox Dolomite and its greater depth in the central uplift also may contribute to the local anomaly. Modeling of the gravity anomaly was not performed for this study, but would be required to separate the local gravity anomaly from the regional anomaly.

MAGNETIC DATA

Sedimentary rocks generally contain few magnetic minerals; consequently, **magnetic anomalies** measured in sedimentary terrains typically are associated with buried Precambrian crystalline basement rocks (Hildenbrand and Kucks, 1984a). Magnetic anomalies caused by impacting meteorites are more complex than associated gravity anomalies because of the wide variation in the magnetic properties of the target rocks. Magnetic anomalies associated with meteorite impact sites are generally negative and may truncate the regional magnetic trends (Grieve and Pilkington, 1996).

The residual total intensity magnetic map of Ohio (Hildenbrand and Kucks, 1984a) is characterized by many circular magnetic anomalies that have steep magnetic gradients along a 49-km (30-mile)-wide north-south zone in west-central Ohio. These anomalies are both positive and negative and indicate a complex geologic history for the basement rocks of Ohio along the Grenville Front Tectonic Zone.

Sappenfield (1951) conducted a ground magnetic survey over approximately 388 square km (150 square miles) of northeastern Adams, southeastern Highland, and southwestern Pike Counties. The Serpent Mound disturbance lies at the approximate center of the surveyed area. The survey delineated a northwest-southeast-trending magnetic anomaly in the form of a "ridge" passing through the center of the Serpent Mound disturbance. The anomaly is about 12 km (7.5 miles) long and has a local high offset to the south of the central uplift, in the ring graben of the disturbance.

In 1996, as part of the present investigation, a regional magnetic survey was conducted over nearly the same area as Sappenfield's (1951) investigation using two EG&G Geometrics 856 recording proton precession magnetometers. One of the magnetometers sampled the Earth's **magnetic field** every 2 minutes at a base station for diurnal corrections and the other, identical magnetometer was used for the actual survey. Lines were initially surveyed (fig. 22) within the boundary of the disturbance using an optical theodolite and GPS stations for location to determine if short-wavelength anomalies associated with mineralized zones were present. These initial lines had station intervals of 10 meters (33 feet) and were conducted in fields and woods, away from roads and possible sources of cultural magnetic noise. After it was established that no short-wavelength anomalies of natural origin were present, lines were surveyed (fig. 22) along roads and the station spacing was increased as the distance from the center of the disturbance increased. On these lines, three to five readings were taken over an area of 10 square meters (108 square feet) to determine whether a strong gradient (greater than 5 **nanoteslas**/meter, 1.5 nanoteslas/foot) was present. Stations having strong gradients were likely to be contaminated by cultural noise. The magnetic survey line coincident with seismic line BV-1-92 and the gravity line between Parker Ridge Road and Horner Chapel Road (fig. 22, G-1 to G-2) had a station interval of 50 meters. The station spacing

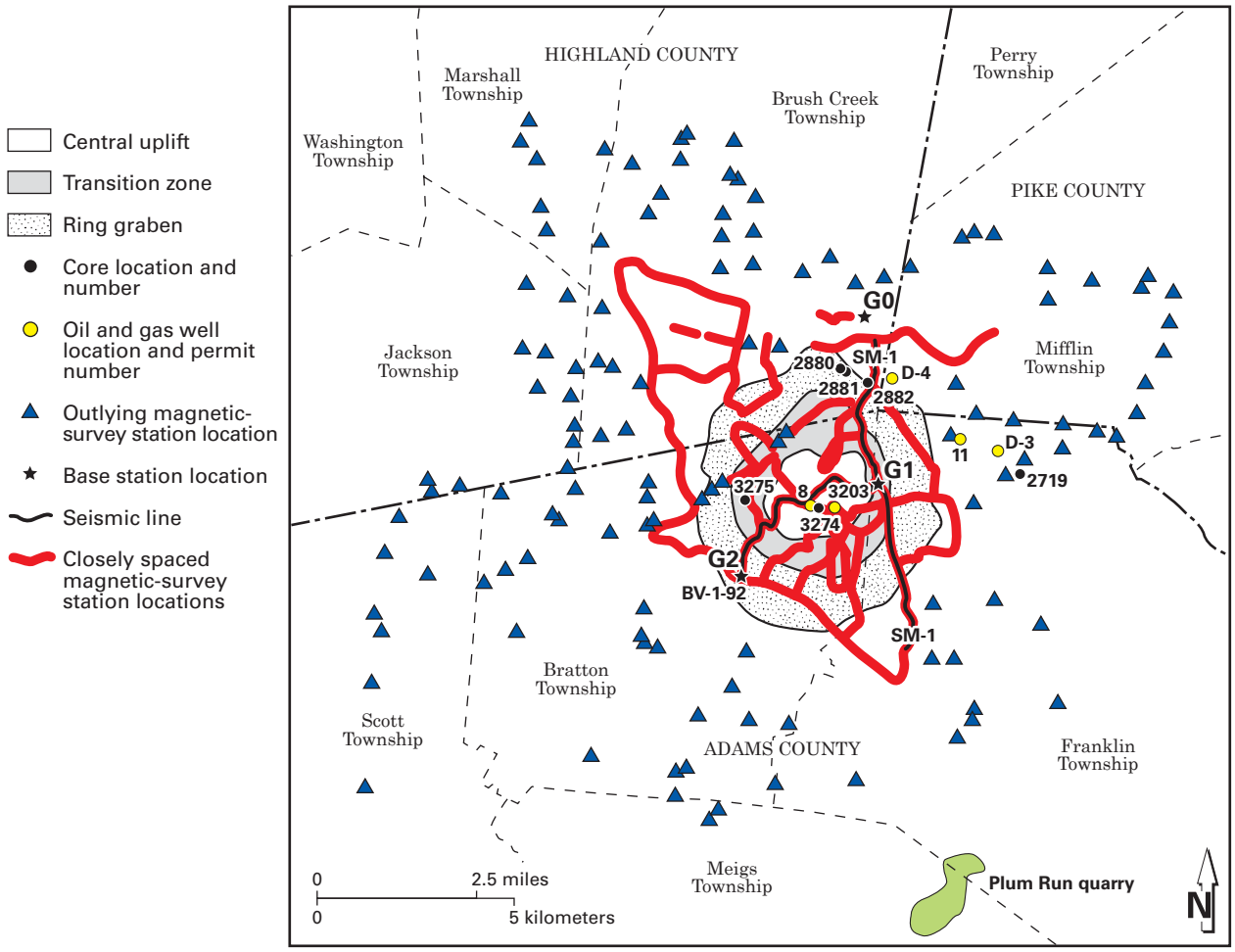

FIGURE 22.—Location of closely spaced magnetic survey stations (10-, 50-, and 100-meter intervals) and outlying stations in the area of the Serpent Mound disturbance. Location data for base stations: **G0**, U.S. Geological Survey bench mark at intersection of Ohio Routes 124 and 41 in Sinking Spring, Highland County; elevation 261.8 meters (859 feet), latitude 39°04'43.0"N, longitude 83°23'18.0"W. **G1**, intersection of Ohio Route 41 and Parker Ridge Rd., Franklin Twp., Adams County; elevation 229.9 meters (754 feet), latitude 39°02'20.83"N, longitude 83°23'10.02"W. **G2**, intersection of Ohio Route 73 and Horner Chapel Rd., Bratton Twp., Adams County; elevation 218.9 meters (718 feet), latitude 39°00'58.76"N, longitude 83°25'32.71"W.

along all other roads was nominally 100 meters and was adjusted to coincide with locations easily identified on the 1:24,000 topographic map. Outlying stations (fig. 22) were established at road intersections.

The data were edited to remove any stations that had a high magnetic gradient. Cultural features such as fence lines and power cables were noted, and stations adjacent to such features were either not recorded or removed from the data. Three strong local anomalies were associated with casing from the Parker well, the Kaeser well, and the core DGS 3274 site. These anomalies were removed from the database to produce the magnetic anomaly map in figure 23. After correcting for diurnal drift and subtracting the reference geomagnetic field, the data were computer contoured on a 500-meter (1,640-foot) grid; a median filter was applied to further suppress cultural noise, revealing the long-wavelength anomaly.

The magnetic anomaly map of the Serpent Mound disturbance (fig. 23) shows a linear positive magnetic anomaly trending northwest to southeast through the central uplift. Maximum amplitude of the anomaly is about 1,000 nT. The maximum amplitude appears to be offset to the northwest of the central uplift. Cultural noise limits the precision with which the high can be located, and it is possible that the magnetic high could be closer to the central uplift. Our map is a significant revision of Sappenfield's (1951) map, which placed the maximum amplitude south of the central uplift, near the outer boundary of the disturbance. Because our survey has a considerably higher station density and used more sensitive magnetometers, there can be no doubt that the magnetic high is north (northwest), not south, of the central uplift. The magnetic high has an adjacent low near the east-

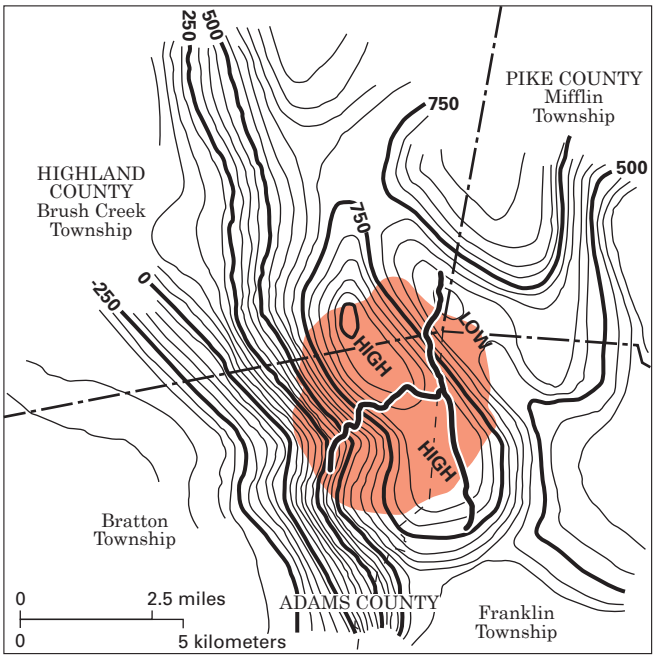

FIGURE 23.—Contour map of magnetic anomalies in the area of the Serpent Mound disturbance. Contour interval is 50 nanoteslas (nT); contours were interpreted after correcting for diurnal drift, subtracting the reference geomagnetic field, and removing cultural anomalies.

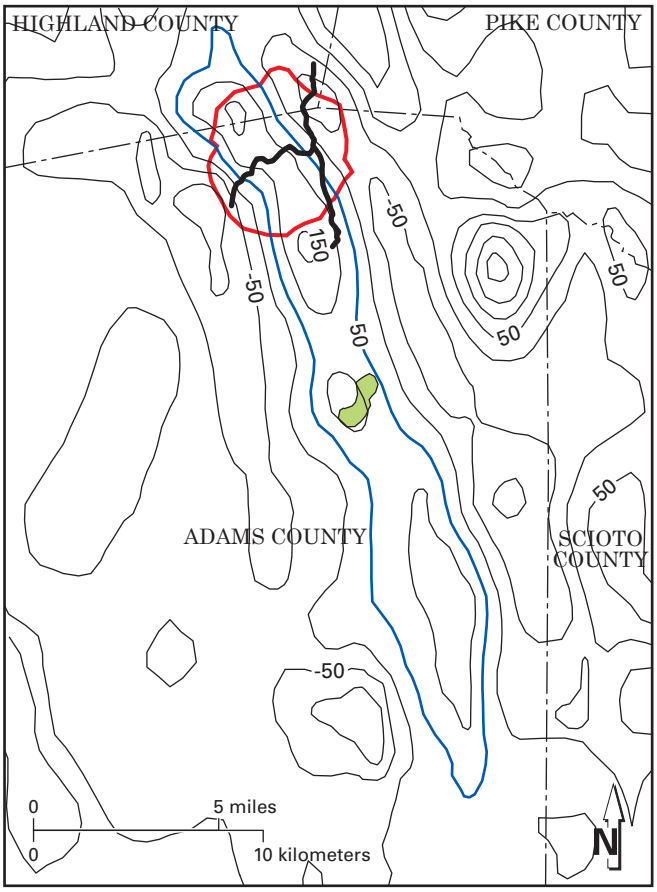

FIGURE 24.—Second-derivative map of the Serpent Mound area based on magnetic data from Hildenbrand and Kucks (1984a). Locations of the Serpent Mound disturbance and the structurally disturbed Plum Run quarry are shown in relation to a linear magnetic high anomaly in northeastern Adams County and southeastern Highland County.

ern boundary of the disturbance. The magnetic low is shown on Sappenfield's map, but it is not as prominent as that displayed in figure 23. The western margin of the magnetic anomaly beneath the Serpent Mound disturbance coincides with the boundary of a prominent north-south-trending regional magnetic anomaly on Hildenbrand and Kucks' (1984a) map. The **second-derivative map** (fig. 24) of these magnetic data shows that the disturbance is located along a 40-km-long northwest-trending anomaly. This northwest- trending second-derivative magnetic anomaly is coincident with thin Cambrian reflectors observed on seismic line BV-1-92 (pl. 3).

PALEOMAGNETIC DATA

The direction of the **magnetization** preserved in rocks can be used to date geological events. For example, Jackson and Van der Voo (1986) used magnetization directions to date the origin of the Kentland structure in Indiana. To determine if similar information was preserved in the Serpent Mound disturbance, sample cylinders from DGS cores were collected to examine the magnetization of subsurface rocks within and outside the disturbance. Doyle Watts performed the analysis while he was at the University of Glasgow (Scotland). The methods and technical discussion of the results of his analysis are described in Watts (in press).

Forty-two hematite-rich samples from the Silurian-age Brassfield Formation from cores DGS 3275, 2880, 2881, 2882, and 2626 and 30 samples of Ordovician- and Silurian-age carbonates from cores DGS 3274 and 3275 (see pl. 1) were collected and analyzed. Analysis of the hematite-rich Brassfield samples indicates the age of magnetization of the Serpent Mound disturbance is 256 million years (+25/-22 million years). Because the magnetization postdates the structure, this date represents an upper limit to its age.

This estimate represents the best constraint for the upper age limit of the Serpent Mound disturbance to date. The estimate is not likely to be improved by radiometric methods, as no datable material has been found associ-

ated with the disturbance. The age estimate provides a much better upper age constraint than that afforded by the geological relationships. It does raise the possibility that ejecta associated with the structure may be preserved in Pennsylvanian or Permian rocks within 100 km (62 miles) of the site. The identification of microfossils or lithologies from allochthonous breccias in cores DGS 3274 and 3275 and in breccias exposed at the surface within the disturbance may yield more diagnostic information.

ORIGIN OF THE SERPENT MOUND DISTURBANCE

The two dominant processes that have been proposed over the years to explain the origin of the Serpent Mound disturbance are endogenic, in which forces from within the Earth are involved, and exogenic, due to impact of an extraterrestrial object. Bucher (1936, 1963) was the main proponent of the endogenic hypothesis for the Serpent Mound disturbance. In his model, sudden crystallization of magma at the base of the Earth's crust created large amounts of water vapor under high pressure. If this water vapor was rapidly transported and emplaced near the surface in porous rocks, beneath an impermeable cap rock, an explosion might occur, creating a feature similar to the Serpent Mound disturbance. The exogenic model proposes that an extraterrestrial body, such as a meteorite or a comet, struck the Earth at hypervelocity, resulting in the release of sufficient energy to create the Serpent Mound disturbance.

Dietz (1960) and Cohen and others (1961, 1962) were the first to suggest a meteorite-impact origin. Dietz (1960) reported finding numerous shatter cones upon breaking open cobbles at the surface in the central uplift. Cohen and others (1961) reported coesite, a high-pressure form of quartz found at many well-documented impact craters, in the Lilley Formation within the Serpent Mound disturbance. Reidel and others (1982), after an extensive search, could not find coesite in the area of the disturbance and thus discounted Cohen's discovery as a probable misidentification of a diffuse X-ray diffraction line. According to Hansen (1994), other workers have searched for but have not been able to confirm the presence of coesite.

Heyl and Brock (1962) and Reidel and others (1982) reported Mississippi Valley-type mineral deposits in the Serpent Mound disturbance. Sphalerite is the primary mineral and occurs as fracture fillings, fault-breccia cement, and replacement of the carbonate host rock. Most of the sphalerite occurs along fault zones, indicating the mineralization occurred after the disturbance formed (Reidel and others, 1982). Within the fault zones, sphalerite cements the breccia, and massive sphalerite and sparry calcite fill open spaces. According to Reidel and others (1982), much of the sphalerite along faults has been fractured and pulverized to a very fine powder, indicating multiple episodes of fault movement.

McFarland and Carlson (1995a), in their study of the mineralogy, sulfur isotopes, and trace elements from the Serpent Mound disturbance, found no differences in the sequence of mineralization inside and outside the structure. They accepted the meteorite-impact origin and provided a model for mineralization that does not require an endogenic origin. McFarland and Carlson (1995a) proposed that mineralizing fluids moved through the area after the formation of the Serpent Mound disturbance, depositing dolomite and zinc minerals primarily in fractures. Sphalerite was deposited in an area approximately 64 km (40 miles) long in a north-south trend and 32 km (20 miles) wide (Carlson, 1991, p. 29). After this phase of dolomite and sphalerite deposition, one or more episodes of dissolution, primarily along these breccia zones, resulted in solution collapse and additional brecciation of the original dolomite-cemented breccia and sphalerite. Rocks were brecciated further along faults by the settling and adjustment of large blocks. Later, local, less intense episodes of mineralization occurred (Reidel and others, 1982; McFarland and Carlson, 1995a).

In their magnetic and gravity studies, Sappenfield (1951), Flaugher (1973), and Langford (1984) supported an endogenic origin for the Serpent Mound disturbance. Sappenfield (1951) attributed the magnetic anomaly to the intrusion of basic magma into the upper part of the more siliceous basement. He suggested that this model supports Bucher's (1936, 1963) endogenic model for the formation of the Serpent Mound disturbance. Evidence of igneous rocks has not been discovered at the surface nor in cores studied for this report. Flaugher (1973) favored a model for the gravity anomaly in which basic magma was intruded into lower density siliceous rocks to create the gravity high adjacent to the Serpent Mound disturbance. In his model, gases from this intrusion eventually migrated along faults, became trapped, and after a buildup of pressure, exploded, forming the Serpent Mound disturbance. Flaugher (1973) concluded that his data do not definitely prove or disprove Bucher's (1936, 1963) gas-explosion hypothesis or the meteorite-impact hypothesis. Langford (1984) believed the gravity anomaly was the result of an ultramafic intrusion, favoring a sill extending into the Serpent Mound area from the northwest.

The work of Heyl and Brock (1962), Reidel and others (1982), and McFarland and Carlson (1995a, 1995b) indicates a complex history for the Serpent Mound disturbance, including two or more periods of deformation. The presence of northwest-trending faults outside the structure are well known in the literature (Bucher, 1933, 1936; Galbraith, 1968; Reidel and others, 1982; Swinford, 1985). Reidel and others (1982) noted that the faults within the disturbance are aligned approximately with the gravity and magnetic anomaly trends in the area. They concluded that the northwest-trending regional fault zone predates the disturbance, was probably a zone of crustal weakness when the disturbance formed, and controlled to a certain extent the orientation of faults within the disturbance.

Several facts have led some geologists to question the impact hypothesis: (1) the presence of coesite has not been confirmed, (2) at least two widely separated episodes of deformation occurred, and (3) the Serpent Mound disturbance is directly above a zone of crustal weakness. Reidel and others (1982) admitted that the structural relationships within the disturbance are not fully understood, but do provide the proper conditions for an endogenic origin. They considered shatter cones as inconclusive evidence for meteorite impact and stressed the multiple episodes of deformation as strong evidence for an endogenic origin.

Conversely, Koeberl and Anderson (1996) consider the Serpent Mound disturbance an impact site based on the work of Bucher (1936), Deitz (1960), Cohen and others (1961), and Reidel and others (1982). The two most significant pieces of evidence for an impact origin for the Serpent Mound disturbance come from core DGS 3274, where PDF's and above-normal levels of iridium have been discovered (Carlton and others, 1998b). When a meteorite strikes Earth, characteristic changes may occur in the crystalline lattice of quartz found in the impact area as a result of shock metamorphism. In recent years, shock metamorphism of minerals, particularly quartz, has been well documented; excellent reviews on this subject have been published by Stöffler and Langenhorst (1994) and Grieve and others (1996). It should be carefully noted and understood that the conditions for endogenic metamorphism of crustal rocks are distinctly different from the conditions necessary for shock metamorphism (Koeberl and Reimold, 1995; Grieve and others, 1996, and references therein; Koeberl and Anderson, 1996). The lowest pressure necessary for shock metamorphism in quartz is about 5 **gigapascals** (GPa) and is well above the approximate maximum pressure of 2.0 GPa in crustal rocks (Koeberl, 1997). The formation of PDF's requires very high strain rates, and pressure durations are on the order of nanoseconds to seconds. Typically, for tectonic deformation, strain rates are much lower and pressure durations much longer (Grieve and others, 1996).

The occurrence of PDF's in quartz is generally accepted as diagnostic evidence for shock resulting from impact (French and Short, 1968; Alexopoulos and others, 1988; Sharpton and Grieve, 1990; Grieve and others, 1996). As viewed through an optical microscope (see fig. 14), PDF's appear as intersecting sets of parallel, planar, amorphous lamellae. The lamellae are spaced 2 to 10 micrometers apart and are less than 3 micrometers thick (Alexopoulos and others, 1988; Stöffler and Langenhorst, 1994). PDF's were observed in seven samples examined from core DGS 3274 and confirm the impact origin of the Serpent Mound disturbance (Carlton and others, 1998b).

The presence of iridium (Ir), as well as other platinum group elements, commonly is used to identify rocks impacted by a meteorite (Koeberl and Shirey, 1996). The 0.2 parts per billion (ppb) Ir concentration found in two breccias analyzed for this investigation (see p. 21) strongly suggests a small chondritic or iron meteorite component. The 0.2 ppb value for these samples is about 10 times higher than concentrations found in average crustal sedimentary rocks.

Shatter cones are believed to form in rocks subjected to intense shock waves. Experimental evidence from explosion-crater experiments (Milton, 1977) suggests shatter cones form at pressures in the range of 2 to 30 GPa, depending on the type of rock, far above pressures generally found in endogenic processes. Shatter cones have been identified at the surface of the Serpent Mound disturbance and are abundant in both cores DGS 3274 and 3275 (pl. 1).

DISCUSSION

In the nearly eight decades since Bucher (1925) named the disturbance the Serpent Mound cryptovolcanic structure, many investigators have proposed various mechanisms for the origin of the disturbance. In spite of the fact that the disturbance has many of the classic features of an impact crater such as shatter cones, circular shape, central uplift, and highly brecciated and faulted strata, many investigators have favored an endogenic origin over an impact origin (Bucher, 1936, 1963; Sappenfield, 1951; Galbraith, 1968; Reidel and others, 1982; Langford, 1984). However, Dietz (1960), Cohen and others (1961), and McFarland and Carlson (1995b) have supported an impact origin. The discovery of PDF's and an Ir anomaly, along with the known presence of shatter cones, provides overwhelming evidence for an impact origin of the Serpent Mound disturbance (Carlton and others, 1998b).

The impact of a meteorite into a pre-existing structural zone tends to complicate and confuse the origin issue. For some investigators, it is difficult to accept that a meteorite could precisely hit a fault zone (as shown on seismic profile BV-1-92, pl. 3). The presence of a fault zone or structural weakness in the basement below the Serpent Mound disturbance also makes it easier to propose deep-seated magmas that are necessary for the endogenic formation of the disturbance as postulated by Bucher (1963). However, surface rocks and deep cores in the area of the Serpent Mound disturbance are devoid of minerals indicative of deep-seated magmas and fluids required to support an endogenic origin. Detailed study of deep cores indicates complex cross-cutting structural relationships and establishes relative timing of structural events over a long period of geologic time.

Impacts into pre-existing structures have been reported, for example, the Wells Creek structure in Tennessee (Wilson and Stearns, 1968) and the Avak structure in Alaska (Kirschner and others, 1992). In Ohio, where seismic reflection and deep well data are available, structures and faults have been documented in the Precambrian and Paleozoic rocks (Baranoski and Wickstrom, 1994; Baranoski, 2002). It follows that many more structures and faults are present in the subsurface than presently mapped, thus increasing the possibility of an impact into a pre-existing structure throughout geologic time. Northwest-trending geophysical anomalies, satellite imagery lineaments, surface faulting, subsurface mapping based on well and seismic data, and cross-cutting structural relationships from deep cores support the presence of pre-existing structure at the Serpent Mound disturbance.

The Russell/Tener well, just outside the boundaries of the Serpent Mound disturbance, suggests the possible presence of arkose beneath typical Mount Simon Sandstone, and seismic data beneath the central uplift indicate about 250 meters more rock between the Mount Simon Sandstone reflector and the pre-Mount Simon reflector than found in the Russell/Tener well. Presumably, this arkose also is present beneath the central uplift and along the northwest-trending magnetic anomaly. The increased thickness of the arkose (?) beneath the central uplift strongly suggests a Precambrian or Early Cambrian basin/graben at the impact site. Wicks (1996) presented another well-documented case in which localized structural grabens on Precambrian ter-

rane are filled with pre-Mount Simon sediments. Figure 25 presents a diagrammatic model to illustrate the possible geologic sequence of events, from the Precambrian to modern day, that may have occurred along the northwest- trending magnetic anomaly in southern Ohio. Figure 25A shows localized normal faulting and rift-basin fill, which is analogous to Precambrian features reported by Wicks (1996) in Holmes County, Ohio. Figure 25B indicates the Precambrian surface was eroded down into the rift-basin fill, then was subjected to a westward regional tilt. The Cambrian Mount Simon Sandstone and Rome Formation were deposited on this eroded, tilted surface.

During the Cambrian and Early Ordovician, the area beneath what is now the central uplift gradually and episodically became a structural high as a result of regional tectonic forces, causing the uppermost part of the Rome Formation, the Conasauga Formation, and the Knox Dolomite to be thinner than observed outside the Serpent Mound area. The structural high probably was the result of uplift along pre-existing Precambrian zones of weakness. Thinning of the Rome and Conasauga Formations and the Knox Dolomite in the vicinity of the Serpent Mound disturbance supports the idea of a gradually emerging structural high at this time. This thinning is illustrated in figure 25C. Tectonic inversion in the form of uplift along the northwest- trending magnetic anomaly started at the end of Rome Formation deposition and ceased prior to deposition of the Middle Ordovician Black River Group.

There are no noticeable thickness variations in the Carntown unit of the Black River Group in the vicinity of the Serpent Mound disturbance. The Carntown is broken by faults extending upward from the Precambrian and is about 276 meters deeper beneath the disturbance than elsewhere. None of the post-Carntown strata reveal any strong evidence for a significant structural event in the vicinity of the Serpent Mound disturbance, although several major unconformities are present throughout the Paleozoic sequence of southwestern Ohio. Local structure had little or no effect on the deposition of post-Knox-unconformity units (fig. 25D).

Minor graben development in the area of the Plum Run quarry indicates an episode of post-Silurian faulting, on the basis of the presence of possible Upper Devonian Ohio Shale clasts in a fault zone in the quarry. As mentioned earlier, deposition of asphaltic material in the Peebles Dolomite in the Plum Run quarry may have been inhibited because of faulting. If the asphaltic material was emplaced during the Alleghany Orogeny, then faulting must have occurred prior to the orogeny. Therefore, some faulting at Plum Run is at least post-Silurian and pre-orogeny. In core DGS 3275, asphaltic material is found in pores and fractures within the Peebles Dolomite as well as in anastomosing fractures; no hydrocarbons are found in the non-Peebles breccia in the core. Hydrocarbons most likely were in place at the time of impact, but did not migrate following the impact into overlying units and breccia.

An examination of gravity (Hildenbrand and Kucks, 1984b) and magnetic (Hildenbrand and Kucks, 1984a) anomaly maps indicates magnetic and gravity anomalies throughout Ohio, particularly along the Grenville Front Tectonic Zone. The second-derivative map in figure 24 is based on data from Hildenbrand and Kucks (1984a) and indicates a north-northwest-trending magnetic anomaly that is approximately 25 miles long. Both the Serpent Mound disturbance and the Plum Run Quarry Fault are situated directly over a portion of this anomaly. It is clear that there are a number of densely spaced gravity and magnetic anomalies in this part of Ohio. It is possible that a meteorite impact simply coincided with a magnetic anomaly.

The magnetic anomaly high beneath the Serpent Mound disturbance is just one of many in southwestern Ohio and has the same trend as regional magnetic anomalies in the area. In past studies of the Serpent Mound disturbance (for example Sappenfield, 1951), investigators have used the magnetic anomaly as support for an endogenic origin. They associated the anomaly with an intrusive igneous body into either the Paleozoic sedimentary rocks or Precambrian igneous and metamorphic rocks underlying the disturbance. Such an intrusion could have provided gases for an explosive endogenic event. However, scanning the deep core DGS 3274 with a kappa meter showed only weakly magnetized sedimentary rocks. No evidence for igneous material was found in the core. Zones of mineralization in the core are devoid of magnetite or other strongly magnetic minerals. No evidence for an anomalous thermal gradient, consistent with the presence of an intrusive body, was found in the deep core.

The magnetic and gravity surveys conducted for this investigation confirm a weak magnetic anomaly, which appears parallel to the regional trend, and a small local gravity low (pl. 3) associated with the central uplift. The local negative gravity anomaly is probably due to the lower average density of the highly faulted and brecciated rocks in the central uplift. The thinning of the Knox Dolomite and its greater depth in the central uplift also may contribute to the local anomaly.

In general, the core and seismic data indicate a decrease in structural complexity with depth and away from the central uplift of the disturbance, which supports an impact-origin hypothesis. Figure 25E illustrates our structural model immediately following impact along the northwest-trending magnetic anomaly. In the model, a fault-bounded impact crater having a central uplifted peak and breccia accompanied by ejecta deposits near the surface overlies a structurally reactivated and down-dropped depression. A structural depression beneath a centrally uplifted peak is difficult to explain on the basis of the typical complex impact-crater model proposed by Pilkington and Grieve (1992) (fig. 26). To complicate matters further, cross-cutting structural relationships and mineralization events noted in core samples and outcrops strongly suggest a complex structural history prior to and following the impact. Figure 25F illustrates our model of the present-day disturbance based on well control and geophysical data. Erosion has removed a significant portion of the centrally uplifted peak and all evidence of an impact crater and ejecta deposits. The structural depression beneath the central uplift shown in the model possibly formed independent of the impact, but, as indicated in the section on geophysical data, the actual mode of formation is poorly understood.

Most of the circumstantial evidence suggests reactivation of Precambrian faulting during the Cambrian and Early Ordovician.

Most of the breccias observed in the cores undoubtedly were produced by recurrent fault movement related to the Precambrian basement in addition to impact. Sedimentary breccias are known to be present in the Peebles and Knox Dolomites outside the Serpent Mound disturbance, and some of the breccias in cores DGS 3274 and 3275 most likely are sedimentary breccias. In most cases, we were unable to conclusively distinguish between breccia types in the Peebles and Knox Dolomites. The mixed-lithic breccias are almost certainly impact related because of the presence of PDF's in many of them.

In rare instances, the breccia-filled fractures contain clasts and matrix of a darker lithology (see figs. 16, 17, and 20). Carlton and others (1998a, b) speculated that this anomalous lithology is an altered impact-melt rock (?) replaced by dark-gray carbonate and pyrite. Impact-melt rock has been reported at the Manson, Iowa, crater (Anderson and others, 1996) and other North American craters (Koeberl and Anderson, 1996). Further mineralogical work needs to done on this dark material to determine origin and diagenetic relationships.

The apparent absence of coesite in the Serpent Mound disturbance should not be used as evidence against an impact origin. If coesite was formed in the Serpent Mound disturbance, it was probably near ground zero, where shock pressures were highest. The disturbance is between 256 and 330 million years old and highly eroded. It is quite possible that any coesite formed has been removed and dispersed by erosion.

CONCLUSIONS

The discovery of PDF's and an Ir anomaly, along with a myriad of supporting evidence, confirms the meteorite impact origin for the Serpent Mound disturbance. Paleomagnetic data indicate the structure cannot be younger than Late Permian, and Mississippi Valley-type mineralization restrict it to being no older than Late Pennsylvanian.

The Paleozoic and Precambrian rocks at the site of the Serpent Mound meteorite impact have had a long and complex geologic history. Seismic and core data indicate movement on pre-existing faults in Precambrian rocks. Some of this movement occurred before the impact took place, but certainly some occurred afterward, modifying and collapsing the original impact structure. Reactivation of these faults apparently has occurred throughout the Paleozoic. Prior to the impact, basement faulting, uplift, depositional facies changes, and possibly subsidence occurred. In the time since the impact, geologic events, including erosion, faulting, mineralization, and continued subsidence, have drastically modified the structure.

The exact relationship between the Serpent Mound disturbance and the geologic anomalies beneath the central uplift are far from completely understood. More work is required to determine whether the meteorite impacted precisely in the center of a subsurface structural trend or to the side of such feature. The Serpent Mound meteorite impact locally affected the rocks in a spectacular way, creating a structure that can still be recognized after more than 256 million years. Although our understanding of this structure is incomplete, it can now be said with authority that a meteorite impacting the Earth created the structure.

EXPLANATION

- Ejecta breccia
- Crater fall-back breccia
- Breccia zone
- Mixed-lithic breccia zone
- Mississippian, Pennsylvanian, and Permian rocks
- Salina Group through Berea Sandstone
- Bisher Formation through Tymochtee Dolomite
- Estill Shale
- Ordovician and Silurian rocks through top of Dayton Formation
- Black River Group
- Carntown unit of the Black River Group and Wells Creek Formation
- Knox Dolomite
- Conasauga and Kerbel Formations
- Rome Formation reflector
- Rome Formation
- Mount Simon Sandstone
- Pre-Mount Simon arkosic sediments?
- Precambrian Grenville basement
- Northwest-trending magnetic high anomaly
- Unconformity
- Fault, arrow indicates relative direction of movement
- Reactivated Precambrian fault
- Well/core location
- ? Contact questionable

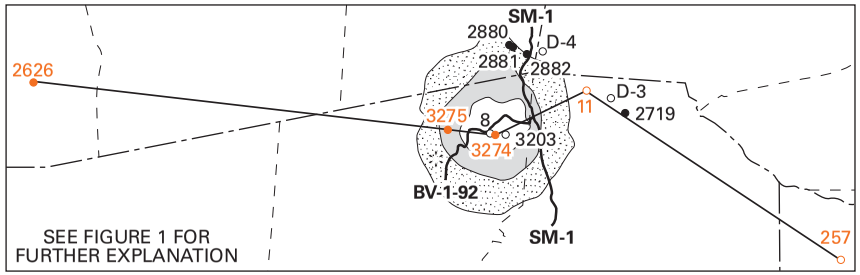

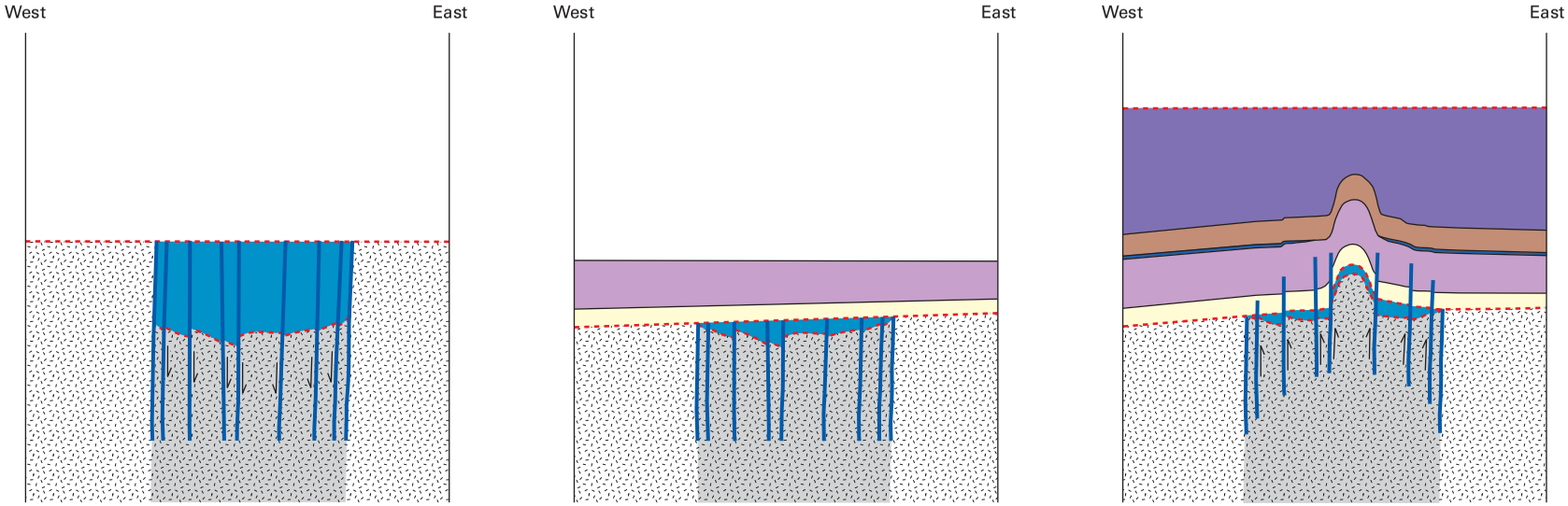

A Pre-Mount Simon sediments accumulate in a rift basin developed on an eroding, tectonically active Grenville landscape. Normal faults develop contemporaneously with sedimentation in response to rift extension forces acting on Grenville basement rocks. Axis of rifting is oriented along a northwest-trending magnetic high anomaly.

B Rifting and rift sedimentation cease. Erosion removes most of the sediments that had accumulated in the rift basin. Regional tectonism tilts eroded Precambrian Grenville and pre-Mount Simon rocks toward the west. Transgressing seas deposit sediments of the Mount Simon Sandstone and the Rome Formation across the region.

C Active tectonism resumes along the magnetic anomaly near the end of Rome Formation deposition and causes a structural high area and possible strike-slip fault movement above pre-existing faults. Structural uplift diminishes during deposition of the Conasauga and Kerbel Formations and resumes during Knox Dolomite deposition. Deposition ceases and a period of erosion begins on the Knox surface. Tectonic inversion and erosion cease by the end of Middle Ordovician time.

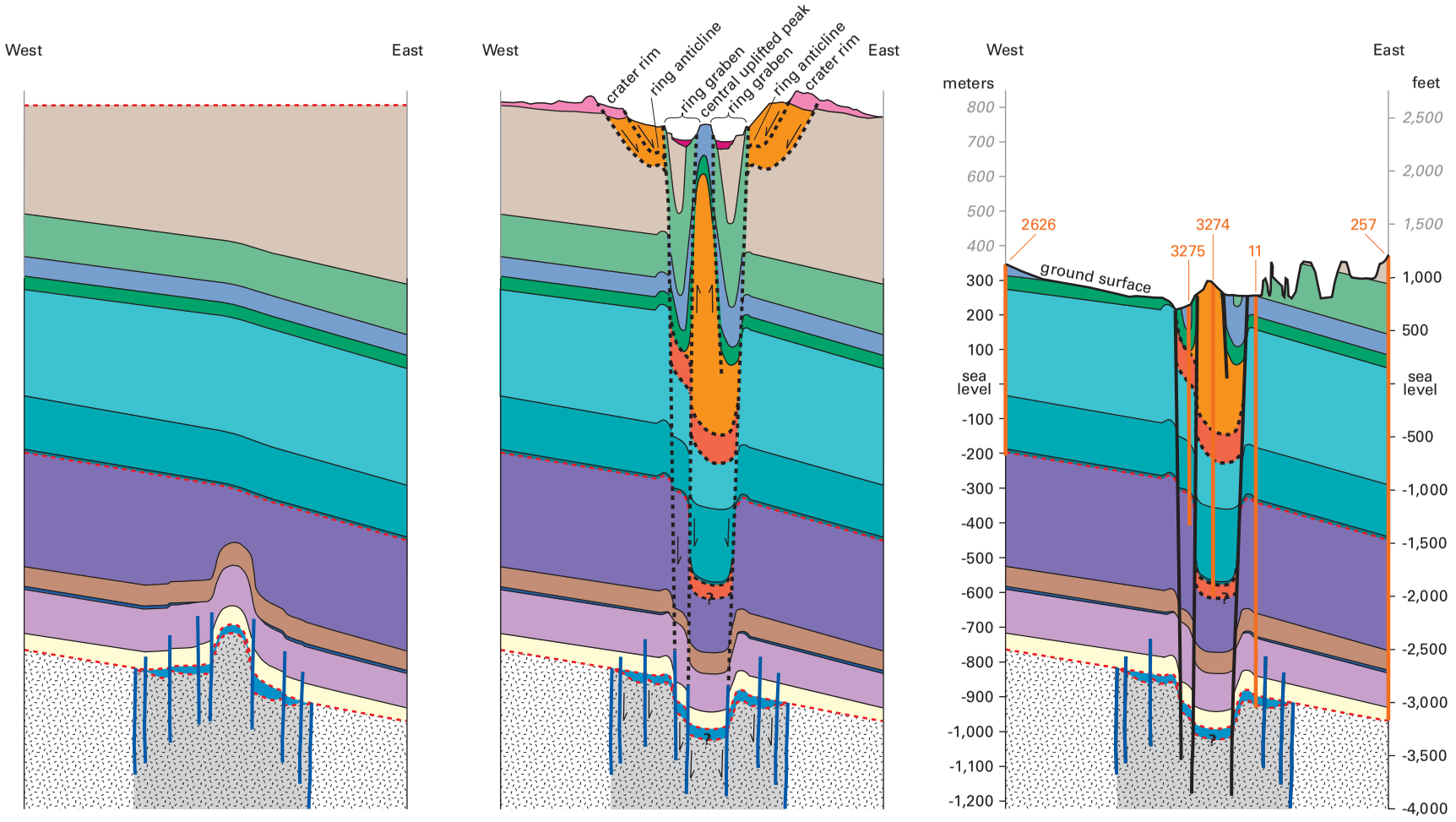

D Sedimentation across the region resumes in Middle Ordovician time and continues through Permian time. Subsidence of the Appalachian Basin beginning in Middle Ordovician time causes basement rocks and overlying strata to dip eastward. By late Paleozoic time, strata and basement rocks attain current extent of eastward dip. A pronounced monocline of more steeply dipping rocks develops on the east side of the magnetic anomaly.

E Some time in the late Paleozoic (Pennsylvanian-Permian time), a meteorite impacts northern Adams County along the existing northwest-trending magnetic anomaly/structurally disturbed zone. The force of the impact depresses underlying Paleozoic strata and Precambrian basement rocks along the reactivated basement-fault trend. Deep strata (Black River Group and deeper) remain depressed; however, strata overlying the Black River Group rebound following initial depression.

F Strata structurally disturbed by impact and impact breccia settle and collapse along new and existing faults. Erosion removes hundreds of feet of overlying strata to create present topography. This model of the subsurface geology underlying the disturbance is based on core samples (note core-hole locations) and seismic data collected within and outside the impact zone. Surface geology and topography across the feature are based on Reidel (1975) and open-file maps of the Division of Geological Survey.

FIGURE 25.—Proposed sequence of major structural events in the area of the Serpent Mound disturbance, shown in a series of diagrammatic west-east cross sections. See figure 24 for the location and extent of the northwest-trending magnetic high anomaly. See figure 5 for column of stratigraphic units.

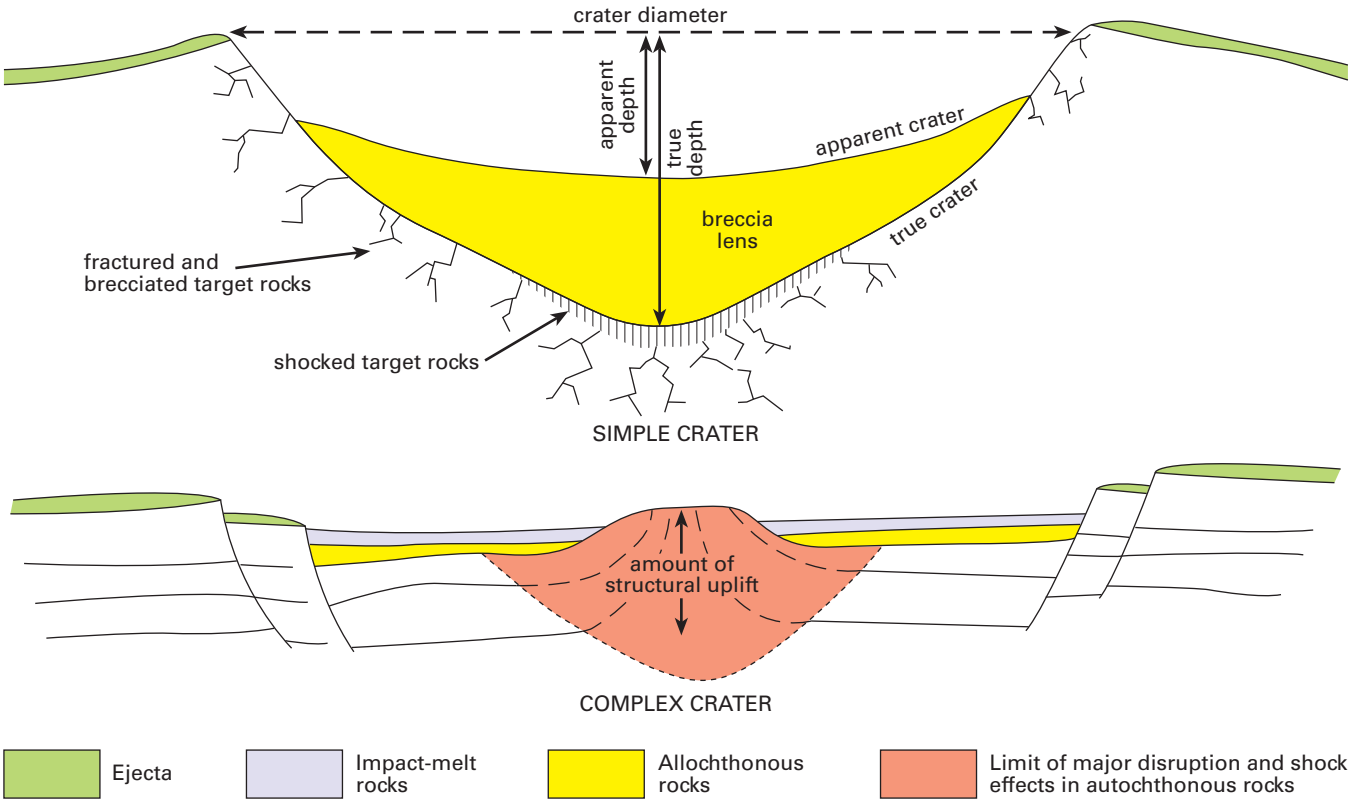

FIGURE 26.—Schematic cross sections of simple and complex craters, modified from Pilkington and Grieve (1992). No scale is implied.

REFERENCES CITED

Alexopoulos, J. S., Grieve, R. A. F., and Robertson, P. B., 1988, Microscopic lamellar deformation features in quartz: discriminative characteristics of shock-generated varieties: Geology, v. 16, p. 796-799.

Ammerman, M. L., and Keller, G. R., 1979, Delineation of Rome Trough in eastern Kentucky by gravity and deep drilling data: American Association of Petroleum Geologists Bulletin, v. 63, p. 341-353.

Anderson, R. R., Witzke, B. J., and Roddy, D. J., 1996, The drilling of the 1991-1992 Geological Survey Bureau and U.S. Geological Survey Manson impact structure cores, *in* Koeberl, Christian, and Anderson, R. R., eds., The Manson impact structure, Iowa: anatomy of an impact crater: Geological Society of America Special Paper 302, p. 45-88.

Baranoski, M. T., 1993, Interpretation of seismic data acquired over the Serpent Mound disturbance in Adams County, Ohio: Paper presented at Ohio Geological Society Special Meeting, An update on Ohio's subsurface geology, Canton, Ohio.

_____ 2002, Structure contour map on the Precambrian unconformity surface in Ohio and related basement features: Ohio Division of Geological Survey Map PG-23, scale 1:500,000, and 18-page text.

Baranoski, M. T., and Brockman, C. S., 1998, Field trip to Plum Run quarry and the Serpent Mound disturbance: American Association of Petroleum Geologists, 1998 Eastern Section Meeting, Columbus, Ohio, 17 p.

Baranoski, M. T., and Riley, R. A., 1993, Map of southeastern Ohio depicting structure contours on the Knox unconformity at 100-foot contour interval: Ohio Division of Geological Survey Digital Chart and Map Series (DCMS) 8, scale 1:250,000.

Baranoski, M. T., Riley, R. A., McDonald, James, and Brown, Tim, 1992, Map of southeastern Ohio showing wells reaching Knox unconformity and deeper: Ohio Division of Geological Survey Digital Chart and Map Series (DCMS) 1, scale 1:250,000.

Baranoski, M. T., Schumacher, G. A., Carlton, R. W., Watts, D. R., El-Saiti, Belgasem, and Koeberl, Christian, 1998, The Serpent Mound disturbance of south-central Ohio: the ultimate geological lottery (abs.): Geological Society of America Abstracts with Programs, v. 30, no. 2, p. 4.

Baranoski, M. T., Schumacher, G. A., Watts, D. R., Carlton, R. W., and El-Saiti, Belgasem, 1997, Hydrocarbon potential beneath the Knox unconformity in the vicinity of the Serpent Mound disturbance based upon new core and geophysical data, *in* Fifth Annual Technical Symposium: Ohio Geological Society Publication 14, p. 1-11.

Baranoski, M. T., and Watts, D. R., 1997,Cambrian hydrocarbon potential in the region of the Serpent Mound disturbance of southern Ohio (abs.): American Association of Petroleum Geologists Bulletin, v. 81, p. 1545.

_____ 2001, The Serpent Mound disturbance of southern Ohio: a structurally complex impact site with hydrocarbon potential from the Ordovician and Cambrian System reservoirs (abs.): American Association of Petroleum Geologists Bulletin, v. 85, p. 1530.

Baranoski, M. T., Watts, D. R., El-Saiti, Belgasem, Schumacher, G. A., and Carlton, R. W., 1998a, Interpretation of seismic and gravity data from the Serpent Mound disturbance of south-central Ohio (abs.): Geological Society of America Abstracts with

Programs, v. 30, no. 2, p. 4.
_____ 1998b, Analysis of core fractures and structure at the Serpent Mound disturbance site in south-central Ohio, U.S.A. (abs.): The Woodworth Conference on Rock Fractures, Abstracts with Programs, Geological Society of London, Tectonic Studies Group, University of Ulster, Coleraine, Northern Ireland (not paged).
Baranoski, M. T., and Wickstrom, L. H., 1994, Map of basement structures in Ohio: Ohio Division of Geological Survey Digital Chart and Map Series (DCMS) 7, scale 1:500,000.
Bass, M. N., 1960, Grenville boundary in Ohio: Journal of Geology, v. 68, p. 673-677.
Bayley, R. W., and Muehlberger, W. R., compilers, 1968, Basement rock map of the United States (exclusive of Alaska and Hawaii): U.S. Geological Survey, scale 1:2,500,000.
Beardsley, R. W., and Cable, M. S., 1983, Overview of the evolution of the Appalachian Basin: Northeastern Geology, v. 5, p. 137-145.
Billings, M. P., 1972, Structural geology: Englewood, New Jersey, Prentice-Hall, Inc., 606 p.
Botoman, George, and Stieglitz, R. D., 1978, The occurrence of sulfide and associated minerals in Ohio: Ohio Division of Geological Survey Report of Investigations 104, 11 p.
Bowman, R. S., 1956, Stratigraphy and paleontology of the Niagaran Series in Highland County, Ohio: Ph.D. dissertation (unpub.), The Ohio State University, 339 p.
Bownocker, J. A., compiler, 1920, Geologic map of Ohio: Ohio Division of Geological Survey Map 1, scale 1:500,000.
Bucher, W. H., 1921, Cryptovolcanic structure in Ohio of the type of the Steinheim Basin (abs.): Geological Society of America Bulletin, v. 32, p. 74-75.
_____ 1925, Über kryptovulkanische Erscheinungen in Ohio und Kentucky: Eclogae Geologie Helvetiae, v. 19, p. 141-143.
_____ 1933, Über eine typische kryptovulkanische Störung im südlichen Ohio: Geologische Rundschau, v. 23a (Salomon-Calvi Festschrift), p. 65-80.
_____ 1935, A crypto-volcanic structure in southern Ohio: Compass, v. 15, p. 157-162.
_____ 1936, Cryptovolcanic structures in the United States: International Geologic Congress, 1933, Report of the 16th Session, v. 2, p. 1055-1084.
_____ 1963, Cryptoexplosion structure caused from without or within the Earth? ("astroblemes" or "geoblemes"): American Journal of Science, v. 261, p. 597-649.
Bull, Colin, Corbató, C. E., and Zahn, J. C., 1967, Gravity survey of the Serpent Mound area, southern Ohio: Ohio Journal of Science, v. 67, p. 359-371.
Cable, M. S., and Beardsley, R.W., 1984, Structural controls on Late Cambrian and Early Ordovician carbonate sedimentation in eastern Kentucky: American Journal of Science, v. 284, p. 797-823.
Carlson, E. H., 1991, Minerals of Ohio: Ohio Division of Geological Survey Bulletin 69, 155 p.
Carlton, R. W., Koeberl, Christian, Baranoski, M. T., and Schumacher, G. A., 1998a, Discovery of planar deformation features at the Serpent Mound disturbance, south-central Ohio: unequivocal evidence for an impact (abs.): Geological Society of America Abstracts with Programs, v. 30, no. 2, p. 8.
_____ 1998b, Discovery of microscopic evidence for shock metamorphism at the Serpent Mound disturbance, south-central Ohio: confirmation of an origin by impact: Earth and Planetary Science Letters, v. 162, p. 177-185.
Carman, J. E., and Schillhahn, E. O., 1930, The Hillsboro Sandstone of Ohio: Ohio Journal of Science, v. 30, p. 246-261.
Cohen, A. J., Bunch, T. E., and Reid, A. M., 1961, Coesite discoveries establish cryptovolcanics as fossil meteorite craters: Science, v. 134, p. 1624-1625.
Cohen, A. J., Reid, A. M., and Bunch, T. E., 1962, Central uplifts of terrestrial and lunar craters. Part 1, Kentland and Serpent Mound disturbances (abs.): Journal of Geophysical Research, v. 67, p. 1632-1633.
Court, P. R., and Kahle, C. F., 1993, Stratigraphy and sedimentology of some Silurian rocks in southwestern Ohio: Society for Sedimentary Geology (SEPM), Great Lakes Section fall field trip, 30 p.
Cramer, F. H., and Díez de Cramer, M. C. R., 1972, North American Silurian palynofacies and their spatial arrangement: acritarchs: Palaeontographica Abteilung, v. B138, p. 107-180.
Cressman, E. R., 1973, Lithostratigraphy and depositional environments of the Lexington Limestone of central Kentucky: U.S. Geological Survey Professional Paper 768, 61 p.
Culotta, R. C., Pratt, T., and Oliver, J., 1990, A tale of two sutures: COCORP deep seismic surveys of the Grenville province in the eastern U.S. midcontinent: Geology, v. 18, p. 646-649.
Denison, R. E., Lidiak, E. G., Bickford, M. E., and Kisvarsanyi, E. B., 1984, Geology and geochronology of Precambrian rocks in the Central Interior region of the United States: U.S. Geological Survey Professional Paper 1241-C, 20 p.
Dennison, J. M., 1976, Appalachian Queenston delta related to eustatic sea-level drop accompanying Late Ordovician glaciation centered in Africa, *in* Bassett, M. G., ed., The Ordovician System: Proceedings of a Palaeontological Association Symposium: Cardiff, Wales, University of Wales Press and National Museum of Wales, p. 107-120.
Dietz, R. S., 1959, Shatter cones in cryptoexplosion structures (meteorite impact?): Journal of Geology, v. 67, p. 496-505.
_____1960, Meteorite impact suggested by shatter cones in rock: Science, v. 131, p. 1781-1784.
_____ 1968, Shatter cones in cryptoexplosion structures, *in* French, B. M., and Short, N. M., eds., Proceedings of the 1st Conference on Shock Metamorphism of Natural Materials (1966): Baltimore, Maryland, Mono Book Corp., p. 267-285.
Dolly, E. D., and Busch, D. A., 1972, Stratigraphic, structural, and geomorphologic factors controlling oil accumulation in Upper Cambrian strata of central Ohio: American Association of Petroleum Geologists Bulletin, v. 56, p. 2335-2368.
Drahovzal, J. A., Harris, D. C., Wickstrom, L. H., Walker, Dan, Baranoski, M. T., Keith, Brian, and Furer, L. C., 1992, The East Continent Rift Basin: a new discovery: Ohio Division of Geological Survey Information Circular 57, 25 p.
Elias, R. J., 1983, Middle and Late Ordovician solitary rugose corals of the Cincinnati Arch region: U.S. Geological Survey Professional Paper 1066-N, p. 1-13.
El-Saiti, B. M. B., 1998, Geophysical studies of the Serpent Mound structure, Adams County, Ohio, U.S.A.: Ph.D. dissertation (unpub.), University of Glasgow (Scotland), 341 p.
Ettensohn, F. R., 1985, The Catskill Delta complex and the Acadian orogeny, *in* Woodrow, D. W., and Devon, W. D., eds, The Catskill Delta: Geological Society of America Special Paper 201, p. 39-49.
_____ 1987, Rates of relative plate motion during the Acadian orogeny based on the spatial distribution of black shales: Journal of Geology, v. 95, p. 572-582.
_____ 1991, Flexural interpretation of relationships between Ordovician tectonism and stratigraphic sequences, central and southern Appalachians, U.S.A., *in* Barnes, C. R., and Williams, S. H., eds., Advances in Ordovician geology: Geological Survey of Canada Paper 90-9, p. 213-224.
_____ 1992, General Devonian paleogeographic and tectonic framework for Kentucky, *in* Ettensohn, F. R., ed., Changing interpretations of Kentucky geology—layer-cake, facies, flexure, and eustacy: Ohio Division of Geological Survey Miscellaneous Report 5, p. 32-40.
Flaugher, D. M., 1973, A gravity survey of the Serpent Mound cryptoexplosion structure and surrounding area in southern Ohio: M.S. thesis (unpub.), Wright State University, 114 p.

Fletcher, R. V., Cameron, T. L., Lepper, B. T., Wymer, D. A., and Pickard, William, 1996, Serpent Mound: a Fort Ancient icon?: Midcontinental Journal of Archaeology, v. 21, p. 105-143.

Foerste, A. F., 1935, Correlation of Silurian formations in southwestern Ohio, southeastern Indiana, Kentucky, and western Tennessee: Journal of the Scientific Laboratories of Denison University, v. 30, p. 119-205.

Forsyth, J. L., and Bowman, R. S., 1963, Geology of the Highland-Adams County area: Guidebook for field trip, Ohio Academy of Science 38th annual field conference, 32 p.

French, B. M., and Short, N. M., eds., 1968, Proceedings of the 1st Conference on Shock Metamorphism of Natural Materials: Baltimore, Maryland, Mono Book Corp., 644 p.

Galbraith, R. M., IV, 1968, Peripheral deformation of the Serpent Mound cryptoexplosion structure in Adams County, Ohio: M.S. thesis (unpub.), University of Cincinnati, 47 p.

Galbraith, R. M., IV, and Koucky, F. L., 1969, Peripheral deformation of the Serpent Mound cryptoexplosion structure in Adams County, Ohio (abs.): Geological Society of America Abstracts with Programs, v. 1, p. 17.

Goddard, E. N., chairman, 1948, Rock color chart: Geological Society of America, Rock-Color Chart Committee.

Goldthwait, R. P., and Van Horn, R. G., 1993, Quaternary geology of Ohio, Columbus quadrangle: Ohio Division of Geological Survey Open-File Map 298, scale 1:250,000.

Gonterman, J. R., 1973, Petrographic study of the Precambrian of Ohio: M.S. thesis (unpub.), Ohio State University, 140 p.

Gordon, L. A., and Ettensohn, F. R., 1984, Stratigraphy, depositional environment, and regional dolomitization of the Brassfield Formation (Llandoverian) in east-central Kentucky: Southeastern Geology, v. 25, p. 101-115.

Grahn, Yngve, 1985, Llandoverian and early Wenlockian Chitinozoa from southern Ohio and northern Kentucky, U.S.A.: Palynology, v. 9, p. 147-164.

Grahn, Yngve, and Bergström, S. M., 1985, Chitinozoans from the Ordovician-Silurian boundary beds in the eastern Cincinnati region in Ohio and Kentucky: Ohio Journal of Science, v. 85, p. 175-183.

Green, D. A., 1957, Trenton structure in Ohio, Indiana and northern Illinois: American Association of Petroleum Geologists Bulletin, v. 41, p. 627-642.

Grieve, R. A. F., Langenhorst, Falko, and Stöffler, Dieter, 1996, Shock metamorphism of quartz in nature and experiment: II. Significance in geoscience: Meteoritics & Planetary Science, v. 31, p. 6-35.

Grieve, R. A. F., and Pilkington, Mark, 1996, The signature of terrestrial impacts: AGSO Journal of Geology and Geophysics, v. 16, p. 399-420.

Hambrey, M. J., 1985, The Late Ordovician-Early Silurian glacial period: Paleogeography, Paleoclimatology, Paleoecology, v. 51, p. 273-289.

Hansen, M. C., 1982, Diamonds from Ohio: Ohio Geology Newsletter, Fall, p. 1-3.

_____ 1984, "Journey to the center of the Earth"—the aeromagnetic map of Ohio: Ohio Geology Newsletter, Summer, p. 1-6.

_____ 1994, Return to Sunken Mountain: the Serpent Mound cryptoexplosion structure: Ohio Geology Newsletter, Winter, p. 1-7.

_____ 1998, The Serpent Mound disturbance: Timeline (Ohio Historical Society), v. 15, p. 46-51.

Heirendt, K. M., 1988, An analysis of ^{222}Rn soil gas concentrations in the Serpent Mound area, southwestern Ohio: M.S. thesis (unpub.), University of Akron, 86 p.

Heiskanen, W. A., and Uotila, U. A., 1956, Gravity survey of the State of Ohio: Ohio Division of Geological Survey Report of Investigations 30, 34 p.

Heyl, A. V., and Brock, M. R., 1962, Zinc occurrence in the Serpent Mound disturbance of southern Ohio: U.S. Geological Survey Professional Paper 450-D, p. 95-97.

Hildenbrand, T. G., and Kucks, R. P., 1984a, Residual total intensity magnetic map of Ohio: U.S. Geological Survey Geophysical Investigations Map GP-961, scale 1:500,000.

Hildenbrand, T. G., and Kucks, R. P., 1984b, Complete Bouguer gravity anomaly map of Ohio: U.S. Geological Survey Geophysical Investigations Map GP-962, scale 1:500,000.

Horvath, A. L., 1967, Relationships of Lower Silurian strata in Ohio, West Virginia, and northern Kentucky: Ohio Journal of Science, v. 67, p. 341-359.

_____ 1969, Relationships of Middle Silurian strata in Ohio and West Virginia: Ohio Journal of Science, v. 69, p. 321-342.

Hyde, J. E., 1953, The Mississippian formations of central and southern Ohio: Ohio Division of Geological Survey Bulletin 51, 355 p.

Ingram, R. L., 1954, Terminology for the thickness of stratification and parting units in sedimentary rocks: Geological Society of America Bulletin, v. 65, p. 937-938.

Istok, J. D., 1978, Paleomagnetism at Serpent Mound: B.S. thesis (unpub.), Ohio State University, 16 p.

Jackson, J. A., ed., 1997, Glossary of geology (4th ed.): Falls Church, Virginia, American Geological Institute, 769 p.

Jackson, Mike, and Van der Voo, Rob, 1986, A paleomagnetic estimate of the age and thermal history of the Kentland, Indiana cryptoexplosion structure: Journal of Geology, v. 94, p. 713-723.

Jacobs, A. J., 1971, The geology of southern Adams County, Ohio: Senior thesis (unpub.), University of Cincinnati, 25 p.

Janssens, Adriaan, 1973, Stratigraphy of the Cambrian and Lower Ordovician rocks in Ohio: Ohio Division of Geological Survey Bulletin 64, 197 p.

_____ 1977, Silurian rocks in the subsurface of northwestern Ohio: Ohio Division of Geological Survey Report of Investigations 100, 96 p.

Kahle, C. F., 1988, Surface and subsurface paleokarst, Silurian Lockport, and Peebles Dolomites, western Ohio, *in* James, N. P., and Choquette, P. W., eds., Paleokarst: New York, Springer-Verlag, 416 p.

Kepferle, R. C., and Roen, J. B., 1981, Chattanooga and Ohio Shales of the southern Appalachian basin, *in* Roberts, T. G., ed., GSA Cincinnati '81 Field Trip Guidebooks: American Geological Institute, v. 2, p. 259-362.

Kieffer, S. W., 1980, The role of volatiles and lithology in the impact cratering process: Reviews of Geophysics and Space Physics, v. 18, p. 143-181.

Kirschner, C. E., Grantz, Arthur, and Mullen, M. W., 1992, Impact origin of the Avak structure, Arctic Alaska, and genesis of the Barrow gas fields: American Association of Petroleum Geologists Bulletin, v. 76, p. 651-679.

Kleffner, M. A., 1987, Conodonts of the Estill Shale and Bisher Formation (Silurian, southern Ohio): biostratigraphy and distribution: Ohio Journal of Science, v. 87, p.78-89.

Kleffner, M. A., and Ausich, W. I., 1988, Lower and Middle Silurian of the eastern flank of the Cincinnati Arch and the Appalachian Basin margin, Ohio: Field trip guidebook, Society of Economic Paleontologists and Mineralogists, 5th midyear meeting, Columbus, Ohio, 25 p.

Koeberl, Christian, 1997, Impact cratering: the mineralogical and geochemical evidence, *in* Johnson, K. S., and Campbell, J. A., eds., Ames structure in northwest Oklahoma and similar features: origin and petroleum production (1995 symposium): Oklahoma Geological Survey Circular 100, p. 30-54.

Koeberl, Christian, and Anderson, R. R., 1996, Manson and company: impact structures in the United States, *in* Koeberl, Christian, and Anderson, R. R., eds., The Manson impact structure, Iowa: anatomy of an impact crater: Geological Society of America Special Paper 302, p. 1-29.

Koeberl, Christian, Buchanan, P. C., and Carlton, R. W., 1998, Petrology and geochemistry of drill core samples from the Serpent Mound disturbance, Ohio: confirmation of impact origin: Lunar and Planetary Science, v. 29, abstract #1392 (CD-ROM).

Koeberl, Christian, and Reimold, W. U., 1995, The Newporte impact structure, North Dakota, USA: Geochimica et Cosmochimica Acta, v. 59, p. 4747-4767.

Koeberl, Christian, and Shirey, S. B., 1996, Manson impact structure, Iowa: Re-Os isotope systematics indicate presence of cosmic component in impact breccia (abs.): Geological Society of America Abstracts with Programs, v. 26, p. 24.

Koucky, F. L., 1975, Serpent Mound cryptoexplosion structure: Field trip guidebook for the 26th annual Ohio Intercollegiate Field Conference, College of Wooster, 60 p.

Koucky, F. L., and Reidel, S. P., 1987, The Serpent Mound disturbance, south-central Ohio, *in* Biggs, D. L., ed., North-Central Section of the Geological Society of America: Geological Society of America Centennial Field Guide, v. 3, p. 431-436.

Kulander, B. R., Dean, S. L., and Ward, B. J., Jr., 1990, Fractured core analysis—interpretation, logging, and use of natural and induced fractures in core: Association of Petroleum Geologists, Methods in Exploration Series, No. 8, 88 p.

Langford, C. S., 1984, A gravity survey of northeastern Adams County, Ohio: M.S. thesis (unpub.), Ohio State University, 170 p.

Lidiak, E. G., and Zietz, Isidore, 1976, Interpretation of aeromagnetic anomalies between latitudes 37ºN and 38ºN in the eastern and central United States: Geological Society of America Special Paper 167, 37 p.

Locke, John, 1838, Geological report (on southwestern Ohio): Ohio Division of Geological Survey Second Annual Report, p. 201-286.

Lucht, T. E., and Brown, D. L., 1994, Soil survey of Adams County, Ohio: U.S. Department of Agriculture, Soil Conservation Service, 199 p.

Lucius, J. E., and Von Frese, R. R. B., 1988, Aeromagnetic and gravity anomaly constraints on the crustal geology of Ohio: Geological Society of America Bulletin, v. 100, p. 104-116.

Luft, S. J., Osborne, R. H., and Weiss, M. P., 1973, Geologic map of the Moscow quadrangle, Ohio–Kentucky: U.S. Geological Survey Geologic Quadrangle Map GQ-1069, scale 1:24,000.

McCabe, Chad, and Elmore, R. D., 1989, The occurrence and origin of Late Paleozoic remagnetization in the sedimentary rocks of North America: Reviews of Geophysics, v. 27, p. 471-494.

McCormick, G. R., 1961, Petrology of Precambrian rocks of Ohio: Ohio Division of Geological Survey Report of Investigations 41, 60 p.

McDowell, R. C., 1983, Stratigraphy of the Silurian outcrop belt on the east side of the Cincinnati Arch in Kentucky, with revisions in the nomenclature: U.S. Geological Survey Professional Paper 1151-F, 27 p.

McFarlan, A. C., and Freeman, L. B., 1935, Rogers Gap and Fulton Formations in central Kentucky: Geological Society of America Bulletin, v. 46, p. 1975-2006.

McFarland, B. P., 1999, Mineralization in the Serpent Mound disturbance: an investigation using sulfur isotopes, fluid inclusions, and trace elements: M.S. thesis (unpub.), Kent State University, 201 p.

McFarland, B. P., and Carlson, E. H., 1994, Sulfur isotope investigation of the Serpent Mound district, southwest Ohio (abs.): EOS (American Geophysical Union), Abstracts with Programs, v. 75, no. 16, p. 356.

_____ 1995a, The Serpent Mound disturbance, southwest Ohio: a new model based on mineralogy, sulfur isotopes, and trace element geochemistry (abs.): Proceedings, International Field Conference on Carbonate-Hosted Lead-Zinc Deposits, St. Louis, p. 204-206.

_____ 1995b, Unraveling the enigma of the Serpent Mound cryptoexplosion structure (abs.): Program and Abstracts, Fifth V. M. Goldschmidt Conference, University Park, Pennsylvania, p. 71.

_____ 1996, Evidence for Late Paleozoic brine migration in the Serpent Mound District, southwestern Ohio (abs.): Geological Society of America Abstracts with Programs, v. 28, no. 3, p. 79.

McFarland, B. P., McMasters, P. C., Sanfrey, S. L., D'Amato, E. J., Miller, T. L., and Carlson, E. H., 1993, Trace metal patterns in stream sediments and panned concentrates, Serpent Mound disturbance, southwest Ohio (abs.): Geological Society of America Abstracts with Programs, v. 25, p. 278.

McFarland, B. P., and Talnagi, J. W., Jr., 1994, Mineralogic and trace element studies from the Serpent Mound District, southwest Ohio (abs.): Geological Society of America Abstracts with Programs, v. 26, no. 7, p. 500.

McGuire, W. H., and Howell, Paul, 1963, Oil and gas possibilities of the Cambrian and Ordovician in Kentucky: Report prepared by Spindletop Research for Department of Commerce, Commonwealth of Kentucky, 134 p.

Meyer, R. F., and Sweeney, J. W., 1968, Asphalt, heavy crude oil, and shallow oil reservoirs, *in* Mineral resources of the Appalachian region: U.S. Geological Survey Professional Paper 580, p. 96-101.

Milton, D. J., 1977, Shatter cones—an outstanding problem in shock mechanics, *in* Roddy, D. J., Pepin, R. O., and Merrill, R. B., eds., Impact and explosion cratering: New York, Pergamon Press, p. 703-714.

Mitchell, C. E., and Bergström, S. M., 1991, New graptolite and lithostratigraphic evidence from the Cincinnati region, U.S.A., for the definition and correlation of the base of the Cincinnatian Series (Upper Ordovician), *in* Barnes, C. R., and Williams, S. H., eds., Advances in Ordovician geology: Geological Survey of Canada Paper 90-9, p. 59-77.

Muehlberger, W. R., Denison, R. E., and Lidiak, E. G., 1967, Basement rocks in the continental interior of the United States: American Association of Petroleum Geologists Bulletin, v. 51, p. 2351-2380.

Mussman, W. J., and Read, J. F., 1986, Sedimentology and development of a passive- to convergent-margin unconformity: Middle Ordovician Knox unconformity, Virginia, Appalachians: Geological Society of America Bulletin, v. 97, p. 282-295.

Orton, Edward, 1871, The geology of Highland County: Ohio Division of Geological Survey Report of Progress in 1870, p. 253-310.

Pashin, J. C., and Ettensohn, F. R., 1995, Reevaluation of the Bedford-Berea sequence in Ohio and adjacent states: forced regression in a foreland basin: Geological Society of America Special Paper 298, 68 p.

Peck, J. H., 1966, Upper Ordovician formations in the Maysville area, Kentucky: U.S. Geological Survey Bulletin 1244-B, 30 p.

Pilkington, Mark, and Grieve, R. A., 1992, The geophysical signature of terrestrial impact craters: Reviews of Geophysics, v. 30, p. 161-181.

Potter, P. E., 1996, Exploring the geology of the Cincinnati/northern Kentucky region: Kentucky Geological Survey Special Publication 22, Series XI, 115 p.

Potter, P. E., Ausich, W. I., Klee, John, Krissek, L. A., Mason, C. E., Schumacher, G. A., Wilson, R. T., and Wright, E. M., 1991, Geology of the Alexandria-Ashland Highway (Kentucky Highway 546), Maysville to Garrison (Field trip guidebook and roadlog for the joint field conference of the Geological Society of Kentucky and Ohio Geological Society): Kentucky Geological Survey, 64 p.

Reidel, S. P., 1970, A geochemical survey of the western portion of the Serpent Mound cryptoexplosion structure: B.S. thesis (unpub.), University of Cincinnati, 24 p.

_____ 1972, Geology of the Serpent Mound cryptoexplosion structure: M.S. thesis (unpub.), University of Cincinnati, 150 p.
_____ 1975, Bedrock geology of the Serpent Mound cryptoexplosion structure, Adams, Highland, and Pike Counties, Ohio: Ohio Division of Geological Survey Report of Investigations 95, map with text.
_____1981, The Serpent Mound disturbance, south-central Ohio: an example of hydrotectonics (abs.): EOS (American Geophysical Union), v. 62, no. 45, p. 1047.
Reidel, S. P., and Koucky, F. L., 1981, The Serpent Mound cryptoexplosion structure, southwestern Ohio, *in* Roberts, T. G., ed., GSA Cincinnati '81 Field Trip Guidebooks: American Geological Institute, v. 2, p. 391-403.
Reidel, S. P., Koucky, F. L., and Stryker, J. R., 1982, The Serpent Mound disturbance, southwestern Ohio: American Journal of Science, v. 282, p. 1343-1377.
Rexroad, C. B., 1967, Stratigraphy and conodont paleontology of the Brassfield (Silurian) in the Cincinnati Arch area: Indiana Geological Survey Bulletin 36, 64 p.
Rexroad, C. B., and Kleffner, M. A., 1984, The Silurian stratigraphy of east-central Kentucky and adjacent Ohio, *in* Rast, Nicholas, and Hay, H. B., eds., Field trip guides for the Geological Society of America Annual Meeting, Southeastern and North-Central Sections, Lexington, Kentucky: University of Kentucky, p. 44-65.
Rexroad, C. B., Branson, E. R., Smith, M. O., Summerson, Charles, and Boucot, A. J., 1965, The Silurian formations of east-central Kentucky and adjacent Ohio: Kentucky Geological Survey Bulletin 2, Series X, 34 p.
Riley, R. A., Harper, J. A., Baranoski, M. T., Laughrey, C. D., and Carlton, R. W., 1993, Measuring and predicting reservoir heterogeneity in complex deposystems: the Late Cambrian Rose Run sandstone of eastern Ohio and western Pennsylvania: Report prepared for U.S. Department of Energy, Contract No. DE-AC22-90BC14657, 257 p.
Rogers, J. K., 1936, Geology of Highland County: Ohio Division of Geological Survey Bulletin 38, 148 p.
Rudman, A. J., Summerson, C. H., and Hinze, W. J., 1965, Geology of basement in midwestern United States: American Association of Petroleum Geologists Bulletin, v. 49, p. 894-904.
Sappenfield, L. W., 1950, A magnetic survey of the Adams County cryptovolcanic structure: M.S. thesis (unpub.), University of Cincinnati, 27 p.
_____ 1951, A magnetic survey of the Adams County, Ohio cryptovolcanic structure: Compass, v. 28, p. 115-124.
Schmidt, R. G., McFarlan, A. C., Nosow, Edmund, Bowman, R. S., and Alberts, Robert, 1961, Examination of Ordovician through Devonian stratigraphy and the Serpent Mound chaotic structure area, Field trip 8: Geological Society of America, Guidebook for Field Trips, Cincinnati meeting, p. 259-293.
Schumacher, G. A., 1992, Lithostratigraphy, cyclic sedimentation, and event stratigraphy of the Maysville, Kentucky, area, Day 3, Stop 8, *in* Ettensohn, F. R., ed., Changing interpretations of Kentucky geology—layer-cake, facies, flexure, and eustacy: Ohio Division of Geological Survey Miscellaneous Report 5, p. 165-172.
Schumacher, G. A., Baranoski, M. T., Carlton, R. W., Watts, D. R., and El-Saiti, B. M., 1998, The Serpent Mound disturbance revisited: new core data (abs.): Geological Society of America Abstracts with Programs, v. 30, no. 2, p. 70.
Schumacher, G. A., Bergström, S. M., and Mitchell, C. E., 1991, The Sebree Trough Project 4: preliminary tracing of surficial Upper Ordovician lithostratigraphic units into the subsurface of western and northern Ohio (abs.): Geological Society of America Abstracts with Programs, v. 23, no. 3, p. 59.
Schumacher, G. A., and Hay, H. B., 1995, Cyclic sedimentation in the Arnheim Formation (Upper Ordovician) of Ohio, Indiana, and northeastern Kentucky: lithostratigraphic implications (abs.): Geological Society of America Abstracts with Programs, v. 27, no. 2, p. 85.
Schumacher, G. A., Swinford, E. M., and Shrake, D. L., 1991, Lithostratigraphy of the Grant Lake Limestone and Grant Lake Formation (Upper Ordovician) in southwestern Ohio: Ohio Journal of Science, v. 91, p. 56-68.
Scotese, C. R., and McKerrow, W. S., 1990, Revised World maps and introduction, *in* McKerrow, W. S., and Scotese, C. R., eds., Paleozoic paleogeography and biogeography: Geological Society of London Memoir 12, p. 1-21.
Sharpton, V. L., and Grieve, R. A. F., 1990, Meteorite impact, cryptoexplosion, and shock metamorphism: a perspective on the evidence at the K/T boundary, *in* Sharpton, V. L., and Ward, P. D., eds., Global catastrophes in Earth history: Geological Society of America Special Paper 247, p. 301-318.
Sheriff, R. E., 1982, Encyclopedic dictionary of exploration geophysics: Society of Exploration Geophysicists, 266 p.
Shrake, D. L., 1991, The Middle Run Formation: a new stratigraphic unit in the subsurface of southwestern Ohio: Ohio Journal of Science, v. 91, p. 49-55.
Shrake, D. L., Carlton, R. W., Wickstrom, L. H., Potter, P. E., Richard, B. H., Wolfe, P. J., and Sitler, G. W., 1991, Pre-Mount Simon basin under the Cincinnati Arch: Geology, v. 19, p. 139-142.
Shrake, D. L., Schumacher, G. A., and Swinford, E. M., 1988, The stratigraphy, sedimentology, and paleontology of the Upper Ordovician Cincinnati group of southwest Ohio: Field trip guidebook, Society of Economic Paleontologists and Mineralogists (SEPM), 5th midyear meeting, Columbus, Ohio, 83 p.
Stith, D. A., 1979, Chemical composition, stratigraphy, and depositional environments of the Black River Group (Middle Ordovician), southwestern Ohio: Ohio Division of Geological Survey Report of Investigations 113, 36 p.
_____ 1986, Supplemental core investigations for high-calcium limestones in western Ohio and discussion of natural gas and stratigraphic relationships in the Middle and Upper Ordovician rocks of southwestern Ohio: Ohio Division of Geological Survey Report of Investigations 132, 16 p.
Stith, D. A., and Stieglitz, R. D., 1979, An evaluation of "Newberry" analysis data on the Brassfield Formation (Silurian), southwestern Ohio: Ohio Division of Geological Survey Report of Investigations 108, 25 p.
Stöffler, Dieter, and Langenhorst, Falko, 1994, Shock metamorphism of quartz in nature and experiment: I. Basic observations and theory: Meteoritics, v. 29, p. 155-181.
Stout, Wilber, 1941, Dolomites and limestones of western Ohio: Ohio Division of Geological Survey Bulletin 42, 468 p.
Stryker, J. R., 1971, Geologic and geochemical survey of the area south of Sinking Springs, Highland County, Ohio: B.S. thesis (unpub.), University of Cincinnati, 25 p.
Summerson, C. H., Forsyth, J. L., Hoover, K. V., and Ulteig, J. R., 1963, Stratigraphy of the Silurian rocks in western Ohio: Guidebook for the Michigan Basin Geological Society Annual Field Excursion, Michigan Geological Survey, 71 p.
Summerson, C. H., and Swann, D. H., 1970, Patterns of Devonian sand on the North American craton and their interpretation: Geological Society of America Bulletin, v. 81, p. 469-490.
Swanson, R. G., 1981, Sample examination manual: American Association of Petroleum Geologists Methods in Exploration Series, 31 p. plus 4 appendixes.
Sweet, W. C., 1979, Conodonts and conodont biostratigraphy of post-Tyrone Ordovician rocks of the Cincinnati region: U.S. Geological Survey Professional Paper 1066-G, 26 p.
Swinford, E. M., 1983, Geology of the Peebles quadrangle, Adams County, Ohio: M.S. thesis (unpub.), Eastern Kentucky University, 104 p.
_____ 1985, Geology of the Peebles quadrangle, Adams County, Ohio: Ohio Journal of Science, v. 85, p. 218-230.
_____ 1991, Bedrock geologic map of the Peebles quad-

rangle: Ohio Division of Geological Survey open-file map, scale 1:24,000.

Swinford, E. M., Schumacher, G. A., Shrake, D. L., Larsen, G. E., and Slucher, E. R., 1998, Descriptions of geologic map units, a compendium to accompany Division of Geological Survey open-file bedrock-geology maps: Ohio Division of Geological Survey Open-File Report 98-1, 8 p.

Taylor, S. R., and McLennan, S. M., 1985, The continental crust: its composition and evolution: Oxford, Blackwell Scientific Publications, 312 p.

Wachter, J., 1971, A geochemical study of the southwestern border of the Serpent Mound cryptoexplosion structure: B.S. thesis (unpub.), University of Cincinnati, 42 p.

Watts, D. R., in press, Paleomagnetic determination of the age of the Serpent Mound structure: Ohio Journal of Science.

Watts, D. R., El-Saiti, Belgasem, Baranoski, M. T., and Schumacher, G. A., 1998, Paleomagnetic constraints on the age of the Serpent Mound disturbance (abs.): Geological Society of America Abstracts with Programs, v. 30, no. 2, p. 77.

Watts, D. R., El-Saiti, Belgasem, Memmi, J. M., Weaver, John, and Baranoski, M. B., 1998, The Serpent Mound magnetic anomaly: fingerprint of a meteorite impact? (abs.): American Association of Petroleum Geologists Bulletin, v. 82, p. 1776.

Wicks, John, 1996, Structural history of the Killbuck area, Holmes County, Ohio, with implications for Knox exploration: Ohio Geological Society, 4th Annual Technical Symposium, p. 173-182.

Wickstrom, L. H., 1990, A new look at Trenton (Ordovician) structure in northwestern Ohio: Northeastern Geology, v. 12, p. 103-113.

Williams, N. L., Kerr, J. W., and McLoda, N. A., 1977, Soil survey of Highland County, Ohio: U.S. Department of Agriculture, Soil Conservation Service, 206 p.

Wilson, C. W., and Stearns, R. G., 1968, Geology of the Wells Creek structure, Tennessee: Tennessee Division of Geology Bulletin 68, 236 p.

Witzke, B. J., and Anderson, R. R., 1996, Sedimentary-clast breccias of the Manson impact structure, *in* Koeberl, Christian, and Anderson, R. R., eds., The Manson impact structure, Iowa: anatomy of an impact crater: Geological Society of America Special Paper 302, p. 115-144.

Woodward, H. P., 1961, Preliminary subsurface study of southeastern Appalachian Interior Plateau: American Association of Petroleum Geologists Bulletin, v. 45, p. 1634-1655.

Worthing, R. W., 1965, Structural evidence of regional block movement of the craton in the eastern interior of the North American continent: Shale Shaker, v. 15, p. 101-108.

Zahn, J. C., 1965, A gravity survey of the Serpent Mound area in southern Ohio: M.S. thesis (unpub.), Ohio State University, 37 p.

APPENDIX A.—GLOSSARY

Sources for definitions include *Glossary of geology* (Jackson, 1997), *Encyclopedic dictionary of exploration geophysics* (Sheriff, 1982), and *Structural geology* (Billings, 1972).

acoustic impedance The product of seismic velocity and density.

allochthonous Refers to a rock or block that was formed or produced elsewhere then moved to its present place. The antonym is *autochthonous*, which refers to a rock or block that is in place.

anastomosing Refers to irregular, subparallel, typically branching fractures that are commonly mineral filled.

aulocogen A sediment-filled continental rift that trends at a high angle to the adjacent continental margin.

cataclastic Refers to the structure or texture produced in a rock by the action of severe mechanical stress (crushing); characteristic features include the bending, breaking, and granulation of mineral grains.

chrondritic Refers to a meteorite that contains spheroidal granules or aggregates consisting chiefly of olivine and/or orthopyroxene. In contrast, iron meteorites are composed predominantly of iron-nickel.

cryptovolcanic A term used to describe circular structures on the Earth's surface resulting from deep-seated Earth processes. *Cryptoexplosion* is an alternate term.

density log On a geophysical log of a borehole, the curve of induced radioactivity that shows the bulk density of rocks and their contained fluids.

endogenic Refers to a geologic process that originates within the Earth, such as volcanism or igneous intrusion.

en echelon tension gashes Short fractures offset in a stair-step fashion (en echelon) by pull-apart (tension) forces; the fractures are commonly mineralized but may be open.

exogenic Refers to objects of extraterrestrial origin, such as meteorites or comets.

fold In regard to a seismic survey, where a common-depth point is sampled from multiple geophones; for example, if the same common depth point is sampled at 30 different offset distances, the resultant data are referred to as 30-fold.

frequency The rate of repetition of a periodic waveform, measured in seconds or in hertz (Hz); the reciprocal of period.

gigapascal (Gpa) 10^9 pascals. A pascal is the SI (Système Internationale) unit for pressure representing one newton/meter^2.

gravity anomaly The natural variation in the Earth's gravitational field or the difference between the observed value of gravity at a point and the theoretically calculated value. Measurement of gravity anomalies enables geologists to map differences in rock and mineral densities in the subsurface. Gravity data must be corrected for many factors, such as latitude, terrain, elevation (free-air correction), and rock (or lack of rock), between the gravity station and the datum plane. The corrected value is called the *Bouguer anomaly*.

gravity survey Measurement of the gravitational field at a series of different locations. Gravitational variations are related to differences in the distribution of rock densities and thus rock types.

magnetic anomaly The natural variation in the Earth's **magnetic field**, or the difference between the observed magnetic value at a point and the theoretically calculated value. Local magnetic anomalies reflect variations in the magnetic mineral content of near-surface rocks.

magnetic field The region of influence of a magnetized body or an electric current. A magnetic field is characterized by seven magnetic elements: declination, inclination, total intensity, horizontal intensity, vertical intensity, north component, and east component. The Earth's magnetic field is referred to as the geomagnetic field.

magnetic survey Measurement of the total magnetic intensity (or rarely another magnetic element) at different locations.

magnetization The sum of a rock's two types of magnetization, induced and remanent. *Induced magnetization* is the **magnetic field** spontaneously induced in a volume of rock by the uniform action of an applied magnetic field. *Remanent magnetization* is the component that has a fixed direction relative to the rock and is independent of moderate, applied magnetic fields, such as the Earth's magnetic field.

migration The process by which **reflectors** on a seismogram are plotted in true spatial position, rather than beneath a common-depth-point location.

milligal (mGal) In the centimeter-gram-second system of measurement, a unit (10^{-3} cm/sec/sec) used to measure acceleration of gravity.

nanotesla (nT) In the meter-kilogram-second (SI) system of measurement, a unit used to measure magnetic-field strength; equivalent to the gamma in the centimeter-gram-second system of measurement.

paleomagnetic analysis The study of the natural remanent **magnetization** of Earth materials in order to determine the intensity and direction of the Earth's **magnetic field** in the geologic past.

planar deformation features (PDF's) Submicroscopic amorphous lamellae occurring in shocked minerals as multiple sets of planar lamellae parallel to crystallographic planes. PDF's are indicative of shock metamorphism resulting from passage of high-pressure shock waves, whose only known cause is a hypervelocity impact.

reflector (reflected wave) On seismic profiles, the result of seismic energy returned from a down-going wave incident on a subsurface interface separating two contrasting rock types. The reflection coefficient is the ratio of the **amplitude** of the reflected wave to the corresponding incident wave amplitude, assuming incidence is vertical (perpendicular) to the rock interface.

resolution In geophysics, the limit of separation of two features that are very close together on a seismic section, gravity map, or magnetic map.

rifting The formation of a long, narrow continental trough that is bounded by normal faults. A rift marks a zone along which the entire thickness of the lithosphere has ruptured under extension.

ring anticline A curved or circular, structurally high fold.

ring graben A curved or circular, structurally low fault block.

second-derivative map A contour map of the second vertical derivative of a potential field such as the Earth's gravity or magnetic field. The values are normally derived by mathematical processing of the observed component.

seismic reflection profile A seismic recording of the sound energy reflected by subsurface rocks subjected to a manmade energy force, either a pulse source such as an explosion or a vibrating source placed against the surface of the Earth. The energy source is deployed at surface stations (shotpoints), commonly spaced at approximately equal intervals along a line or grid. Geophones (a type of seismometer) placed at intervals along the same line or grid record the ground motion resulting from the reflection of the imparted energy as it is reflected back from the subsurface rock interfaces. The arrival time (or two-way travel time) is the amount of time between the instant the energy is propagated and its arrival back from a subsurface **reflector** to a geophone. The velocity at which seismic energy passes through the Earth is dependent primarily on the physical properties of the rock and can change rapidly even where the geology is relatively simple. The relationship of the true depth of the reflector to two-way travel time generally is complex because of rapid changes and uncertainty in the subsurface seismic velocity.

shatter cone A distinctively striated conical structure, ranging in length from less than 1 cm to several meters, along which fracturing of the rock has occurred. Shatter cones are commonly found in nested or composite groups in rocks of impact structures and were formed by shock waves generated by hypervelocity impact. They are most common in carbonate rocks but are known from other rock types. The striated surfaces radiate outward from the apex.

slickenlines The lineations on a **slickenside**; they are generally parallel to the direction of slip along the fault.

slickensides A polished and striated surface resulting from friction during movement of rock along a fault plane.

sonic log On a geophysical log of a liquid-filled borehole, the interval-transit time of compressional seismic waves in rocks near the well bore. Also called a velocity log.

stylolite An irregular, interlocking, tooth-shaped surface, generally marked by dark-colored insoluble residues, formed by pressure solution; most common in carbonate rocks. The interlocking tooth-shaped axes trend parallel to the maximum direction of compressive stress.

synthetic seismogram An artificial seismic reflection record, generally manufactured from **sonic-log** data, that is compared with an actual seismogram to aid in identifying events or stratigraphic units.

APPENDIX B.—GENERALIZED DESCRIPTIONS OF LITHOSTRATIGRAPHIC UNITS

See figure 5 (p. 10) for a graphic representation of the stratigraphic units

PRECAMBRIAN

On the basis of work by Bass (1960), McCormick (1961), and Gonterman (1973), Precambrian basement rocks in the vicinity of the Serpent Mound disturbance consist predominantly of granite gneiss, schist, amphibolite, and marble of the Grenville Province. Sample cuttings from the Russell/Tener well (Adams County) indicate granite gneiss at 917 meters below sea level. Sample examination from this well also indicates a possible pre-Mount Simon (?) unit consisting of arkose with limonite cement, which is tentatively assigned to the Precambrian. The upper contact of the Precambrian is interpreted as unconformable with the pre-Mount Simon (?) arkose; the contact of the pre-Mount Simon (?) arkose with the Mount Simon Sandstone also is interpreted as unconformable. Depth to basement within the disturbed area is estimated at 914 meters to 1,189 meters below sea level on the basis of seismic data and sparse well control.

CAMBRIAN

Mount Simon Sandstone

The Mount Simon Sandstone consists of fine- to coarse-grained sandstone, siltstone, and dolomite (Janssens, 1973). The basal Mount Simon may contain high percentages of feldspar and lesser amounts of grains derived from the underlying Precambrian. In southern Ohio, the Mount Simon is quartz dominated toward the west and changes facies eastward, where it is dominated by dolomite and lesser amounts of quartz sandstone. The thickness of the unit is variable locally because of Precambrian paleotopography and is estimated to be 30 meters thick in the vicinity of the disturbance (Janssens, 1973). In western Ohio, the Mount Simon is overlain by the Eau Claire Formation; to the east and south the Mount Simon intertongues with the Rome Formation. The upper contact of the Mount Simon is interpreted as gradational and conformable with the overlying Eau Claire Formation or Rome Formation.

Eau Claire Formation

The Eau Claire Formation is present in western Ohio and consists of glauconitic sandstone, siltstone, and shale with lesser amounts of dolomite (Janssens, 1973). The unit is in facies transition in central Ohio with the Rome, Conasauga, and Kerbel Formations. Janssens (1973, pl. 2) does not show the Eau Claire present in the vicinity of the Serpent Mound disturbance.

Rome Formation

The following description is from Janssens (1973). The Rome Formation consists of dolomite and fine- to coarse-grained sandstone. It is dominantly sandstone in south-central Ohio, where a thicker north-south-trending sandstone facies occurs. East of the Serpent Mound disturbance, the Rome Formation is primarily dolomite. In western Ohio, the Rome intertongues with sandstone, siltstone, shale, and dolomite of the Eau Claire Formation. The Rome Formation is approximately 84 meters thick in the vicinity of the disturbance. The upper contact of the Rome Formation is interpreted as gradational and conformable with the overlying Conasauga Formation.

Conasauga Formation

In southern Ohio, the Conasauga Formation consists of interbedded shale, siltstone, sandstone, and limestone in three facies that are genetically related to the overlying Kerbel Formation (Janssens, 1973). The Conasauga is approximately 90 meters thick in the vicinity of the Serpent Mound disturbance. The upper and lower parts of the Conasauga intertongue with the Kerbel and the Eau Claire Formations, respectively. The upper contact of the Conasauga Formation is interpreted as gradational and conformable with the overlying Kerbel Formation, where present, or the Knox Dolomite.

Kerbel Formation

The Kerbel Formation consists of fine- to coarse-grained sandstone, siltstone, and dolomite (Janssens, 1973). The Serpent Mound disturbance is located near the southern limit of the Kerbel, which ranges in thickness from zero to 48 meters in southern Ohio. The upper contact of the Kerbel Formation is interpreted as gradational and conformable with the overlying Knox Dolomite.

CAMBRIAN-ORDOVICIAN

Knox Dolomite

The Knox Dolomite consists predominantly of dolomite but includes fine- to coarse-grained sandstone and siltstone (Janssens, 1973). The top of the Knox is marked by a regional unconformity; older subunits are present in central Ohio. The Knox is informally subdivided, in ascending order, into the Copper Ridge dolomite, Rose Run sandstone, and Beekmantown dolomite. Thickness of the Knox outside the area of the Serpent Mound disturbance is approximately 305 meters. The upper part of the Knox Dolomite, as observed in core DGS 3275, consists of dolomite and arenaceous dolomite interbedded with quartz sandstone and rare shale. Baranoski and others (1992) and Riley and others (1993) mapped the inferred southern limit of the Rose Run sandstone subcrop as passing just north of the Serpent Mound disturbance, and the Beekmantown dolomite as present in the vicinity of the disturbance. The Rose Run sandstone

apparently changes to a carbonate-dominated sandstone west of the Waverly Arch, which would include the area of the Serpent Mound disturbance (Riley and others, 1993). Thus, we tentatively suggest that the upper part of the Knox Dolomite in core DGS 3275 may correlate with the Rose Run sandstone and the underlying Copper Ridge dolomite. The upper contact of the Knox Dolomite is interpreted as sharp to gradational and unconformable with the overlying Wells Creek Formation.

ORDOVICIAN

"St. Peter sandstone"

"St. Peter sandstone" is a drillers' term for an unnamed sandstone at the base of the Wells Creek Formation on the Knox unconformity. The presence of the unit is spotty throughout southern Ohio.

Wells Creek Formation

The Wells Creek Formation consists of dolomite, argillaceous and arenaceous dolomite, dolomitic shale, siltstone, and sandstone (Janssens, 1973). The names "Glenwood" shale, "Glenwood-St. Peter," and lower dolomite member of the Chazy Limestone have been used to describe this stratigraphic interval. The unit ranges in thickness from less than 30 cm to more than 18 meters. The upper contact is gradational over 60 cm and is placed arbitrarily halfway within the gradational zone between the Wells Creek lithologies and the interbedded micritic limestones and calcareous shales of the overlying Black River Group.

Black River Group

The Black River Group consists of micritic limestone and subordinate amounts of dolomite, dolomitic limestone, and skeletal limestone interbedded with minor amounts of shale (Stith, 1979, 1986). Stith (1979) subdivided the Black River Group into three informal units—upper argillaceous, Carntown, and lower argillaceous—and eight informal marker beds. The Carntown unit is equivalent to the "Gull River" limestone of drillers.

The upper and lower argillaceous units are interbedded micritic limestone and shale. The Carntown unit is micritic limestone that displays prominent burrow mottling. The contacts between the units are sharp and placed at the top and bottom of the Carntown unit micritic limestone. Five of the eight marker beds are K-bentonites; the others are a burrowed micritic to pelletal limestone and two beds of shaly to argillaceous limestone and shale or carbonaceous shale.

The Black River Group ranges in thickness from 122 to 152 meters. The thickness of the upper argillaceous unit ranges from 12 to 20 meters, the Carntown ranges from 15 to 23 meters, and the lower argillaceous unit ranges from 7 to 13 meters (Stith, 1979).

The upper contact of the Black River Group with the overlying Curdsville Limestone Member of the Lexington Limestone is sharp and is placed at the top of the last micritic limestone bed underlying the interbedded skeletal limestone and shale of the Curdsville.

Lexington Limestone

The name Lexington Limestone has been adopted as a replacement for the Trenton Limestone throughout southwestern Ohio (Stith, 1986). In southwestern Ohio, the Trenton Limestone is now considered an informal drillers' term. The Lexington Limestone consists of fossiliferous gray to brownish-gray limestone (70 percent) interbedded with sparsely fossiliferous to fossiliferous gray to black shale (30 precent). Cressman (1973, pl. 10) traced the Curdsville Limestone Member, the Logana Member, and the Grier Member of the Lexington Limestone into the Cincinnati, Ohio, region. Stith (1986) recognized the Curdsville and Logana Members of the Lexington Limestone throughout southwestern Ohio, but could not recognize the Grier Member. Stith (1986) referred to the rocks between the top of the Logana Member and the base of the Point Pleasant Formation as the Lexington Limestone undifferentiated.

The Curdsville Limestone Member is approximately 90 percent fossiliferous brownish-gray to gray limestone and 10 percent sparsely fossiliferous gray shale. The Logana Member averages 60 percent sparsely fossiliferous to brachiopod-rich olive-gray to black shale interbedded with fossiliferous to brachiopod-coquina brownish-gray limestone. The Lexington Limestone undifferentiated averages 70 percent fossiliferous gray to brownish-gray limestone interbedded with sparsely fossiliferous gray shale.

The Lexington Limestone ranges in thickness from 45 to 64 meters throughout southern Ohio (Stith, 1986). The Curdsville Limestone Member ranges in thickness from 6 to 15 meters, the Logana Member ranges in thickness from 9 to 17 meters, and the Lexington Limestone undifferentiated ranges in thickness from 30 to 40 meters.

The upper contact of the Lexington Limestone undifferentiated with the overlying Point Pleasant Formation is gradational over 60 cm. The contact is placed arbitrarily midway through the gradational zone between an average 70 percent limestone interbedded with shale characterizing the Lexington Limestone and the average 60 percent limestone interbedded with shale of the Point Pleasant Formation. The upper contact of the Logana Member is gradational over 60 cm and is arbitrarily placed midway within a transition zone between the lithologies of the Logana Member and the Lexington Limestone undifferentiated. The upper contact of the Curdsville Limestone Member is sharp and is placed at the top of the first limestone bed below the lowermost shale bed of the Logana Member.

Point Pleasant Formation

The interbedded fossiliferous limestones and sparsely fossiliferous shales of the Point Pleasant Formation are exposed along the Ohio River and its tributaries in southwestern Ohio, making the Point Pleasant Formation the oldest unit exposed at the surface in Ohio. Limestone averages 60 percent in the Point Pleasant.

Luft and others (1973) reported the thickness of the Point Pleasant as ranging from 32 to 35 meters in exposures near Carntown, Kentucky. In Ohio, the entire unit is not exposed (Swinford and others, 1998). Stith (1986) and Mitchell and Bergström (1991) traced the Point Pleasant into the subsurface of southern Ohio. Stith (1986) reported that the subsurface thickness ranges from 34 to 37 meters.

The upper contact of the Point Pleasant Formation in southwestern Ohio is sharp and is placed at the top of the uppermost limestone bed of the Point Pleasant underlying the basal, thick-bedded shale of the Kope Formation.

Kope Formation

The Kope Formation consists of medium- to thick-bedded, planar, sparsely fossiliferous shale (75 percent) interbedded with thin- to medium-bedded, fossiliferous limestone. The unit is exposed in the valleys of the Ohio River and its tributaries throughout southwestern Ohio. The Kope Formation has been correlated from surface exposures into the subsurface by comparing shale-percentage logs of measured stratigraphic sections to shale-percentage logs of continuous cores and geophysical well-log suites (Stith, 1986; Shrake and others, 1988; Mitchell and Bergström, 1991; Potter and others, 1991; Schumacher, Swinford, and Shrake, 1991; Schumacher, 1992). The Kope ranges in thickness from 61 to 79 meters (Swinford and others, 1998).

McFarlan and Freeman (1935) studied the ranges of fossils from Ordovician rocks of Kentucky and found that the crinoid *Merocrinus curtas* occurs in great abundance in the basal part of the Kope Formation. This index fossil is easily recognized because *M. curtas* columnals are two to three times larger than the columnals of other crinoid or cystoid species present in the basal Kope. The basal Kope Formation containing *M. curtas* occurs twice in core DGS 3274 and once in core DGS 3275 (see pl. 1).

The upper contact of the Kope Formation with the overlying Fairview Formation is sharp and is placed at the top of the last medium- to thick-bedded, planar, sparsely fossiliferous shale bed of the Kope Formation.

Fairview Formation

The Fairview Formation is characterized by interbedded limestone and shale, which each average 50 percent of the formation. Limestone and shale beds are planar to irregular bedded; limestone beds are fossiliferous and shale beds are sparsely fossiliferous.

The Fairview Formation is widely exposed throughout southwestern Ohio in the valleys and tributaries of the Ohio, the Great Miami, and the Little Miami Rivers. The formation has been traced into the subsurface by comparing shale-percentage logs of measured stratigraphic sections and continuous cores to geophysical-log suites from core holes and oil and gas wells (Shrake and others, 1988; Mitchell and Bergström, 1991; Potter and others, 1991; Schumacher, Bergström, and Mitchell, 1991; Schumacher, Swinford, and Shrake, 1991; Schumacher, 1992).

Swinford and others (1998) reported the thickness of the Fairview ranges from 15 to 37 meters. The upper contact of the Fairview Formation with the Grant Lake Limestone is sharp and is placed at the top of the uppermost planar- to irregular-bedded fossiliferous limestone or the uppermost planar- to irregular-bedded sparsely fossiliferous shale underlying the wavy-bedded, fossiliferous limestone and shale of the Grant Lake Limestone.

Grant Lake Limestone

The Grant Lake Limestone consists of irregular- to wavy-bedded, fossiliferous limestone and minor amounts of planar-bedded fossiliferous limestone interbedded with fossiliferous to sparsely fossiliferous shale. Limestone averages 70 percent of the unit and shale 30 percent. The Grant Lake Limestone has been mapped in outcrop and into the subsurface of Adams, Brown, and Highland Counties, Ohio (Schumacher, Swinford, and Shrake, 1991; Schumacher, Bergström, and Mitchell, 1991).

Between Maysville, Kentucky, and Cincinnati, Ohio, the Grant Lake Limestone grades laterally into the Grant Lake Formation as the shale percentage increases from 20-30 percent to 50-60 percent north of Cincinnati in Butler County, Ohio (Schumacher, Swinford, and Shrake, 1991). The two formations are separated by a lateral transition zone, located in Clermont, northern Brown, and northwestern Highland Counties, in which the shale percentage is approximately 50 percent.

The thickness of the Grant Lake Limestone ranges from 23 to 36 meters (Swinford and others, 1998). The unit thins northwestward from the Ohio River (Schumacher, Swinford, and Shrake, 1991). The upper contact of the Grant Lake Limestone with the overlying Arnheim formation is sharp and is placed at the top of the uppermost irregular- to wavy-bedded, fossiliferous limestone or shale bed of the Grant Lake underlying the lowermost planar-bedded, fossiliferous limestone bed or planar-bedded, sparsely fossiliferous shale bed of the Arnheim formation.

Arnheim formation (informal)

The Arnheim formation consists of meter-scale alternation of nodular- to wavy-bedded limestone and irregularly bedded, fossiliferous shale with nearly equal amounts of planar-bedded, fossiliferous limestone and sparsely fossiliferous shale (Schumacher and Hay, 1995). The Ohio Division of Geological Survey has mapped the Arnheim unit throughout southwestern Ohio (Schumacher, Swinford, and Shrake, 1991) and informally recognizes the Arnheim formation pending formal reinstatement of this unit. Shrake and others (1988), Schumacher, Swinford, and Shrake (1991), and Schumacher, Bergström, and Mitchell (1991) have recognized this unit on shale-percentage logs and geophysical-log suites in the subsurface.

The Arnheim formation ranges in thickness from 15 to 30 meters (Swinford and others, 1998). The upper contact of the Arnheim formation is sharp and is placed at the top of the nodular- or wavy-bedded limestone bed that underlies the planar-bedded lithologies of the Waynesville Formation.

Waynesville Formation

The Waynesville Formation is characterized by planar-bedded, sparsely fossiliferous, calcareous shale interbedded with planar- to irregular-bedded, fossiliferous limestone. Shale averages 70 percent of the unit and limestone 30 percent. This formation has been mapped throughout southwestern Ohio and has been traced into the subsurface (Shrake and others, 1988). The Waynesville Formation ranges in thickness from 27 to 37 meters (Swinford and others, 1998). The upper contact of the Waynesville with the overlying Drakes Formation is sharp and is placed at the top of the planar-bedded, fossiliferous limestone or planar-bedded, calcareous, sparsely fossiliferous shale underlying the thick, planar-bedded, dolomitic, sparsely fossiliferous shale of the Drakes.

Drakes Formation

The Drakes Formation is approximately 80 percent dolomitic shale and 20 percent interbedded limestone and dolomitic limestone. Shale beds are variable in color, ranging from bluish gray to greenish gray to dark reddish gray, and are generally sparsely fossiliferous. Limestone and dolomitic limestone beds are gray and fossiliferous.

Peck (1966) recognized and mapped the Drakes Formation in the Maysville, Kentucky, region, and the Ohio Division of Geological Survey has mapped the unit throughout southwestern Ohio (Schumacher, Swinford, and Shrake, 1991). Shrake and others (1988) and Schumacher, Bergström, and Mitchell (1991) recognized this unit in the subsurface. The Drakes Formation ranges in thickness from 6 to 9 meters (Swinford and others, 1998).

The contact of the Drakes Formation with the overlying Brassfield Formation is the Ordovician-Silurian systemic boundary in Ohio. Swinford (1985) observed that the Drakes appears to grade into the Brassfield with no sign of erosion south of the Serpent Mound disturbance on exposures mapped in the Peebles quadrangle. Similar observations are reported from sections near Maysville, Kentucky (Peck, 1966). However, biostratigraphic evidence documents that the uppermost Ordovician and lowermost Silurian is missing throughout south-central Ohio (Rexroad and others, 1965; Rexroad, 1967; Cramer and Díez de Cramer, 1972; Sweet, 1979; Rexroad and Kleffner, 1984; Grahn, 1985; Grahn and Bergström, 1985).

SILURIAN

Brassfield Formation

The Brassfield Formation consists of interbedded limestone, cherty limestone, hematitic limestone, dolomite, and shale. The Belfast Member at the base of the Brassfield Formation in southern Ohio consists of massive, argillaceous to silty, sparsely fossiliferous dolomite or interbedded argillaceous to silty dolomite and dolomitic shale (Rexroad and others, 1965; Stith and Steiglitz, 1979). Rexroad and others (1965) and Swinford (1985) indicated the thickness of the Belfast Member ranges from 1.5 to 3 meters in south-central Ohio. The upper contact of the Belfast Member is sharp and is placed at the top of the uppermost argillaceous, sparsely fossiliferous dolomite or dolomitic shale bed underlying the base of the first fossiliferous limestone bed of the Brassfield.

A series of hematitic limestones forms a distinctive stratigraphic marker near the top of the Brassfield in the vicinity of the Serpent Mound disturbance (Foerste, 1935; Rogers, 1936; Reidel and others, 1982). This stratigraphic marker is present in the southeastern and central portions of Highland County and extends southward into Adams County (Rogers, 1936; Stith and Stieglitz, 1979). Horvath (1967) reported this marker in the subsurface of central Ohio.

The top of the Brassfield Formation contains several feet of medium- to coarse-grained, argillaceous, cross-bedded, crinoidal limestone that commonly displays megaripples. Rexroad and others (1965) observed the persistence of this bed(s) and informally referred to this interval as the "bead bed." The term "bead" was used because of large distinctive crinoidal columnals that occur in great abundance. The unconformable upper contact of the Brassfield Formation is at the top of the "bead bed" (Rexroad and others, 1965; Rexroad and Kleffner, 1984; Swinford, 1985). The thickness of the Brassfield ranges from 8 to 15 meters in south-central Ohio (Rogers, 1936; Swinford, 1985).

Noland Formation

As defined by Rexroad and others (1965), the Noland Formation includes all Silurian rocks between the top of the Brassfield Formation and the base of the Estill Shale in eastern Kentucky and southern Ohio, and the Dayton is a member of the Noland Formation. In southern Highland and Adams County, Ohio, the Noland Formation consists of a lower undifferentiated unit of planar-bedded, sparsely fossiliferous, dolomitic shale interbedded with thin to thick, planar beds of fine- to coarse-grained dolomitic limestone and dolomite overlain by the Dayton Limestone Member. North of the Adams-Highland County line, Rexroad and others (1965, p. 22) retained the formational rank of the Dayton because erosion has removed the undifferentiated Noland rocks and the Dayton is separated from the underlying Brassfield by an erosional unconformity.

In recent mapping, the Ohio Division of Geological Survey restricted the Noland Formation to the shale-dominant undifferentiated rocks, retaining the Dayton Formation in southern Highland and Adams County, Ohio (Swinford and others, 1998). The Brassfield Formation, the Noland Formation, and the Dayton Formation are distinct lithologic units throughout southern Ohio and are readily mappable at the 1:24,000 scale, although for expediency these units were mapped as a single undivided unit.

Horvath (1967) successfully correlated the Noland Formation of Rexroad and others (1965) into the subsurface of north-central Kentucky and south-central Ohio. The Noland Formation rapidly thickens across Adams and Scioto Counties from zero to nearly 30 meters. The Noland Formation ranges in thickness from approximately 8 meters in southern Adams County to zero in the area of the Adams-Highland County line (Swinford and others, 1998). The contact with

the Dayton Formation is at the top of the uppermost dolomitic shale bed of the Noland.

Dayton Formation

The Dayton Formation is a persistent ledge-forming, medium- to thick-bedded, finely crystalline to cryptocrystalline limestone or dolomite containing minor shale interbeds. The Dayton is an excellent stratigraphic marker that is easily mapped and is lithologically distinct from the shale-dominant Noland, where the latter is present.

The Dayton ranges in thickness from 0.6 to 2 meters in southern Ohio (Rexroad and others, 1965). The upper contact with the Estill Shale is unconformable and is placed at the top of the upper limestone or dolomite bed of the Dayton underlying the basal glauconitic zone of the Estill Shale (Swinford, 1985).

Estill Shale

The Estill Shale consists of dolomitic shale interbedded with minor amounts of dolomite and limestone. Sparsely fossiliferous shale beds range in color from dark reddish gray to greenish gray and commonly are thick bedded. Sparsely to abundantly fossiliferous dolomite and limestone beds are gray and occur as laminations or thin beds.

A glauconitic zone (Rexroad and others, 1965) at the base of the Estill Shale is 0.3 to 0.6 meter thick and is a shale containing disseminated glauconite and/or concentrated glauconite stringers. This persistent marker bed is recognized throughout much of Ohio (Horvath, 1967, 1969) and has been traced from the Serpent Mound region southward to east-central Kentucky by Rexroad and others (1965).

Horvath (1969) and Janssens (1977) traced the Estill Shale into the subsurface of eastern, central, and northern Ohio. Both authors described the rapid thinning of the unit in central Ohio; Janssens (1977) used the name Rochester Formation for the Estill in the subsurface of Ohio.

The Estill Shale ranges in thickness from 9 to 55 meters in southern Ohio (Swinford and others, 1998). The unit thickens to the southeast from northern Clinton County to southern Adams County. The upper contact of the Estill with the Bisher Formation is sharp and is placed at the top of the uppermost dolomitic shale bed of the Estill.

Bisher Formation

The Bisher Formation as exposed in southern Highland and northern Adams Counties is a fine-grained, silty to argillaceous dolomite containing minor dolomitic shale interbeds (Bowman, 1956; Swinford, 1985). Horvath (1969) traced the Bisher into the subsurface of southern and eastern Ohio. The Bisher Formation ranges in thickness from 6 to 26 meters (Bowman, 1956; Swinford, 1985) and is highly variable because of an intertonguing relationship with the overlying Lilley Formation. The upper contact of the Bisher Formation is the top of the uppermost argillaceous dolomite bed underlying the medium- to coarse-grained crinoidal dolomite beds of the Lilley Formation.

Lilley Formation

The Lilley Formation consists of two distinct lithologies: (1) silty to argillaceous dolomite and (2) medium- to coarse-grained, crystalline, crinoidal dolomite (Bowman, 1956). In many sections, the two lithologies are interbedded. The thickness of the Lilley ranges from 5.5 to 24 meters (Bowman, 1956; Swinford, 1985). Bowman (1956) and Swinford (1985) reported that the thickness of the Lilley is highly variable in Highland and Adams Counties because of the intertonguing relationship with the underlying Bisher Formation.

Horvath (1969) observed that the Lilley Formation and the overlying Peebles Dolomite lose their distinctive lithologies as they are traced into the subsurface. Horvath (1969) and Janssens (1977) correlated the Lilley Formation and the Peebles Dolomite to the subsurface Lockport Group. The upper contact of the Lilley Formation with the overlying Peebles Dolomite is gradational over 0.3 meter. The contact is placed arbitrarily midway within a transition between the lithologies of the Lilley Formation and the fine- to medium-grained, vuggy dolomite of the Peebles.

Peebles Dolomite

The Peebles Dolomite is a finely to coarsely crystalline, fossiliferous dolomite in thick to massive beds. Argillaceous material is rare, and moldic and vuggy porosity is very abundant in comparison to the underlying Lilley Formation. The Peebles is a resistant, cliff-forming unit in stream valleys and forms broad, flat areas on the uplands. Caves and sinkholes are very common in this unit.

The thickness of the Peebles Dolomite is difficult to determine because the upper contact is unconformable; topographic relief on the unconformity ranges from zero to 1.5 meters (Swinford, 1985; Kahle, 1988), and the contact generally is not exposed on the flat uplands (Bowman, 1956; Swinford, 1985). Swinford (1985) estimated that the thickness of the Peebles ranges from 12 to 21 meters in northern Adams County. Bowman (1956) estimated that the thickness of the Peebles ranges from less than 15 meters to greater than 36 meters in Highland County.

Greenfield Dolomite

The Greenfield Dolomite consists of fine-grained to cryptocrystalline, sparsely fossiliferous dolomite in thin to thick, planar-bedded, discontinuous beds. Carbonaceous laminae and intervals of thick- to massive-bedded, vuggy, fossiliferous dolomite are present locally (Rogers, 1936; Schmidt and others, 1961).

Erosion has removed the Greenfield Dolomite and the overlying Tymochtee Dolomite in some areas of southern Ohio. Thus, the Devonian units of southern Ohio rest unconformably on the Tymochtee, the Greenfield, or the Peebles Dolomite, and in central and southern Adams County on the Lilley or the Bisher Formation.

The thickness of the Greenfield is highly variable, ranging from zero to 30 meters (Rogers, 1936; Swinford and

others, 1998). The conformable upper contact is gradational and difficult to recognize because of lithologic similarities between the Greenfield and the overlying Tymochtee Dolomite (Swinford, 1985). The Plum Run quarry in northeastern Adams County contains the most extensive exposure of this contact in southern Ohio.

Tymochtee Dolomite

The lithology of the Tymochtee Dolomite is similar to the Greenfield except argillaceous laminae and shale beds are common and the thick- to massive-bedded, vuggy facies of the Greenfield is absent. Thickness of the Tymochtee ranges from zero to 15 meters (Swinford and others, 1998). The upper contact of the Tymochtee is unconformable; the Upper Devonian Olentangy Shale generally overlies the Tymochtee but in rare cases the Lower? Devonian Hillsboro Sandstone is present.

DEVONIAN

Hillsboro Sandstone

The Hillsboro Sandstone is a fine-grained, well-rounded, well-sorted, friable quartz sandstone. Orton (1871), Carman and Schillhahn (1930), and Rogers (1936) described in detail the known exposures of this unit in Highland and Adams Counties. The Hillsboro is present as unconformable cavity fillings within the underlying Silurian dolomites or as locally restricted bedded sandstone unconformably overlying the Silurian dolomites and underlying the Olentangy Shale. The Hillsboro Sandstone is highly variable in thickness, ranging from a few centimeters up to 6 meters (Rogers, 1936).

Olentangy and Ohio Shales

The Olentangy Shale consists of greenish-gray clay shale and rare limestone nodules and nodular beds. The overlying Ohio Shale consists of black, carbonaceous shale; greenish-gray clay shale interbeds are present in places (Kepferle and Roen, 1981). The Olentangy Shale ranges in thickness from 6 to 17 meters, and the Ohio Shale ranges from 76 to 152 meters (Swinford and others, 1998). The conformable contact between the Olentangy Shale and the Ohio Shale is placed arbitrarily midway within a gradational zone characterized by interbedded clay shale and carbonaceous shale of both units. The upper contact of the Ohio Shale with the overlying Bedford Shale is sharp and is placed at the top of the last carbonaceous shale of the Ohio.

Bedford Shale

The Bedford Shale consists of gray shale interbedded with sandstone. The number of sandstone beds increases in the upper half of the unit. Swinford and others (1998) reported the thickness of the Bedford ranges from 24 to 30 meters. The upper contact of the Bedford Shale with the Berea Sandstone is gradational and is placed arbitrarily where the upward-increasing sandstone content exceeds 50 percent.

DEVONIAN-MISSISSIPPIAN

Berea Sandstone

The Berea Sandstone consists of thin- and thick-bedded sandstone interbedded with shale. The resistance to erosion of the upper portion of the Berea Sandstone produces distinctive flat caps to many hills of southern Ohio (Swinford, 1985). The Berea Sandstone ranges in thickness from 3 to 15 meters (Swinford and others, 1998). The upper contact of the Berea Sandstone with the overlying Sunbury Shale is sharp and is placed at the top of the uppermost sandstone bed underlying the carbonaceous shale of the Sunbury.

MISSISSIPPIAN

Sunbury Shale

The Sunbury Shale consists of thin planar beds of carbonaceous shale. Hyde (1953) observed that the upper part of the Sunbury is more argillaceous and grades into the overlying Cuyahoga Formation. The unit ranges in thickness from 3 to 15 meters (Swinford and others, 1998). The upper contact of the Sunbury Shale with the overlying Cuyahoga Formation is sharp and is placed at the top of the uppermost carbonaceous shale underlying the arenaceous shale, siltstone, or sandstone of the Cuyahoga.

Cuyahoga Formation

The Cuyahoga Formation consists of arenaceous shale and intervals of interbedded siltstone and sandstone. The unit ranges in thickness from 15 to 198 meters (Swinford and others, 1998). The Cuyahoga Formation is the youngest bedrock unit in the area of the Serpent Mound disturbance. The upper contact of the Cuyahoga with the overlying Logan Formation is not present.

APPENDIX C.—CHECKLIST USED IN DESCRIBING CORES

1. Determine core intervals to be described, using the following criteria:
   - A. Formational contacts
   - B. Lithologic contacts
   - C. Faults
   - D. Stylolitic contacts
   - E. Bedding dip
2. Check and physically fit top and bottom of core between adjacent boxes to determine upside-down boxes, displaced core, etc.
3. Determine intervals of core lost or missing
4. Measure apparent thickness
5. Describe lithology
   - A. Gross lithology (list dominant lithology first)
   - B. Estimate percent of rock types
   - C. Color (Goddard, 1948)
   - D. Texture (see Swanson, 1981, Appendix 3)
     - a. grain size
     - b. shape
     - c. roundness and sphericity
     - d. sorting
     - e. cement
   - E. Bedding and laminations (planar, wavy, etc.)
   - F. Bed thickness (Ingram, 1954)
   - G. Sedimentary structures
     - a. primary (sole marks, graded bedding, etc.)
     - b. secondary (deformed bedding, ball and pillow, etc.)
   - H. Fossils (body and trace)
   - I. Contacts
     - a. unit
     - b. bedding contacts
   - J. Accessory minerals (vein fillings, clasts, etc.)
   - K. Porosity and oil shows (see Swanson, 1981, p. I-14)
   - L. Fluorescence (mineral and hydrocarbon)
6. Structural description
   - A. Bedding dip
   - B. Natural fractures (dip, plume axes, mineralization, etc.)
   - C. Coring-induced fractures
   - D. Faulting (dip, relative movement, brecciation, etc.)
   - E. Folding
   - F. Stylolites (orientation)
   - G. Slickenlines (orientation and direction)
   - H. Shatter cones (orientation)
   - I. Overprinting/cross-cutting relationships (fractures, folds, faults, etc.)

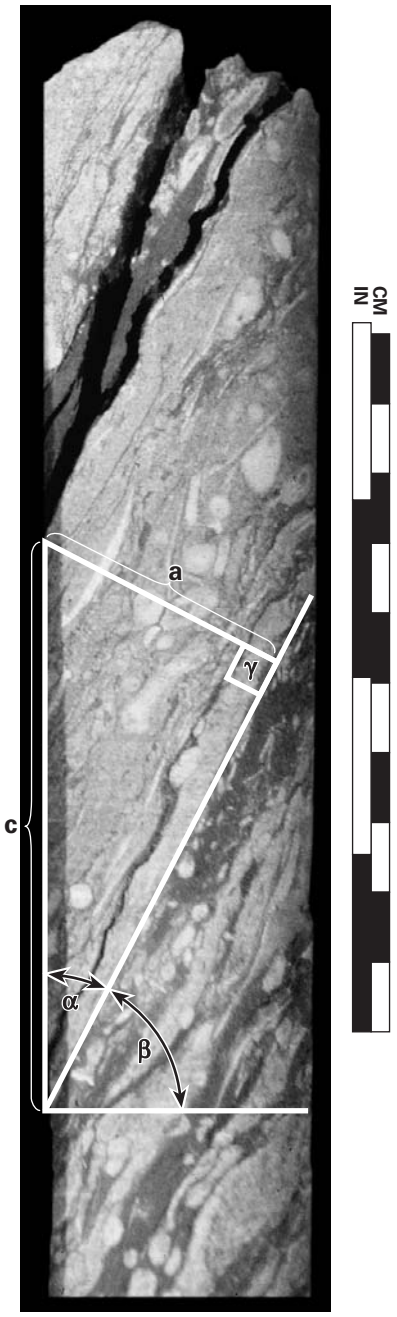

angle β (in degrees) = apparent bedding dip
angle α (in degrees) = 90° - β

c = length of core
a = bedding thickness, (sine α) x c
γ = 90°

Simple diagram showing trigonometry used to calculate bedding thickness.

APPENDIX D.—SELECTED MEGASCOPIC DESCRIPTIONS OF THIN SECTIONS AND SAMPLES FROM CORES DGS 3274 AND DGS 3275

Megascopic descriptions are based on thin-section blanks and represent a cross-sectional area of approximately 1.1 by 1.8 inches (27 by 46 mm). Because of core loss and depth uncertainty in some core boxes, depth intervals are approximate. A 30X binocular microscope was used to examine and describe 44 rock specimens collected from cores DGS 3274 and DGS 3275. Samples are listed in order from top to bottom of core. See plate 1 for sample locations and tables 4 and 5 for lists of samples. Depths are in feet with metric equivalents in parentheses.

A nongenetic breccia classification based on clast type was used. Where a single clast type is present in quantities greater than 70 percent, the clast type is used in the breccia name. If no clast type represents 70 percent or more of the rock, the breccia is termed a mixed-lithic breccia. Clasts are considered to be fragmental material approximately 0.04 inch (1.0 mm) or greater in diameter. Color terminology is descriptive (subjective) for individual breccia clasts. Breccia matrix and whole-rock colors were determined using the rock-color chart of Goddard (1948). For all samples, colors were described when wet.

CORE DGS 3274

Sample SM1-05
Hand sample
Depth: 265.8 to 266.3 feet (81.0 to 81.2 meters)
Claystone-clast breccia

The matrix is moderately calcareous; the rock as a whole is very poorly sorted. The largest clast is a 0.6-inch (1.5-cm) limestone fragment. Claystone clasts are greenish gray, calcareous, and silty and disaggregate readily in water. Limestone clasts are mottled white and gray, are finely to medium crystalline, and contain tiny, rodlike pyritized fossil fragments 0.004 inch wide by 0.008 inch long (0.1 mm by 0.2 mm). The matrix consists of finely pulverized claystone. The matrix is grayish olive green (5GY 3/2).

Sample SM1-07
Hand sample, thin section
Depth: 960.9 to 961.1 feet (292.9 to 292.9 meters)
Claystone-clast breccia

The matrix is moderately to highly calcareous; the rock as a whole is very poorly sorted. The largest clast is a 1.8-inch (4.5-cm) breccia fragment within the claystone-clast breccia. There are a few white and gray mottled, fossiliferous limestone fragments. The majority of the clasts are greenish-gray claystone that disaggregates readily in water. Breccia clasts contain black aphanitic clasts. The matrix consists of calcareous clay and some silt- and sand-size material. The matrix is olive gray (5Y 4/1). There appears to be two episodes of brecciation in this sample.

Sample SM1-08
Hand sample
Depth: 1,019.0 to 1,019.3 feet (310.6 to 310.7 meters)
Shale and limestone, interbedded

The shale is olive gray (5Y 4/1), moderately calcareous, slightly silty, and dissagregates readily in water. The limestone is mottled light gray (N7) and white (N9), medium crystalline, fossiliferous (brachiopods and bryozoans), and has a sharp, slightly irregular contact with the shale.

Sample SM1-09
Hand sample, thin section
Depth: 1,122.4 to 1,122.6 feet (342.1 to 342.2 meters)
Limestone-clast breccia

The matrix is moderately to highly calcareous; the rock as a whole is very poorly sorted. The largest clast is a 0.4-inch (1.0-cm) limestone fragment. Limestone clasts are white and medium gray mottled, medium crystalline, and fossiliferous. Claystone clasts are medium to light gray; claystone clasts and matrix readily disaggregate in water. Matrix is mostly calcareous clay but has minor amounts of silt- and sand-size limestone fragments of a composition similar to the coarser material. The matrix is olive gray (5Y 4/1).

Sample SM1-10
Hand sample
Depth: 1,136.2 to 1,136.4 feet (346.3 to 346.4 meters)
Limestone

The limestone is medium gray (N5) to light gray (N7), finely crystalline, silty, and fossiliferous. Many small black and amber silt-size to very fine sand size fossil fragments are present. The rock contains slightly wavy laminae. A sharp contact separates darker and finer grained limestone above from lighter and medium-grained limestone below.

Sample SM1-11
Hand sample
Depth: 1,159.6 to 1,159.8 feet (353.5 to 353.5 meters)
Limestone

The limestone is white (N9) and light gray (N7) mottled, finely to medium crystalline, and fossiliferous (bryozoans). The rock contains abundant black fossil fragments. A cavity about 1 cm in diameter is filled with pink dolomite.

Sample SM1-12
Hand sample
Depth: 1,166.1 to 1,166.3 feet (355.4 to 355.5 meters)
Shale

The shale is grayish olive green (5GY 3/2) and slightly calcareous. Rare pyritized organic matter is present. A weakly developed shatter cone also is present.

Sample SM1-14
Hand sample
Depth: 1,348.6 to 1,348.8 feet (411.1 to 411.1 meters)
Shale

The shale is brownish black (5YR 2/1), highly calcareous, and fossiliferous (brachiopods?). Some pyrite coating on fossils. Rare fine-grained calcareous black clasts (?) occur along bedding plane and scattered throughout shale.

Sample SM1-13
Hand sample, thin section
Depth: 1,348.8 to 1,349.1 feet (411.1 to 411.2 meters)
Mixed-lithic breccia

The matrix is highly calcareous; the rock as a whole is very poorly sorted. The largest clast is a 1.8-inch (4.5-cm) shale fragment containing white and brown limestone lenses. This unusually large clast has microfaults, an irregular wavy contact, and a breccia dike. There are clasts of finely crystalline to microcrystalline light-gray limestone that exhibit cataclastic texture. Black aphanitic clasts up to 0.12 inch (3 mm) in diameter are present in the dike and appear to show flow or compactionlike features. A few stylolites are present in some limestone clasts. The matrix is olive gray (5Y 4/1) to olive black (5Y 2/1).

Sample SM1-15
Hand sample, thin section
Depth: 1,395.1 to 1,395.5 feet (425.2 to 425.4 meters)
Chert

The chert is mottled light gray (N7) to very light gray (N8), slightly calcareous, and exhibits cataclastic texture. Fractures are filled with light-grayish-white clay. Small (0.004 to 0.008 inch/0.1 to 0.2 mm), equant or rod-shaped, black to gray grains are present. Some fossil ghosts also are present.

Sample SM1-16
Hand sample, thin section, trace element analysis
Depth: 1,412.1 to 1,412.6 feet (430.4 to 430.6 meters)
Limestone-clast breccia

The matrix is moderately to highly calcareous; the rock as a whole is very poorly sorted. The largest clast is a limestone fragment in excess of 1.2 inches (3 cm) wide that makes up almost one-third of the sample. This clast is white to light brown, fossiliferous, and contains a 0.2-inch (5-mm) layer of gray limestone that has abundant pyrite grains. Other clasts include green claystone and gray limestone. Black aphanitic clasts up to 0.08 inch (2.0 mm) in diameter are common. The matrix is grayish black (N2), aphanitic, and contains sand- and silt-size limestone fragments as well as larger clasts. The matrix fills dikes in fractured clasts.

Sample SM1-17
Hand sample
Depth: 1,414.7 to 1,414.9 feet (431.2 to 431.3 meters)
Limestone

The limestone is light gray (N7) and mostly finely crystalline. This limestone contains pyrite grains and a large pink-dolomite-filled vug 0.98 inch (2.5 cm) in diameter. Microcrystalline pyrite lines the dolomite-filled vug. Also present is a coarsely to very coarsely crystalline, fossiliferous, light-gray (N7) limestone that has an irregular contact with the finely crystalline limestone.

Sample SM1-01A
Hand sample, thin section, trace element analysis
Depth: 1,435.2 to 1,435.5 feet (437.5 to 437.5 meters)
Mixed-lithic breccia

Clasts of limestone and shale/claystone are imbedded in a slightly calcareous matrix; the sample is very poorly sorted. The largest clast is a 1.1-inch (2.8-cm)-long limestone fragment. A light-gray dolomite clast and a greenish-gray claystone fragment have thin pyrite rims. Claystone clasts are greenish gray and medium gray. Limestone and dolomite clasts vary from light brown to gray and are medium crystalline to aphanitic. The claystone readily disaggregates in water. The matrix consists of sand- to silt-size shale, claystone, and dolomite fragments and minor limestone fragments. The matrix is olive gray (5Y 4/1).

Sample SM1-04
Hand sample, thin section, trace element analysis
Depth: 1,435.8 to 1,436.3 feet (437.6 to 437.8 meters)
Mixed-lithic breccia

The matrix is slightly calcareous; the rock as a whole is very poorly sorted. The largest clast is a 0.8-inch (2-cm) claystone fragment. There are many green and gray shale clasts. Subordinate limestone clasts are faintly mottled, medium-crystalline fragments ranging from white to gray. Claystone clasts readily disaggregate in water. Rare finely crystalline reddish dolomite clasts contain iron oxide. The matrix is sand, silt, and clay material of a composition similar to the clasts. Clayey matrix dominates. The matrix is olive gray (5Y 4/1).

Sample SM1-18
Hand sample
Depth: 1,443.2 to 1,443.4 feet (439.9 to 440.0 meters)
Shale

The shale is dusky brown (5YR 2/2) and noncalcareous to slightly calcareous. Shatter-cone structure is present and is identified by an irregular fracture surface having radiating light-gray streaks and striations. This surface is about 0.004 inch (0.1 mm) thick. The streaks are 0.02 inch (0.5 mm) wide and up to 0.28 inch (7 mm) long and are slightly calcareous.

Sample SM1-32
Hand sample
Depth: 1,479.8 to 1,479.9 feet (451.0 to 451.1 meters)
Dolomite

The dolomite is olive black (5Y 2/1), finely crystalline, silty, and laminated. A possible shatter cone present.

Sample SM1-06
Hand sample
Depth: 1,503.7 to 1,504.2 feet (458.3 to 458.5 meters)
Limestone-clast breccia

The matrix is moderately to highly calcareous; the rock as a whole is very poorly sorted. The largest clast is a 0.98-inch (2.5-cm) limestone fragment. Limestone clasts are mostly white and gray mottled, medium crystalline, and fossiliferous. Pyritized rodlike fossil fragments are present. Claystone clasts are greenish gray to gray, calcareous, and disaggregate readily in water. The matrix consists mostly of pulverized claystone and shale and is dark greenish gray (5GY 4/1).

Sample SM1-02
Hand sample, thin section
Depth: 1,623.6 to 1,624.0 feet (494.8 to 495.0 meters)
Limestone-clast breccia

The matrix is moderately calcareous; the sample is very poorly sorted. The largest clast in this sample is a 0.9-inch (2.3-cm) limestone fragment. The limestone is white to gray, fossiliferous, and medium crystalline. The shale/claystone clasts are medium gray, calcareous, and disaggregate readily in water. These lithologies are the only two recognized in this sample. The matrix consists of clay-, silt-, and sand-size fragments of similar composition to the clasts. The matrix is very light gray (N8) to dark greenish gray (5GY 4/1).

Sample SM1-03A
Hand sample, thin section
Depth: 2,076.5 to 2,076.8 feet (632.9 to 633.0 meters)
Limestone-clast breccia

The matrix is moderately to highly calcareous; the rock as a whole is very poorly sorted. A dark-brown to black, very fine grained (aphanitic) impact-melt (?) clast 0.98 inch (2.5 cm) long contain small inclusions or cavity fillings (calcite?). Edges of the black impact-melt (?) clasts are ragged and irregular. Smaller fragments of this clast type are scattered throughout the sample. There is one large (0.6 inch/1.5 cm long) white and light-brown limestone clast. The remaining clasts are gray limestone and shale. The matrix consists of poorly sorted sand-, silt-, and clay-size fragments. The matrix is olive gray (5Y 4/1).

Sample SM1-03B
Hand sample, thin section
Depth: same as SM1-03A; sampled immediately below SM1-03A
Limestone-clast breccia

The matrix is highly calcareous; the rock as a whole is very poorly sorted. This sample is hard and has wavy, irregular-shaped shale clasts and laminae; the irregular shape was probably caused by compaction. This sample contains black aphanitic clasts similar to SM1-03A. The largest clast is a 0.47-inch (1.2-cm) limestone fragment. Limestone clasts are white to brown, medium crystalline, and fossiliferous or brown, silty, finely crystalline, and slightly fossiliferous. A minor number of shale clasts is present. The matrix consists of sand, silt, and clay of similar composition to the clasts. The matrix is olive gray (5Y 4/1).

Sample SM1-19
Hand sample, thin section
Depth: 2,290.3 to 2,290.4 feet (698.1 to 698.1 meters)
Limestone-clast breccia

The sample as a whole is made up of a single large clast of limestone in contact with much finer (sand- and granule-size) clasts imbedded in a highly calcareous, pulverized, light-gray (N7) matrix. The breccia material may be a dike injected into a fracture of the large limestone clast, or the large limestone clast may be a large clast in the breccia. The large limestone clast is brown to medium brown, mottled, and occupies two-thirds of the sample. The limestone is microcrystalline and has irregular patches (bioturbation) of finely to medium crystalline limestone. The contact is sharp and regular with a limestone-clast breccia. The clasts in the breccia are mostly white limestone, but two are gray breccia clasts (breccia within a breccia). Several small black aphanitic clasts were observed.

Sample SM1-20
Hand sample
Depth: 2,312.6 to 2,312.8 feet (704.9 to 704.9 meters)
Limestone-clast breccia

The matrix is highly calcareous; the rock as a whole is very poorly sorted. Most clasts are 0.12 inch (3 mm) or less in diameter. Several black aphanitic clasts are present. Limestone-clast breccia makes up about 25 percent of the sample. The matrix is light olive gray (5Y 6/1). The remainder of the sample is a large clast? of white and gray mottled limestone. A stylolite up to 0.08 inch (2 mm) thick runs through this large limestone clast and is filled with expandable clay and minor pyrite.

Sample SM1-33A
Hand sample, thin section
Depth: 2,385.1 to 2,385.5 feet (727.0 to 727.1 meters)
Limestone-clast breccia

The matrix is moderately to highly calcareous; the rock as a whole is very poorly sorted. The largest clast is a very finely crystalline, light-brown limestone fragment 0.8 inch (2 cm) long. Other clasts include very finely crystalline gray limestone, medium-grained white sandstone, and black aphanitic clasts. Minor amounts of coarser carbonates are present. Some of the larger clasts are fractured and some are cataclastic. The matrix is light gray (N7) to light olive gray (5Y 6/1).

Sample SM1-33B
Hand sample, thin section
Depth: same as SM1-33A; sampled immediately below SM1-33A
Limestone-clast breccia

The matrix is moderately to highly calcareous; the rock as a whole is very poorly sorted. The largest clast is a 0.7-inch (1.7-cm), mottled white and gray limestone fragment. The sample also contains medium-crystalline, brown to light-brown limestone clasts; white, medium- to coarse-grained sandy limestone clasts; grayish-brown cataclastic limestone clasts; medium- to dark-gray breccia clasts; greenish-gray claystone clasts (readily disaggregate in water), and black aphanitic clasts. The matrix is light olive gray (5Y 6/1).

Sample SM1-22
Hand sample, X-ray diffraction analysis
Depth: 2,479.8 to 2,479.9 feet (755.8 to 755.9 meters)
Mixed-lithic breccia

The matrix is highly calcareous; the rock as a whole is very poorly sorted. The largest clasts are less than 0.12 inch (3 mm) in diameter. Black aphanitic clasts are common. The matrix is mostly very finely pulverized carbonate and is very light gray (N8).

Sample SM1-23
Hand sample, thin section
Depth: 2,480.4 to 2,480.5 feet (756.0 to 756.1 meters)
Limestone-clast breccia

The matrix is highly calcareous; the rock as a whole is very poorly sorted. The largest clasts are about 0.31 inch (8 mm) in diameter. Most clasts are microcrystalline white to light-tan limestone. Some microcrystalline medium-gray limestone clasts are present. Calcareous black aphanitic clasts also were observed; several are about 0.04 inch (1 mm) in diameter and appear to be vesicular and to have irregular, delicate edges. The matrix is mostly pulverized carbonate and is light gray (N7).

Sample SM1-21
Hand sample, thin section
Depth: 2,482.7 to 2,482.9 feet (756.7 to 756.8 meters)
Limestone-clast breccia

The matrix is highly calcareous; the rock as a whole is poorly sorted. Vuggy light-tan limestone or calcareous dolomite is cataclastic in part. Minor sphalerite mineralization is present in the matrix and in vugs. The largest clast is a 1.4-inch (3.5-cm) limestone fragment. The matrix appears to be black (N1) and aphanitic.

Sample SM1-24
Hand sample
Depth: 2,630.8 to 2,630.9 feet (801.9 to 801.9 meters)
Cataclastic limestone

The limestone is brownish gray (5YR 4/1), very fine grained, and has possible fossil fragments and ghosts less than 0.04 inch (1 mm) in diameter. There are hairlike fractures (cataclastic texture) throughout. Stylolites are present and have a black coating on one fracture surface.

Sample SM1-25
Hand sample, thin section, X-ray diffraction analysis
Depth: 2,644.4 to 2,644.7 feet (806.0 to 806.1 meters).
Limestone-clast breccia

The matrix is highly calcareous; the rock as a whole is very poorly sorted. The largest clast is a 0.12-inch (3-mm) limestone fragment. Also present are very fine grained white and light-brown limestone clasts, light-gray limestone clasts that have a cataclastic texture, black aphanitic clasts, and rare greenish-gray claystone clasts. The matrix is mostly sand, silt, and finer sizes of carbonate and is olive gray (5Y 4/1).

Sample SM1-26
Hand sample
Depth: 2,738.6 to 2,738.8 feet (834.7 to 834.8 meters)
Shale

The shale is grayish black (N2), highly calcareous, very friable, and contains some black carbonaceous material.

Sample SM1-28A
Hand sample, thin section
Depth: 2,852.6 to 2,852.9 feet (869.5 to 869.6 meters)
Dolomite-clast breccia

The matrix is slightly calcareous; the rock as a whole is very poorly sorted. The largest clast is a 1.6-inch (4.0-cm) very fine grained gray dolomite fragment that has a cataclastic texture. Also present are very fine grained light-brown dolomite clasts that have a cataclastic texture, medium-grained white sandstone clasts, sandy glauconitic green dolomite clasts, and a few shale/claystone clasts. All clasts appear to be slightly flattened (compressed) and have featherlike edges and a lenticular appearance. Several black aphanitic clasts are present. The matrix is light olive gray (5Y 6/1) to olive gray (5Y 4/1) and is mostly pulverized clay-size material but has some sand- and silt-size material. Stylolites are present in the matrix.

Sample SM1-28B
Hand sample, thin section
Depth: same as SM1-28A
Sandstone-clast breccia

The top one-third of this sample is similar to SM1-28A. The remainder is a noncalcareous, fine- to medium-grained, subrounded, very light gray (N8) sandstone. Sand grains appear to float in a very fine grained, nearly white matrix (clay?). Conjugate fractures are fairly extensive in this sample and are filled with this clay (?) material. Extensive fracturing gives the sandstone a cataclastic texture.

Sample SM1-27
Hand sample, thin section, X-ray diffraction analysis
Depth: 2,856.7 to 2,856.9 feet (870.7 to 870.8 meters)
Sandstone

The sandstone is very light gray (N8) to white (N9), moderately to well sorted, subrounded to rounded, and fine to medium grained. Sand grains appear to be floating in a noncalcareous clay matrix. The sandstone is crossed by conjugate faults and fractures filled with white clay. Rose Run sandstone?

Sample SM1-29A
Hand sample, thin section
Depth: 2,870.6 to 2,871.0 feet (875.0 to 875.1 meters)
Mixed-lithic breccia

The matrix is slightly calcareous; the rock as a whole is very poorly sorted. The largest clast is a 0.8-inch (2.0-cm) greenish-gray claystone fragment. Other types include white to tan calcareous dolomite clasts that have a cataclastic texture and contain minor amounts of glauconite, white sandstone clasts similar to that in sample SM1-28B, brown and gray dolomite clasts, and rare black aphanitic clasts. The matrix is medium light gray (N6).

Sample SM1-29B
Hand sample, thin section
Depth: same as SM1-29A; sampled immediately below SM1-29A
Mixed-lithic breccia

The matrix is slightly calcareous; the rock as a whole is very poorly sorted. The largest clast is a 0.6-inch (1.6-cm) white sandstone fragment. The sandstone clasts are similar to the noncalcareous, fine- to medium-grained sandstone described in the lower part of sample SM1-28B. Other clasts include finely crystalline gray and brown dolomite and limestone and minor amounts of greenish-gray shale.

Black aphanitic clasts up to 0.08 inch (2 mm) in diameter are present. The matrix color is light olive gray (5Y 6/1).

Sample SM1-29C
Hand sample, thin section
Depth: same as SM1-29A; sampled immediately below SM1-29B
Mixed-lithic breccia

The matrix is slightly calcareous; the rock as a whole is very poorly sorted. The breccia is similar to that in sample SM1-29B. Two-thirds of this sample is a white sandstone clast similar to the noncalcareous, fine- to medium-grained sandstone described in the lower part of sample SM1-28B. The matrix is light gray (N7).

Sample SM1-30
Hand sample
Depth: 2,874.6 to 2,875.0 feet (876.2 to 876.3 meters)
Dolomite

The dolomite is light olive gray (5Y 6/1), medium crystalline, glauconitic, and contains minor amounts of pyrite. An indistinct shatter cone and a stylolite that has a dark-greenish-black surface residue are present.

Sample SM1-31
Hand sample, X-ray diffraction analysis
Depth: 2,883.4 to 2,883.8 feet (878.9 to 879.0 meters)
Dolomite

The dolomite is light gray (N7), finely crystalline, and calcareous. Pyrite is disseminated throughout.

CORE 3275

Sample SM2-01
Hand sample
Depth: 1,278.6 to 1,278.9 feet (389.7 to 389.8 meters)
Claystone

The claystone is very light gray (N8), moderately calcareous, and friable. This sample contains abundant biotite, mostly 0.004 to 0.02 inch (0.1 to 0.5 mm) in diameter. This rock is most likely an Ordovician-age K-bentonite.

Sample SM2-02
Hand sample
Depth: 1,312.6 to 1,312.8 feet (400.0 to 400.1 meters)
Chert

The chert is yellowish gray (5Y 8/1), slightly calcareous, hard, brittle, and contains many fractures (cataclastic). Fossil ghosts are present in bluish carbonate; chalky white areas are chert.

Sample SM2-03
Hand sample
Depth: 1,455.8 to 1,456.1 feet (443.7 to 443.8 meters)
Limestone

The limestone is mottled olive gray (5Y 4/1) and very finely crystalline. Coarsely crystalline gray and white limestone fills fractures and replaces fossils. This sample has a vertical fracture (breccia dike) 0.4 to 0.8 inch (1 to 2 cm) wide filled with clasts of the olive-gray limestone up to 0.4 inch (1 cm) in diameter. The matrix of the breccia dike is black (N1), calcareous, and aphanitic.

Sample SM2-04
Hand sample, thin section
Depth: 1,822.4 to 1,822.7 feet (555.5 to 555. 6 meters)
Sandstone

The sandstone is light gray (N7), noncalcareous, fine- to medium-grained, well rounded, well sorted, and hard. Grains float or have point contacts. This sample is similar to sample SM1-27 of core DGS 3274.

Sample SM2-05
Hand sample, thin section
Depth: 1,858.7 to 1,858.9 feet (566.5 to 566.6 meters)
Dolomite

The dolomite is white (N9), cherty, and very slightly calcareous. Randomly distributed fossil fragments are replaced by medium-gray chert. Most of the fossil fragments are rod shaped or curvilinear, 0.004 to 0.12 inch (0.1 to 3 mm) wide, and up to 0.6 inch (1.5 cm) long.

Sample SM2-06
Hand sample, thin section
Depth: 1,866.1 to 1,866.3 feet (568.8 to 568.9 meters)
Sandstone

The sandstone is light gray (N7), fine to medium grained, well sorted, and well rounded. An irregular laminae of clay is present. The sample is noncalcareous. This rock may be Rose Run sandstone.

Baranoski, Schumacher, Watts, Carlton, and El-Saiti—SUBSURFACE GEOLOGY OF THE SERPENT MOUND DISTURBANCE, ADAMS, HIGHLAND, AND PIKE COUNTIES, OHIO—Ohio Division of Geological Survey Report of Investigations 146

CORE DGS 2880

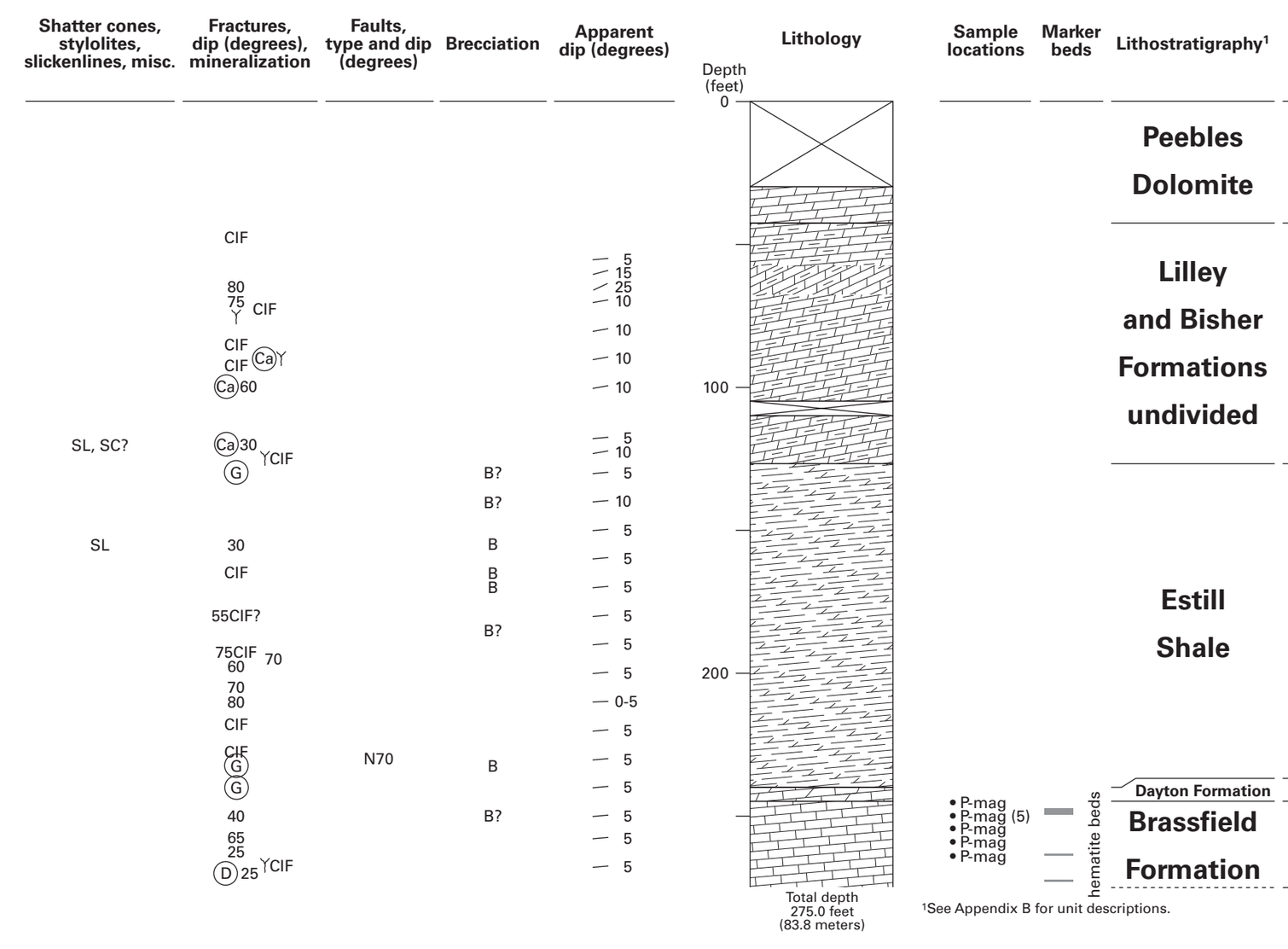

Lithologic description

Reference elevation 812.0 feet (247.5 m)

0-20.0 feet (0-6.1 m)—core missing

Peebles Dolomite

Vuggy, brecciated dolomite
20.0-42.0 feet (6.1-12.8 m)

Dolomite, white (N9) to medium-gray (N5); finely to medium crystalline; crystals anhedral to euhedral; fine to coarse grained; grains subrounded; well sorted; massive bedding; fossiliferous, colonial corals, pelmatozoans, and brachiopods common; rare to moderate bioturbation with local burrow mottling; pyrite, limonite, and minor argillaceous material; vuggy, moldic, fracture, and granular porosity.

Upper contact not cored. Lower contact gradational over 1.0 foot (0.3 m) and arbitrarily placed halfway within gradational zone.

Lilley and Bisher Formations undivided

Dolomite, minor shale, and rare chert
42.0-126.0 feet (12.8-38.4 m)
Core missing between 105.0 and 109.0 feet (32.0-33.2 m)

Dominant lithology: argillaceous dolomite, light-gray (N7) to medium-gray (N5); finely to medium crystalline; crystals euhedral to anhedral; planar to irregular bedding; laminated to thick bedded; cross-laminated; sparsely fossiliferous, disseminated brachiopods and echinoderms; rare to moderate bioturbation; rare burrow mottling; disseminated and laminated glauconite; rare pyrite concentrated in burrows and fractures or disseminated throughout unit; interparticle and fracture porosity.

Subordinate lithology: granular dolomite, medium-gray (N5) to dark-gray (N3); medium to coarse grained; grains subangular to subrounded; moderately sorted; planar bedding; laminated to thick bedded; sparsely to abundantly fossiliferous, echinoderm ossicles abundant; calcite-filled fractures; interparticle and rare fracture porosity.

Shale, medium-dark-gray (N4); planar to irregular bedding; laminated to thin bedded; rare to moderate bioturbation; slightly calcareous; disseminated pyrite.

Chert nodules and beds present between 87.0 and 93.0 feet (26.5-28.3 m).

Lower contact sharp and placed at base of lowermost argillaceous dolomite bed.

Estill Shale

Shale and minor dolomitic limestone and dolomite
126.0-237.9 feet (38.4-72.5 m)

Shale, greenish-gray (5GY 6/1), medium-gray (N5), pale-brown (5YR 5/2), and grayish-red (10R 4/2); dolomitic; planar bedding; laminated to thick bedded; sparsely fossiliferous; rare bioturbation; pyrite in burrow fillings; disseminated glauconite in basal 10.0 feet (3.0 m) of unit.

Dolomitic limestone, light-gray (N7) to medium-gray (N5); finely to coarsely crystalline; crystals euhedral to anhedral; fine to coarse grained; grains angular to subrounded; irregular to wavy bedding, laminated to thin bedded; shale partings; sparsely to abundantly fossiliferous; rare bioturbation.

Dolomite, light-gray (N7); fine grained; grains subrounded; planar bedding and lamination; sparsely fossiliferous; rare bioturbation.

Lower contact sharp and placed at base of lowermost shale bed.

Dayton Formation

Dolomite and minor shale
237.9-243.6 feet (72.5-74.2 m)

Dolomite, light-olive-gray (5Y 6/1) to greenish-gray (5GY 6/1); finely to medium crystalline; crystals subhedral to euhedral; planar bedding; medium to thick bedded; shale partings; sparsely fossiliferous; argillaceous in upper 1.6 feet (0.5 m) of unit; glauconite as clasts, insoluble residue at stylolite seams, and disseminated throughout unit; intercrystal, moldic, and fracture porosity.

Shale, greenish-gray (5GY 6/1); dolomitic; planar bedding; thin bedded; sparsely fossiliferous; rare bioturbation; pyrite in burrow fillings.

Lower contact sharp and placed at base of lowermost dolomite bed.

Brassfield Formation

Limestone and shale interbedded
243.6-275.0 feet (74.2-83.8 m)

Limestone, very light gray (N8), light-olive-gray (5Y 6/1), greenish-gray (5GY 6/1), grayish-red (5R 4/2), and pale-brown (5YR 5/2); fine to coarse grained; grains angular to rounded; finely to coarsely crystalline; crystals subhedral to euhedral; planar to irregular bedding with local nodular bedding; thin to thick bedded; shale partings and clasts; poorly developed graded bedding; abundantly to sparsely fossiliferous; rare bioturbation with local mottling; hematite and limonite beds in three zones: 247.3 to 248.6 feet (75.4-75.8 m), 263.3 to 263.7 feet (80.2-80.4 m), and 271.0 to 272.7 feet (82.6-83.1 m); disseminated glauconite; intercrystal, moldic, and fracture porosity.

Shale, greenish-gray (5GY 6/1) to medium-gray (N5) to brownish-gray (5YR 4/1); calcareous; planar and irregular bedding; thin to thick bedded; sparsely fossiliferous; rare bioturbation; pyrite in burrow fillings.

Lower contact not cored.

CORE DGS 2881

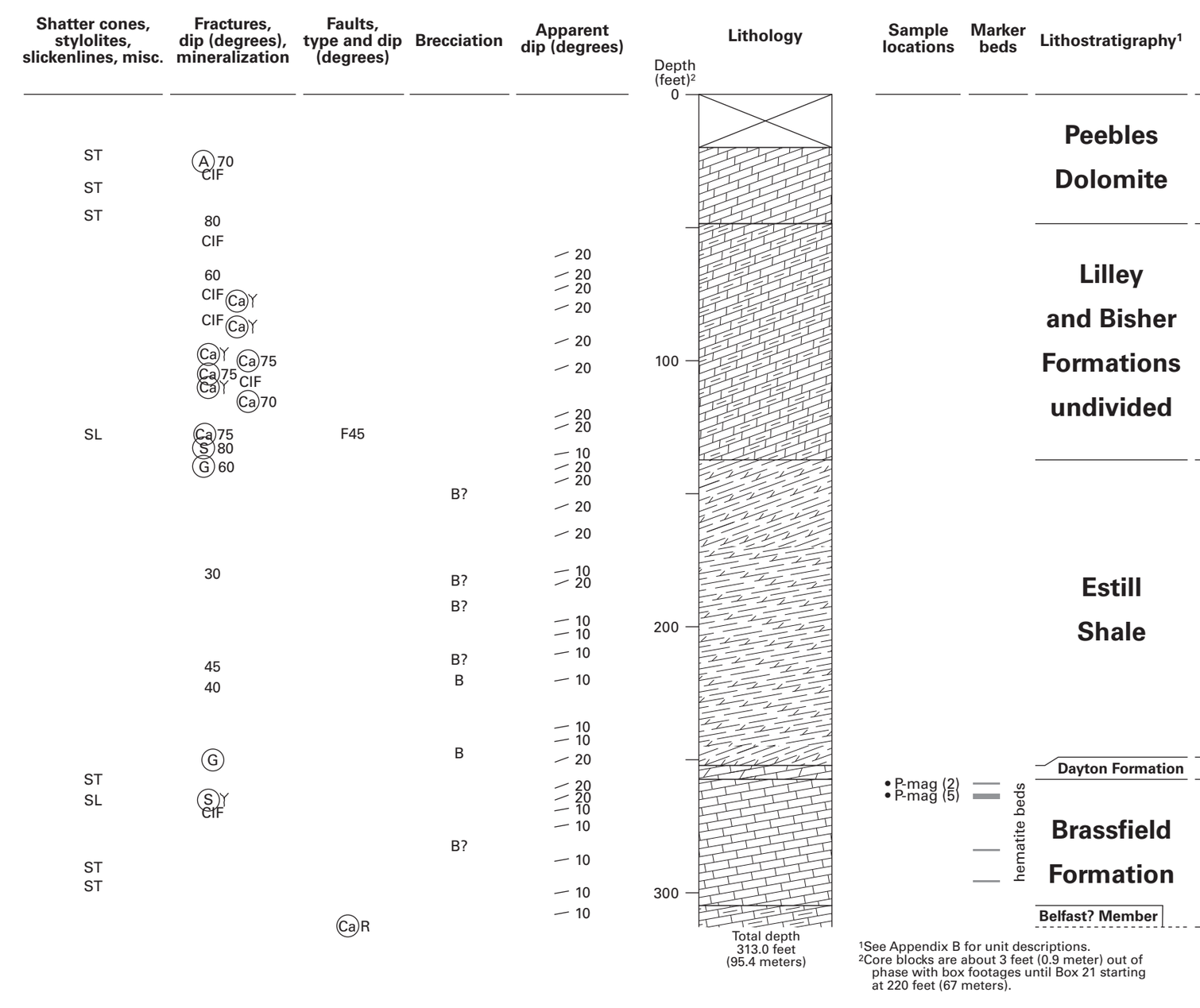

Lithologic description

Reference elevation 749.0 feet (228.3 m)

0-20.0 feet (0-6.1 m)—core missing

Peebles Dolomite

Vuggy, brecciated dolomite
20.0-49.4 feet (6.1-15.1 m)

Dolomite, white (N9) to medium-gray (N5); finely to medium crystalline; crystals anhedral to euhedral; fine to coarse grained; grains subangular to subrounded; well sorted; massive bedded; fossiliferous, colonial corals, pelmatozoans, and brachiopods common; rare to moderate bioturbation with local burrow mottling; pyrite, limonite, and minor argillaceous material; asphalt and asphaltic staining present between 20.0 and 28.0 feet (6.1-8.5 m); vuggy, moldic, fracture, and granular porosity.

Upper contact not cored. Lower contact gradational over 1.0 foot (0.3 m) and arbitrarily placed halfway within gradational zone.

Lilley and Bisher Formations undivided

Dolomite, minor shale, and chert
49.4-138.0 feet (15.1-42.1 m)

Dominant lithology: argillaceous dolomite, light-gray (N7) to medium-gray (N5); finely to medium crystalline; crystals euhedral to anhedral; planar to irregular bedding; laminated to thick bedded, cross-laminated; sparsely fossiliferous, disseminated brachiopods and echinoderms; rare burrow mottling; disseminated and laminated glauconite, rare pyrite concentrated in burrows and fractures or disseminated in laminations; rare calcite and dolomite filling vugs; vuggy, interparticle, and fracture porosity.

Subordinate lithology: granular dolomite, medium-gray (N5) to dark-gray (N3); medium to coarse grained; grains subangular to subrounded; moderately sorted; planar bedding; laminated to thick bedded; abundantly fossiliferous, echinoderm ossicles abundant; calcite-filled fractures; rare interparticle and fracture porosity.

Shale, medium-dark-gray (N4); planar to irregular bedding; laminated to thin bedded; rare to moderate bioturbation; slightly calcareous; disseminated pyrite.

Chert nodules and beds present between 68.0 and 69.0 feet (20.7-21.0 m) and 93.0 and 115.0 feet (28.3-35.0 m).

Lower contact sharp and placed at base of lowermost argillaceous dolomite bed.

Estill Shale

Shale and minor dolomitic limestone and dolomite
138.0-253.0 feet (42.1-77.1 m)

Shale, greenish-gray (5GY 6/1), medium-gray (N5), pale-brown (5YR 5/2), and grayish-red (10R 4/2); dolomitic; planar bedding; laminated to thick bedded; sparsely fossiliferous; rare bioturbation; pyrite in burrow fillings; disseminated glauconite or glauconitic laminations in basal 10.0 feet (3.0 m) of unit.

Dolomitic limestone, light-gray (N7) to medium-gray (N5); finely to coarsely crystalline; crystals euhedral to anhedral; fine to coarse grained; grains subangular; irregular to wavy bedding; laminated to thin bedded; shale partings; sparsely to abundantly fossiliferous; rare bioturbation.

Dolomite, light-gray (N7), fine-grained; grains subangular to subrounded; planar bedding and lamination; sparsely fossiliferous; rare bioturbation.

Lower contact sharp and placed at base of lowermost shale bed.

Dayton Formation

Dolomite and minor shale
253.0-257.6 feet (77.1-78.5 m)

Dolomite, light-olive-gray (5Y 6/1) to greenish-gray (5GY 6/1); finely to medium crystalline; crystals subhedral to euhedral; planar bedding; medium to thick bedded; shale partings; sparsely fossiliferous; glauconite as clasts, insoluble residue at stylolite seams, and disseminated throughout unit; argillaceous in upper 1.0 foot (0.3 m) of unit; intercrystal, moldic, and fracture porosity.

Shale, greenish-gray (5GY 6/1); dolomitic; planar bedding; thin bedded; sparsely fossiliferous; rare bioturbation; pyrite in burrow fillings.

Lower contact sharp and placed at base of lowermost dolomite bed.

Brassfield Formation

Limestone and shale interbedded
257.6-307.0 feet (78.5-93.6 m)

Limestone, very light gray (N8), light-olive-gray (5Y 6/1), greenish-gray (5GY 6/1), grayish-red (5R 4/2), and pale-brown (5YR 5/2); fine to coarse grained; grains angular to rounded; finely to coarsely crystalline; crystals subhedral to euhedral; planar to irregular bedding with local nodular bedding; thin to thick bedded; poorly developed graded bedding; local cross-bedding; shale partings and clasts; abundantly to sparsely fossiliferous; rare bioturbation with local burrow mottling; hematite and limonite common in four zones: 259.1 to 259.4 feet (79.0-79.1 m), 263.4 to 264.7 feet (80.3-80.7 m), 284.2 to 284.5 feet (86.6-86.7 m), 295.1 to 295.8 feet (89.9-90.2 m); disseminated glauconite; intercrystal, moldic, and fracture porosity.

Shale, greenish-gray (5GY 6/1) to medium-gray (N5) to brownish-gray (5YR 4/1); calcareous; planar and irregular bedding; thin to thick bedded; sparsely fossiliferous; rare bioturbation; pyrite in burrow fillings.

Lower contact sharp and placed at base of lowermost fossiliferous granular limestone bed.

Belfast Member?

Limestone and shale interbedded
307.0-313.0 feet (93.6-95.4 m)

Limestone, medium-gray (N5); fine grained; grains subangular to rounded; finely to medium crystalline; crystals euhedral to anhedral; irregular to wavy bedding; thin bedded; abundantly fossiliferous, corals, brachiopods, and pelmatozoan ossicles common; minor bioturbation and burrow mottling; minor intervals of laminated limestone; fracture and rare moldic porosity.

Shale, medium-gray (N5); dolomitic to calcareous; irregular bedding, thin bedded; sparsely fossiliferous; rare bioturbation.

Lower contact not cored.

CORE DGS 2882

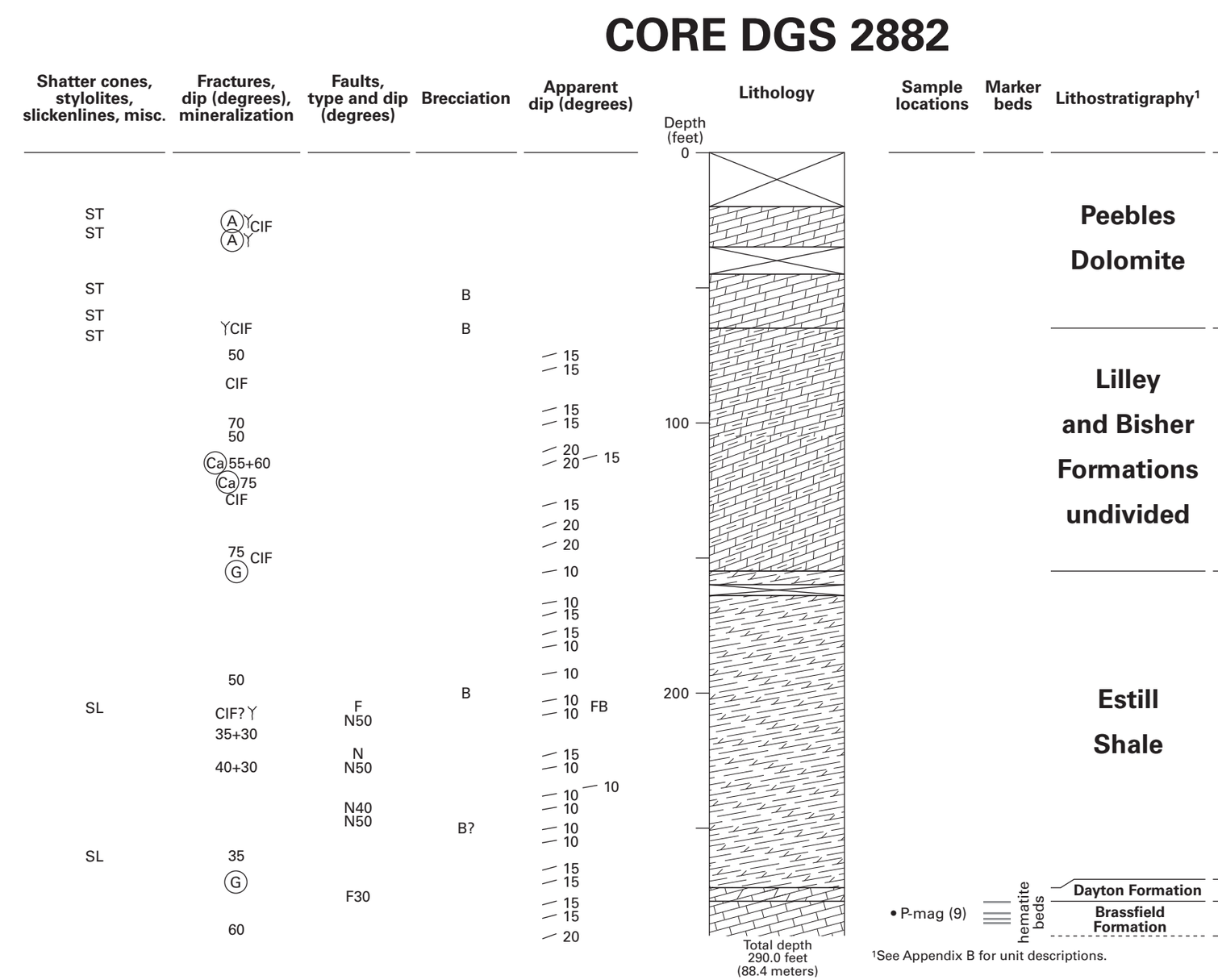

Lithologic description

Reference elevation 735.0 feet (224.0 m)

0-20.0 feet (0-6.1 m)—core missing

Peebles Dolomite

Vuggy, brecciated dolomite
20.0-65.0 feet (6.1-19.8 m)
Core missing between 35.0 and 45.0 feet (10.7-13.7 m)

Dolomite, white (N9) to medium-gray (N5); finely to medium crystalline; crystals anhedral to euhedral; fine to coarse grained; grains subangular to subrounded; well sorted; massive bedded; abundantly to sparsely fossiliferous, colonial corals, pelmatozoans, and brachiopods common; rare to moderate bioturbation with local burrow mottling; pyrite; limonite; minor argillaceous material; asphalt and asphaltic staining between 20.0 and 34.0 feet (6.1-10.4 m); vuggy, moldic, fracture, and granular porosity.

Upper contact not cored. Lower contact gradational over 6.0 feet (1.8 m) and arbitrarily placed halfway within gradational zone.

Lilley and Bisher Formations undivided

Dolomite, minor shale, and rare chert
65.0-154.3 feet (19.8-47.0 m)

Dominant lithology: argillaceous dolomite, light-gray (N7) to medium-gray (N5); finely to medium crystalline; crystals euhedral to anhedral; planar to irregular bedding; laminated to thick bedded; sparsely fossiliferous, disseminated brachiopods and echinoderms; rare to moderate bioturbation; disseminated and laminated glauconite; rare pyrite concentrated in burrows, laminations, and fractures, or disseminated throughout unit; rare calcite and dolomite in vugs; vuggy, interparticle, and fracture porosity.

Subordinate lithology: granular dolomite, medium-gray (N5) to dark-gray (N3); medium to coarse grained; grains subangular to subrounded; planar bedding; laminated to thick bedded; sparsely to abundantly fossiliferous, echinoderm ossicles abundant; rare burrow mottling; interparticle and fracture porosity.

Shale, medium-dark-gray (N4); calcareous; planar to irregular bedding; laminated to thin bedded; rare to moderate bioturbation; disseminated pyrite.

Chert nodules and beds present between 114.5 and 125.5 feet (34.9-38.2 m) and at 146.4 feet (44.6 m).

Lower contact sharp and placed at lowermost argillaceous dolomite bed.

Estill Shale

Shale and minor dolomitic limestone and dolomite
154.3-271.9 feet (47.0-82.9 m)
Core missing between 160.0 and 163.0 feet (48.8-49.7 m)

Shale, greenish-gray (5GY 6/1), medium-gray (N5), pale-brown (5YR 5/2), and grayish-red (10R 4/2); dolomitic; planar bedding; laminated to thick bedded; sparsely fossiliferous; rare bioturbation; pyrite in burrow fillings; disseminated and laminated glauconite in basal 15.0 feet (4.6 m) of unit.

Dolomitic limestone, light-gray (N7) to medium-gray (N5); finely to coarsely crystalline; crystals euhedral to anhedral; fine to coarse grained; grains subangular and subrounded; irregular to wavy bedding; laminated to thin bedded; shale partings; sparsely to abundantly fossiliferous; rare bioturbation.

Dolomite, light-gray (N7); fine grained; grains subrounded; planar bedding and lamination; sparsely fossiliferous; rare bioturbation.

Lower contact sharp and placed at base of lowermost shale bed.

Dayton Formation

Dolomite and minor shale
271.9-276.6 feet (82.9-84.3 m)

Dolomite, light-olive-gray (5Y 6/1) to greenish-gray (5GY 6/1); finely to medium crystalline; crystals subhedral to euhedral; planar bedding; medium to thick bedded; shale partings; sparsely fossiliferous; argillaceous in upper 1.0 foot (0.3 m) of unit; glauconite as clasts and disseminated throughout unit; intercrystal, moldic, and fracture porosity.

Shale, greenish-gray (5GY 6/1); dolomitic; planar bedding; thin bedded; sparsely fossilferous; rare bioturbation; pyrite in burrow fillings.

Stromatoporoids abundant between 274.6 and 275.6 feet (83.7-84.0 m).

Lower contact sharp and placed at base of lowermost dolomite bed.

Brassfield Formation

Limestone and shale interbedded
276.6-290.0 feet (84.3-88.4 m)

Limestone, very light gray (N8), light-olive-gray (5Y 6/1), greenish-gray (5GY 6/1), grayish-red (5R 4/2), and pale-brown (5YR 5/2); fine to coarse grained; grains angular to rounded; finely to coarsely crystalline; crystals subhedral to euhedral; planar to irregular bedding with local nodular bedding; thin to thick bedded; shale partings and clasts; poorly developed graded bedding; abundantly to sparsely fossiliferous; rare bioturbation with local mottling; hematite and limonite common in four zones: 277.9 to 278.0 feet (84.7-84.7 m), 282.1 to 283.7 feet (86.0-86.5 m), 284.0 to 284.5 feet (86.6-86.7 m), 285.0 to 285.2 feet (86.9-86.9 m); disseminated glauconite; intercrystal, moldic, and fracture porosity.

Shale, greenish-gray (5GY 6/1) to medium-gray (N5) to brownish-gray (5YR 4/1), calcareous; planar and irregular bedding; thin to thick bedded; sparsely fossiliferous; rare bioturbation; pyrite in burrow fillings.

Lower contact not cored.

KEY TO SYMBOLS

B	Brecciation
(black bar)	Breccia zone
FB	Bedding-plane breccia
(symbol)	En echelon tension gashes
SC40	Shatter cone and dip value
←	Shatter cone horizontal to bedding
60 ↖	Shatter cone having apex up hole and dip value
60 ↙	Shatter cone having apex down hole and dip value
SL	Slickenlines
ST	Stylolites
(symbol)	Stylolites parallel to bedding
(symbol)	Stylolites oblique to bedding
(symbol)	Stylolites at high angle to bedding
BP80	Bedding-plane fault and dip value
F	Fault
N60	Normal fault and fault angle, where applicable
E	En echelon normal fault
R65	Reverse fault and fault angle, where applicable
S	Strike-slip/rotational fault
M	Multiple episodes of structural movement
Y	Vertical to subvertical anastomosing fractures
CIF	Coring-induced fracture
(A)	Asphalt-filled fractures and staining
(Ca)	Calcite-filled fracture or fault
(D)	Dolomite-filled fracture or fault
(G)	Glauconite
(S)	Sulfide mineralization
K-bent	K-bentonite bed
HS	Hand sample
P-mag (6)	Paleomagnetic analysis sample (number of samples, where applicable)
TE	Trace element analysis sample
TS	Thin section sample
(crossed box)	Missing core

KEY TO LITHOLOGIC PATTERNS

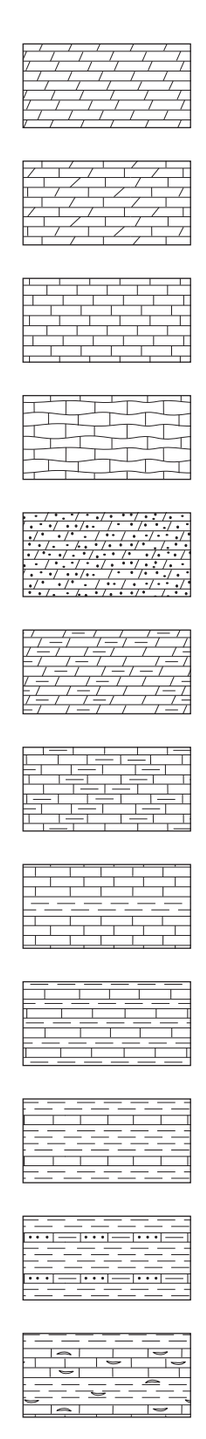

Dolomite
Dolomitic limestone
Limestone
Nodular-, wavy-, or irregular-bedded limestone
Sandy dolomite
Argillaceous dolomite
Argillaceous limestone
Interbedded limestone and shale (limestone dominant)
Interbedded limestone and shale
Interbedded shale and limestone (shale dominant)
Interbedded shale and silty limestone (shale dominant)
Fossiliferous limestone and shale
Dolomitic shale
Sandstone
Breccia

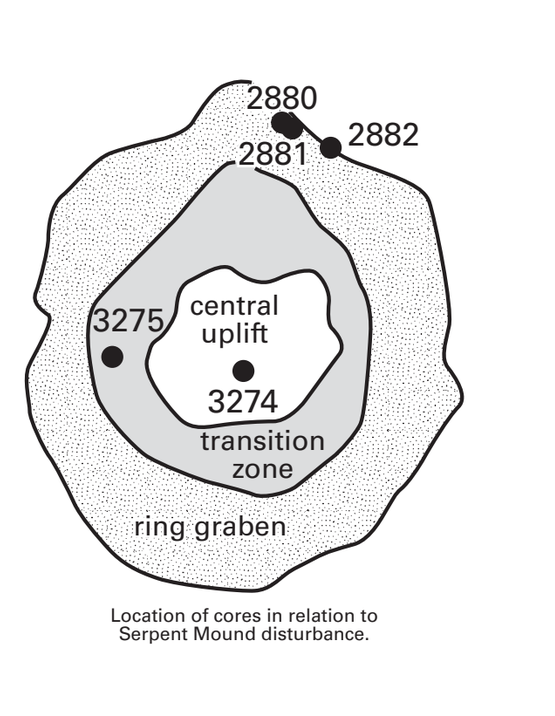

Location of cores in relation to Serpent Mound disturbance.

CORE DGS 3274

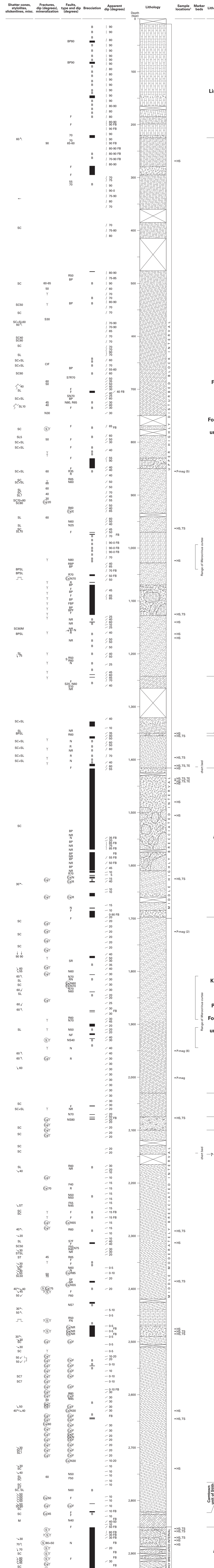

Lithologic description

Reference elevation 960.0 feet (292.6 m)

0-11.0 feet (0-3.3 m)—core missing

Grant Lake Limestone

Limestone (about 80 percent) and shale (about 20 percent) interbedded
11.0-225.3 feet (3.3-68.7 m)
Core missing between 165.0 and 171.0 feet (50.3-52.1 m)

Limestone, light-gray (N7) to medium-gray (N5); finely to coarsely crystalline; crystals subhedral to euhedral; fine to coarse grained; grains subangular to rounded; wavy to irregular bedding; thin to medium bedded; fossiliferous, brachiopods and bryozoans abundant; rare bioturbation; rare sparry-calcite shelter- and moldic-porosity fillings; argillaceous; rare moldic, interparticle, and fracture porosity.

Shale, light-gray (N7); calcareous; wavy to irregular bedding; thin bedded; abundantly fossiliferous; rare bioturbation; fracture porosity.

Possible faulted block of Fairview Formation or Corryville Member of Grant Lake Limestone between 184.5 and 198.2 feet (56.2-60.4 m).

Lower contact removed by faulting.

CORE DGS 3275

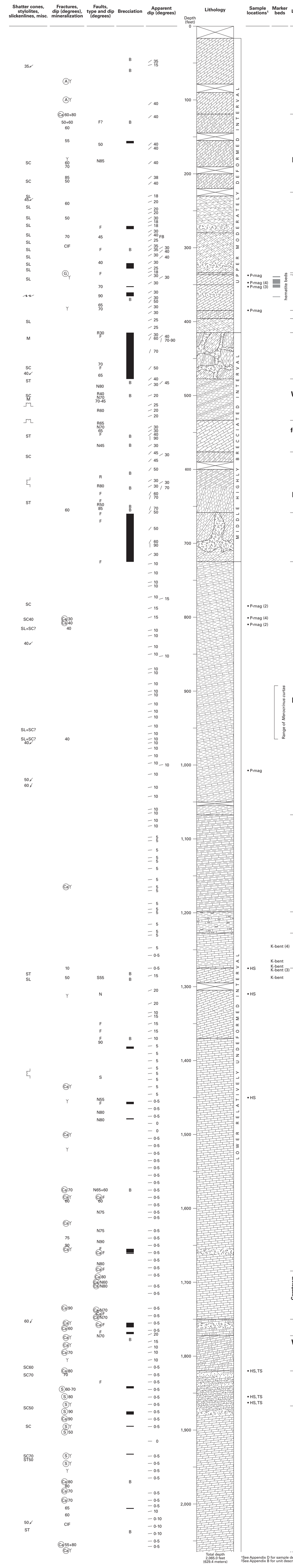

Lithologic description

Reference elevation 735 feet (224.0 m)

0-17.0 feet (0-5.2 m)—core missing

Peebles Dolomite

Vuggy, brecciated dolomite
17.0-118.5 feet (5.2-36.1 m)
Core missing between 78.0 and 88.0 feet (23.8-26.8 m)

Dolomite, white (N9) to medium-gray (N5); finely to medium crystalline; crystals anhedral to euhedral; massive bedded; zone of thin bedding between 58.1 and 62.0 feet (17.7-18.9 m); fossiliferous, colonial corals, pelmatozoans, and brachiopods common; rare to moderate bioturbation with local burrow mottling; pyrite; gypsum?; minor argillaceous material; vug-filling euhedral calcite crystals, well developed at 118.2 feet (36.1 m); limonite crust at 45.2 feet (13.8 m), disseminated asphalt and asphaltic staining between 45.0 and 58.0 feet (13.7 m-17.7 m); asphalt as vug-filling globules and fracture fillings between 107.8 and 118.5 feet (32.9-36.1 m); fracture, vuggy, moldic, and intercrystal porosity.

Upper contact not cored. Lower contact sharp and placed at stylolitic base of lowest massive dolomite bed.

Lilley and Bisher Formations undivided

Argillaceous and granular dolomite and minor shale
118.5-221.0 feet (36.1-67.4 m)
Tongue of Peebles Dolomite present between 122.0 and 123.4 feet (37.2-37.6 m)
Core missing between 145.0 and 154.7 feet (44.2-47.2 m), 192.0 and 200.0 feet (58.5-61.0 m), and 221.0 and 229.0 (67.4-69.8 m)

Dominant lithology: argillaceous dolomite, light-gray (N7) to medium-gray (N5); finely to medium crystalline; crystals euhedral to anhedral; planar to irregular bedding; laminated to thick bedded, cross-laminated; shale intraclasts between 213.0 and 214.0 feet (64.9-65.2 m); disseminated fossils, brachiopods and echinoderms common; rare to moderate bioturbation; disseminated and laminated glauconite in basal 6.0 feet (1.8 m) of unit; rare pyrite concentrated in burrows, fractures, and laminations; rare calcite in vugs; chert nodules at 183.6, 183.9, and 195.5 feet (56.0, 56.1, and 59.6 m); intercrystal and fracture porosity.

Subordinate lithology: granular dolomite, medium-gray (N5) to dark-gray (N3); medium to coarse grained; grains subangular to subrounded, moderately sorted; planar to cross bedding; laminated to thick bedded; sparsely to abundantly fossiliferous, medium-grained echinoderm ossicles; disseminated pyrite and glauconite; interparticle, intercrystal, and fracture porosity.

Shale, medium dark gray (N4); planar to irregular bedding; laminated to thin bedded; rare to moderate bioturbation; dolomitic to slightly calcareous; disseminated pyrite.

Lower contact not present, probably within missing core interval between 221.0 and 229.0 feet (67.4-69.8 m).

Estill Shale

Dolomitic shale and rare dolomite
229.0-333.0 feet (69.8-101.5 m)

Shale, greenish-gray (5GY 6/1), medium-gray (N5), pale-brown (5YR 5/2), and grayish-red (10R 4/2); dolomitic; planar bedding; laminated to thick bedded; sparsely fossiliferous; rare bioturbation; pyrite in burrow fillings; disseminated to laminated glauconite in basal 0.5 foot (0.2 m) of unit.

Dolomite, light-gray (N7); fine grained; planar laminations; sparsely fossiliferous; rare bioturbation.

Lower contact sharp and at base of lowest shale bed.

Dayton Formation

Dolomite and minor shale
333.0-335.5 feet (101.5-102.3 m)

Dolomite, light-olive-gray (5Y 6/1) to greenish-gray (5GY 6/1); finely to medium crystalline; crystals subhedral to euhedral; planar bedding; medium to thick bedded; shale partings; sparsely fossiliferous; glauconite as clasts, insoluble residue along stylolite seams, and disseminated throughout unit; intercrystal, moldic, and fracture porosity.

Shale, greenish-gray (5GY 6/1); dolomitic; planar bedding; thin bedded; sparsely fossiliferous; rare bioturbation; pyrite in burrow fillings.

Lower contact sharp and at base of lowest dolomite bed.

Noland? Formation

Shale
335.5-335.6 feet (102.3-102.3 m)

PLATE 1.—LITHOLOGIC COLUMNS AND DESCRIPTIONS OF CORES FROM THE SERPENT MOUND DISTURBANCE, SOUTHWESTERN OHIO

TIME MIGRATED

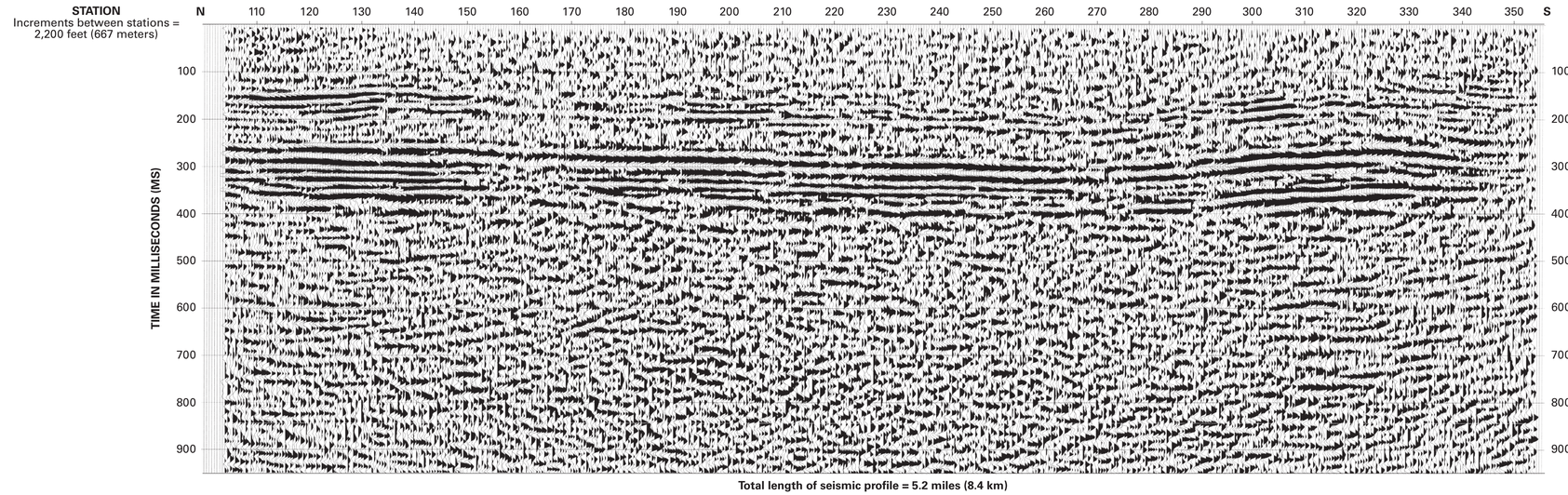

TIME MIGRATED AND INTERPRETED

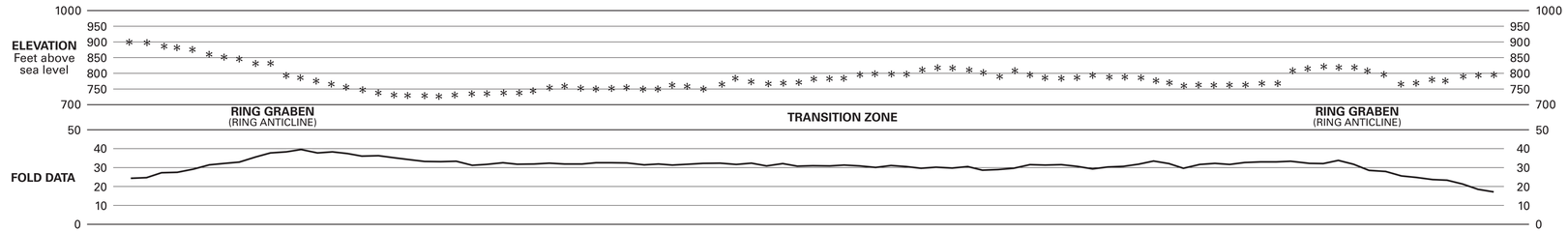

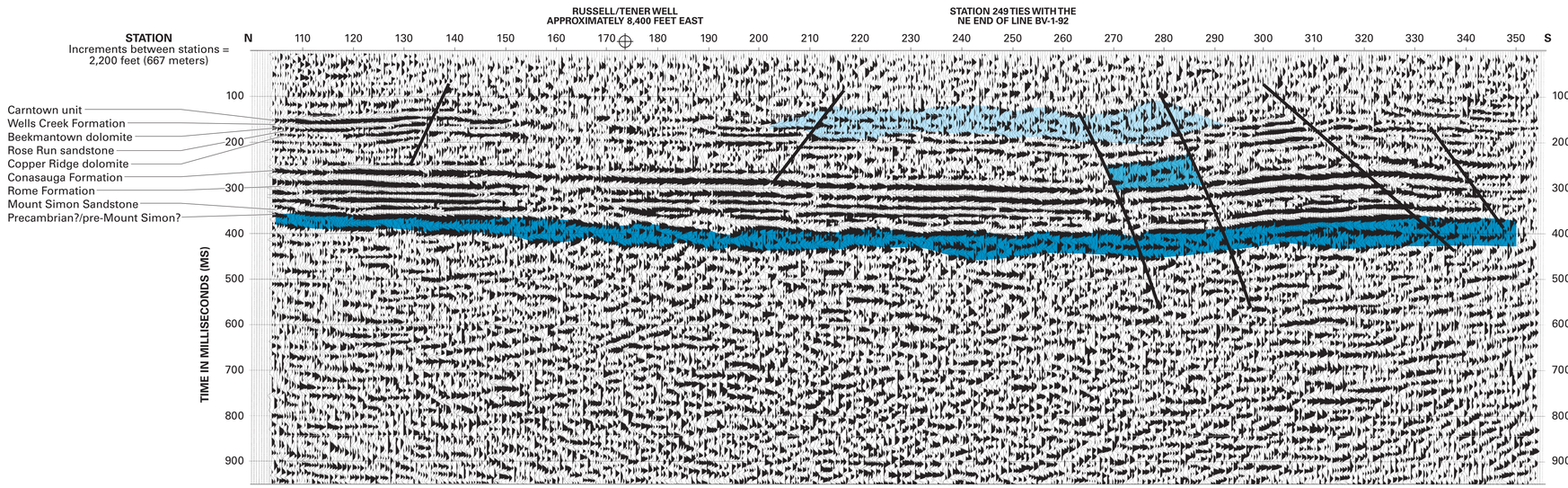

RECORDING PARAMETERS FOR SM-1

Shot by: Western Geophysical, Inc.
Client: Columbia Natural Resources
Date: September 1989
Instruments: DFS-V; Society of Exploration Geophysicists (SEG)-B format; 120 channels; 2-ms sample rate; 12 seconds of recorded data; 12-128 Hz filter
Source: vibrators; in-line array; interval 67 meters (220 feet); 20-12-0 Hz sweep frequency; 7 seconds sweep length; notch filter in; spread geometry 2078.8 m-100.5 m – 100.5 m-2078.8 m (6820 feet-330 feet – 330 feet-6820 feet)
Geophones: in-line array; group interval 33.5 meters (110 feet); 10 Hz; 24 per group

PROCESSING STEPS

Trace kill/reverse
Trace edit
Automatic gain control (AGC): mean
AGC operator length: 300
Basis for scalar application: centered
Bandpass filter
  Type of filter: single
  Type of filter specification: Ormsby bandpass
  Phase of filter: zero
  Apply a notch filter? no
  Ormsby filter frequency values: 10-20-90-120
Phase rotation (first third of line)
  Phase rotation angle: 90
Elevation statics? yes
Residual statics
  Type of residual statics to apply: maximum power autostatics
Frequency-wave number (F-K) filter
  Type of F-K filter: arbitrary polygon
Trace muting
In-line sort
  Select new primary sort key: common depth point (CDP) bin number
  Select new secondary sort key: signed source-receiver offset
  Maximum traces per output ensemble: 50
Normal moveout correction
CDP/ensemble stack
  Sort order of input ensembles: CDP
  Method for trace summing: mean
  Root power scalar for stack normalization: 0.5
  Apply final datum statics after stack? yes
Implicit finite difference (FD) depth migration
  Maximum frequency vs depth to migration: 0 ft-80 Hz, 20000 ft-80 Hz
  Specify migration interval vs depth velocity field: 0 ms-14500 ft/sec, 300 ms-15000 ft/sec, 1500 ms-17000 ft/sec
  Percent velocity scale factor: 100
  Define largest angle for proper migration: 15
  Output migration in depth or time? time
  Re-kill dead traces? yes
Trace display

EXPLANATION

- Anomalous lens-shaped reflector breakup
- Anomalous stratigraphically thin or faulted? Knox Dolomite intervals
- Anomalous thick Precambrian? or pre-Mount Simon? reflectors
- Fault
- Projected well location

NOTE: Carntown unit is equivalent to “Gull River” of drillers
Lexington Limestone is equivalent to Trenton Limestone of drillers

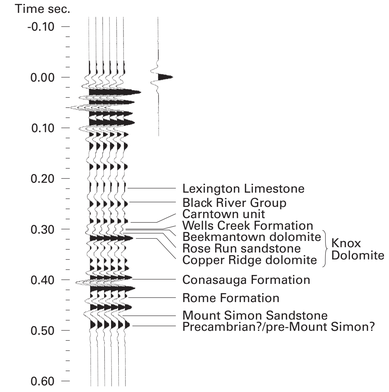

Synthetic seismogram model for the Russell/Tener well (permit no. 11) in Adams County, Ohio. Datum of synthetic seismogram in relation to seismic profile is top of the Precambrian?/pre-Mount Simon?. Density-log data and Ormsby wavelet (0 degree phase; 10-20-50-70 Hz frequency) were used to create a normal polarity model.

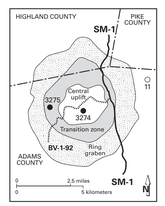

Location of seismic line SM-1

PLATE 2.—SEISMIC REFLECTION PROFILE OF SEISMIC LINE SM-1 ACROSS THE SERPENT MOUND DISTURBANCE, SOUTHWESTERN OHIO

TIME MIGRATED

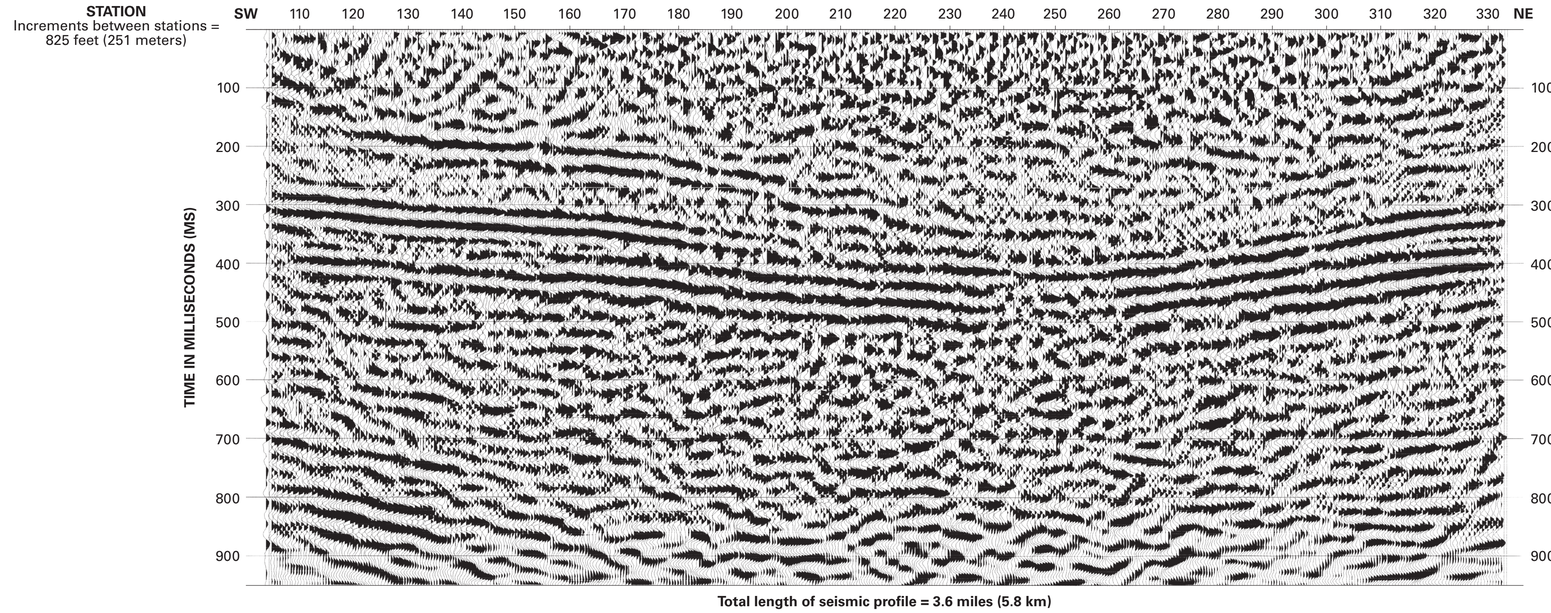

TIME MIGRATED AND INTERPRETED

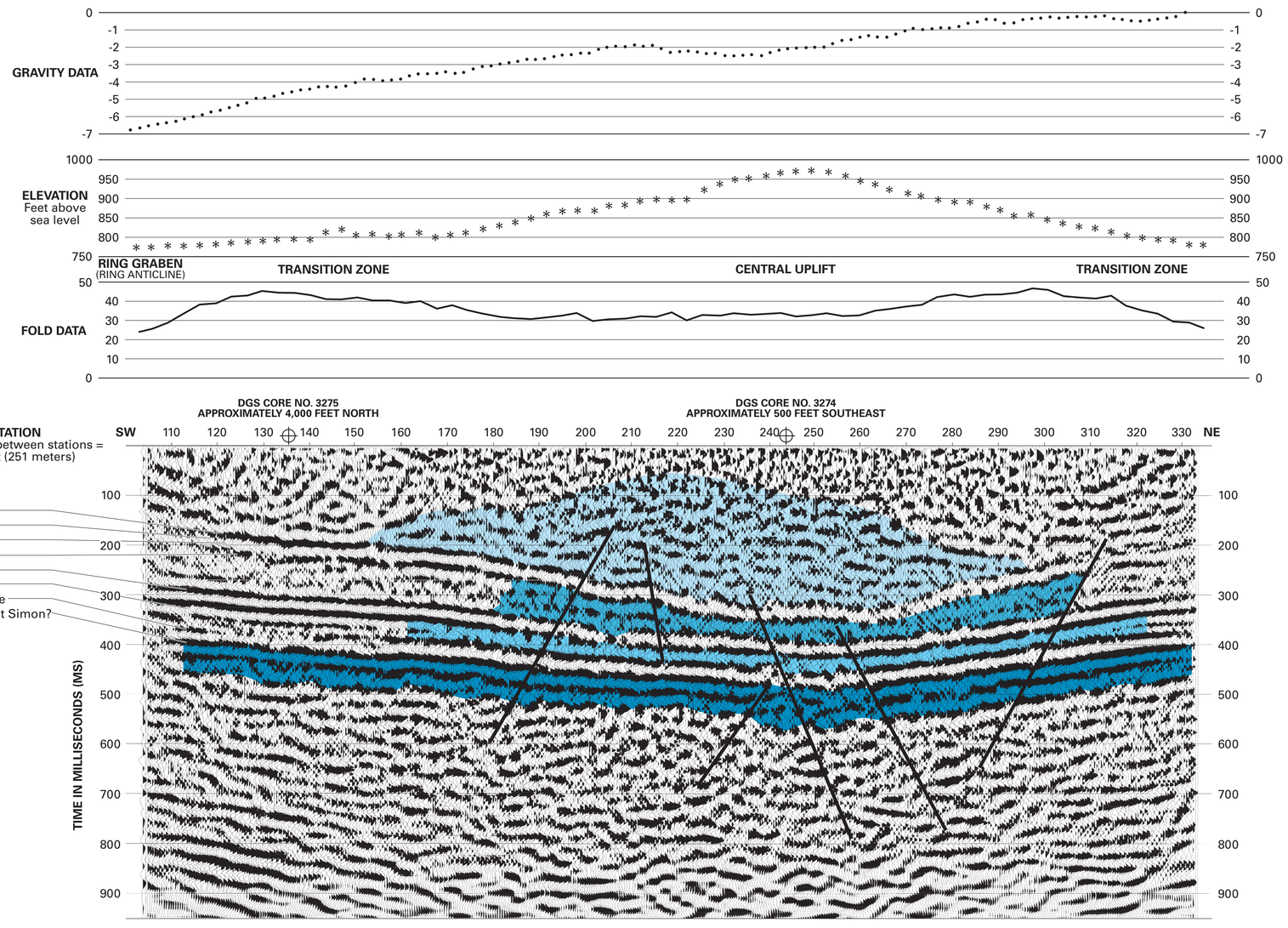

RECORDING PARAMETERS FOR BV-1-92

Shot by: Paragon Geophysical Inc.
Client: Ohio Department of Natural Resources
Date: April 1992
Instruments: DFS-V; Society of Exploration Geophysicists (SEG)-B format; 120 channels; 2-ms sample rate; 3 seconds of data; 18-128 Hz filter
Source: vibrators; in-line array; interval 25.1 meters (82.5 feet); 20-110 Hz sweep frequency; 6 seconds sweep length; notch filter in; spread geometry 1609 meters-75.3 meters – 75.3 meters-1609 meters (5280 feet-247 feet – 247 feet-5280 feet)
Geophones: in-line array; group interval 25.1 meters (82.5 feet); 8 Hz; 24 per group

PROCESSING STEPS

Trace kill/reverse
Trace edit
Automatic gain control (AGC): mean
AGC operator length: 300
Basis for scalar application: centered
Bandpass filter
- Type of filter: single
- Type of filter specification: Ormsby bandpass
- Phase of filter: zero
- Apply a notch filter? no
- Ormsby filter frequency values: 10-20-90-120

Elevation statics? yes
Residual statics
- Type of residual statics to apply: maximum power autostatics

Frequency-wave number (F-K) filter
- Type of F-K filter: arbitrary polygon

Trace muting
In-line sort
- Select new primary sort key: common depth point (CDP) bin number
- Select new secondary sort key: signed source-receiver offset
- Maximum traces per output ensemble: 70

Normal moveout correction
CDP/ensemble stack
- Sort order of input ensembles: CDP
- Method for trace summing: mean
- Root power scalar for stack normalization: 0.5
- Apply final datum statics after stack? yes

Implicit finite difference (FD) depth migration
- Maximum frequency vs depth to migration: 0 ft-80 Hz, 20000 ft-80 Hz
- Specify migration interval vs depth velocity field: 0 ms-14500 ft/sec, 300 ms-15000 ft/sec, 1500 ms-17000 ft/sec
- Percent velocity scale factor: 100
- Define largest angle for proper migration: 15
- Output migration in depth or time? time
- Re-kill dead traces ? yes

Trace display

EXPLANATION

- Anomalous lens-shaped reflector breakup
- Anomalous stratigraphically thin or faulted? Knox Dolomite intervals
- Anomalous stratigraphically thin Rome Formation
- Anomalous thick Precambrian? or pre-Mount Simon? reflectors
- Fault
- Projected well location

NOTE: Carntown unit is equivalent to “Gull River” of drillers
Lexington Limestone is equivalent to Trenton Limestone of drillers

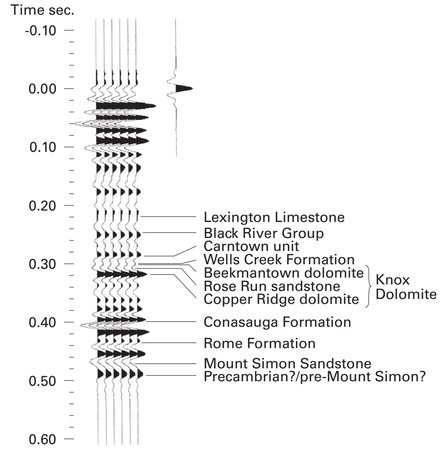

Synthetic seismogram model for the Russell/Tener well (permit no. 11) in Adams County, Ohio. Datum of synthetic seismogram in relation to seismic profile is top of the Precambrian?/pre-Mount Simon?. Density-log data and Ormsby wavelet (0 degree phase; 10-20-50-70 Hz frequency) were used to create a normal polarity model.

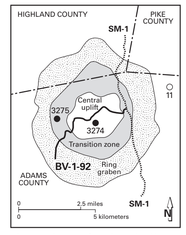

Location of seismic line BV-1-92

PLATE 3.—SEISMIC REFLECTION PROFILE OF SEISMIC LINE BV-1-92 ACROSS THE SERPENT MOUND DISTURBANCE, SOUTHWESTERN OHIO